

## Chapter 6

### ANALYSIS AND DISCUSSION OF EXPERIMENTAL RESULTS

The results of the experimental study of silt behavior performed in this research will now be discussed in terms of cavitation and air coming out of solution from pore water due to a reduction in pore pressure. The pore pressure responses measured in the Q tests will be considered in terms of the information presented in Chapter 4. The results of the undrained unloading tests will be used to consider the pore pressure changes which may occur during sampling along with the possible release of air from solution due to the pressure reductions. The behavior observed in the Q tests performed on specimens trimmed from the unloading test specimens will be considered relative to cavitation. The results of the Q tests performed in the prepressurization study will also be discussed in relation to cavitation of soil pore water. The undrained strength parameters measured for LMVD silt will be discussed and compared. The growth of gas bubbles within the pore water of saturated, dilatant silts will be considered in terms of its potential influence on the stress-strain behavior of these soils in Q tests, and will be related to the stress-strain behavior observed in this research.

C.2

LD  
5655  
V856  
1994  
R 673  
V.2  
C.2

## **6.1 Analysis of Q Tests with Midheight Pore Pressure Measurements**

The results of the Q tests with midheight pore pressure measurements will now be discussed and the pore pressure reductions measured will be used in further analyses.

### **6.1.1 Discussion of Measured Pore Pressures**

The numerous plots of measured change in pore pressure vs. axial strain presented in Sections 5.4 and 5.5 showed variations in the pore pressure responses and values of pore pressure measured in the Q tests performed in this research. A number of tests showed erratic pore pressure measurements. In most of these tests (UU-1, UU-2, UU-4, UU-5, UU-7, UU-16, and UU-23), the erratic pore pressure measurements are believed to have resulted from the failure of the rubber cement seal where the pore pressure needle passed through the rubber membrane.

When failure of the rubber cement seal occurred, the specimens would have experienced drainage to some extent, and the assumption that the Q test specimens maintained a constant volume throughout the tests would be incorrect. In this case, the strengths measured in these Q test would not be accurate, and meaningful comparisons of the results from these tests with the results of other tests would be questionable. In some cases the erratic pore pressure

measurements did not occur until higher values of axial strain had been reached. Strength interpretations using these tests, at levels of axial strain prior to the occurrence of the erratic pore pressure measurements, would still appear to be reasonable. Values of peak deviator stress, which often corresponded with the occurrence of erratic pore pressure measurements, may not be accurate and should not be considered in determining the undrained shear strength of the soil.

In one test (UU-13), a failure of the rubber cement seal may have occurred as well, because no change in pore pressure was measured during the test until after an axial strain of about 12 percent. The condition observed in test UU-13 also could have possibly resulted from the specimen being considerably less than fully saturated or air being present within the pore pressure monitoring system. In this situation, as the deviator stress was applied, the free air present in the specimen or measuring system would compress or expand due to the applied load and a measurable change in pore water pressure may not have been detectable until the air had dissolved and the specimen had a higher degree of saturation. In either case, test UU-13 probably does not provide reliable results for an undrained test on a saturated specimen.

For the ten tests discussed in Section 5.4 in which the measured change in pore pressure vs. axial strain behavior was reasonable, the test results obtained can be used in meaningful comparisons. Figure 6.1 shows the deviator stress-strain behavior for the ten Q tests in which reasonable pore pressure measurements occurred. Plots of the change in pore pressure measured in each test are presented in Figure 6.2.

It can be seen from Figure 6.1 that the deviator stress-strain behavior measured in these tests varied considerably. All of these tests were performed on remolded samples of the same silt. The silt had been  $K_0$  consolidated from a slurry in a batch consolidometer to an effective vertical consolidation pressure,  $\sigma'_v$ , of 56 psi. When tested in Q tests, the saturated specimens would have been expected to give the same undrained strength for the soil.

Based on 10 percent axial strain as a failure criterion or a peak in the deviator stress-strain curve before 10% axial strain, the total stress Mohr's circles for these ten tests have been plotted in Figure 6.3. This figure shows that the tests yielded erratic undrained strengths for the LMVD silt. Two groups of three circles, however, do approach  $\phi_u = 0$ ,  $S_u = c$  envelopes in this plot. The three circles from tests UU-12, UU-15, and UU-18, have been

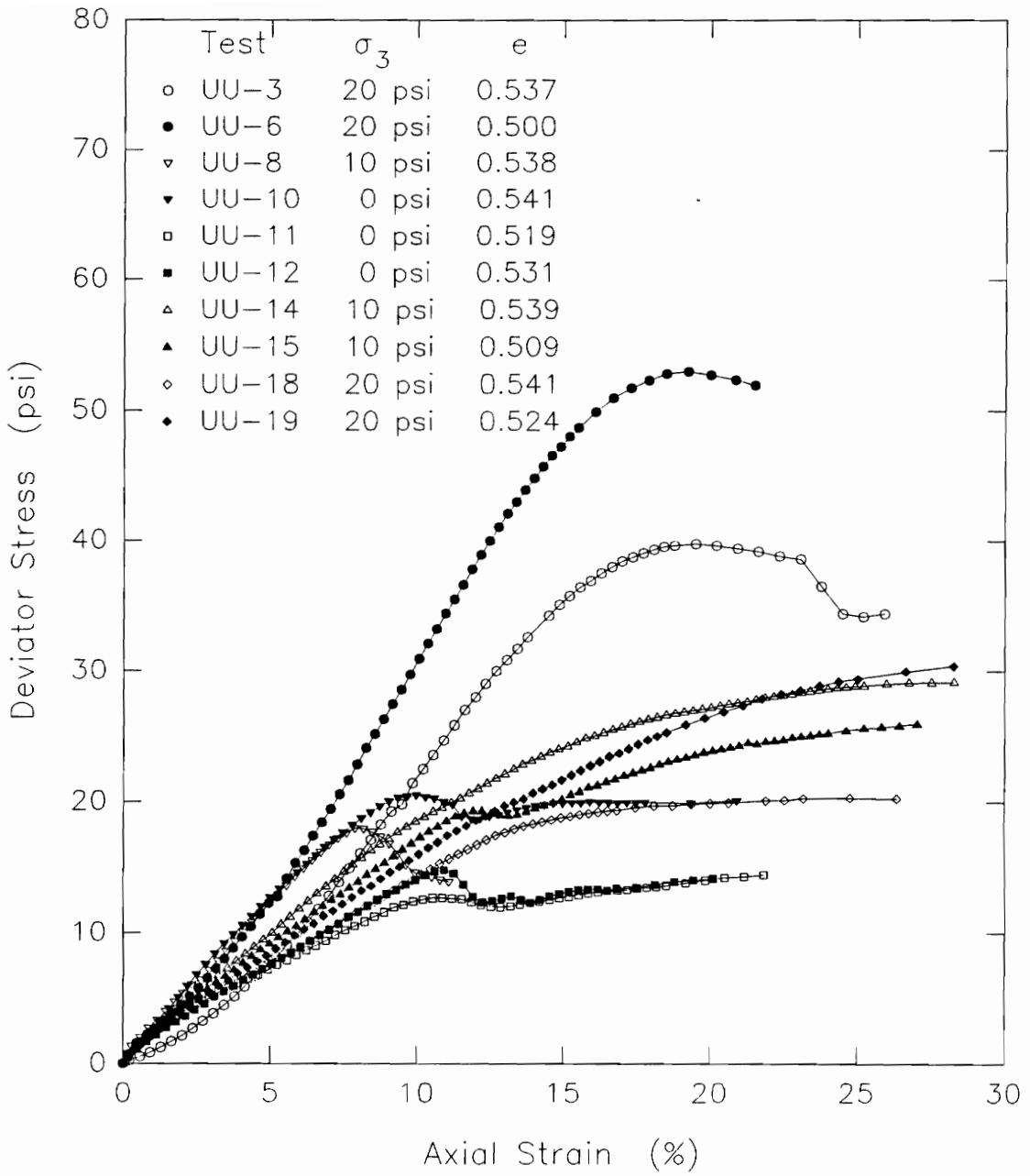


**Figure 6.1. Deviator stress vs. axial strain relationships measured in Q tests in which erratic pore pressure measurements were not observed**

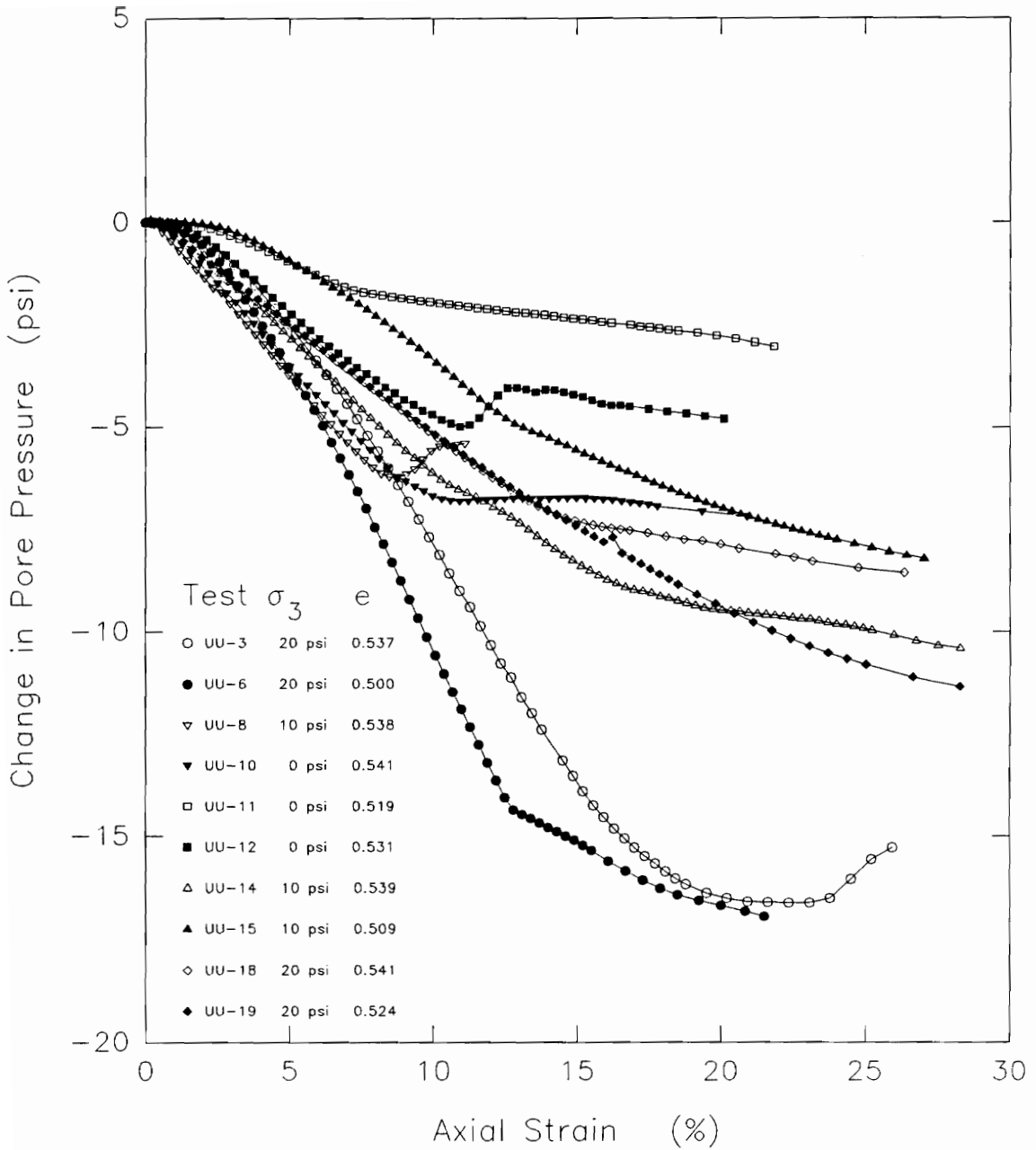


**Figure 6.2.** Change in pore pressure vs. axial strain relationships measured in Q tests in which erratic pore pressure measurements were not observed

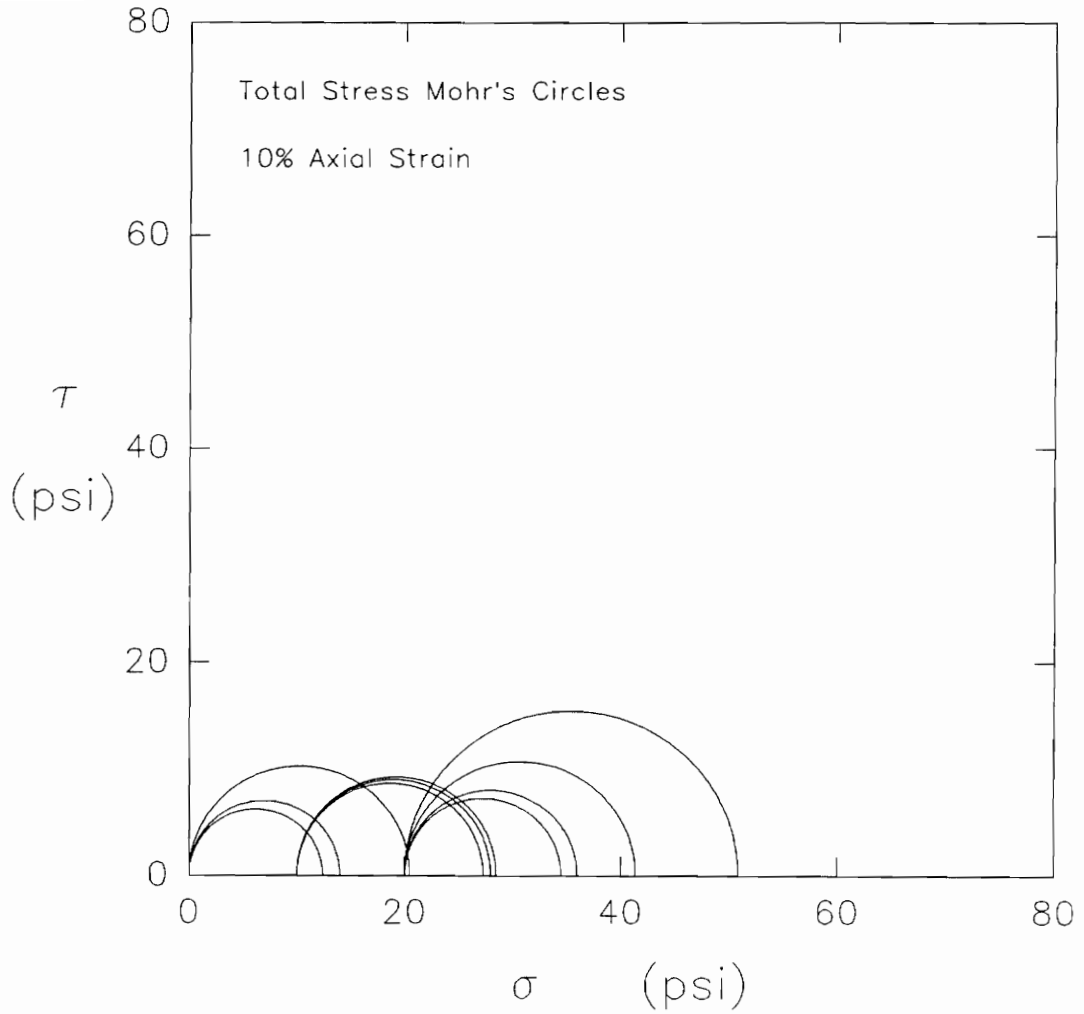


**Figure 6.3. Total stress Mohr's circles for remolded old LMVD silt at 10% axial strain for Q tests in which erratic pore pressure measurements were not observed**

replotted in Figure 6.4. These specimens had void ratios of 0.531, 0.509, and 0.541. For these three tests, at 10% axial strain, the undrained strength of the soil is defined by the parameters  $c = 7.3$  psi and  $\phi_u = 1.1^\circ$ .

Figure 6.5 shows the Mohr's circles for tests UU-3, UU-10, and UU-14. These specimens had void ratios of 0.537, 0.541, and 0.539. From these three Q tests at 10% axial strain, the undrained strength of the soil is defined by the parameters  $c = 9.5$  psi and  $\phi_u = 1.5^\circ$ . The two undrained strength envelopes shown in Figures 6.4 and 6.5 illustrate the variation in undrained strength parameters often obtained for saturated, dilatant silts.

As can be seen from Figure 6.2, in the ten tests in which erratic pore pressure measurements are felt not to have occurred, considerable differences between the measured pore pressure responses were observed. The differences in the observed pore water pressure responses could possibly be due the variations in specimen void ratio. Different void ratios would give specimens which tended to dilate to different extents during shear.

All of these specimens were  $K_0$  consolidated to the same vertical effective confining pressure in the remolding process. If the void ratio of the soil was a function of the vertical effective consolidation pressure, the specimens

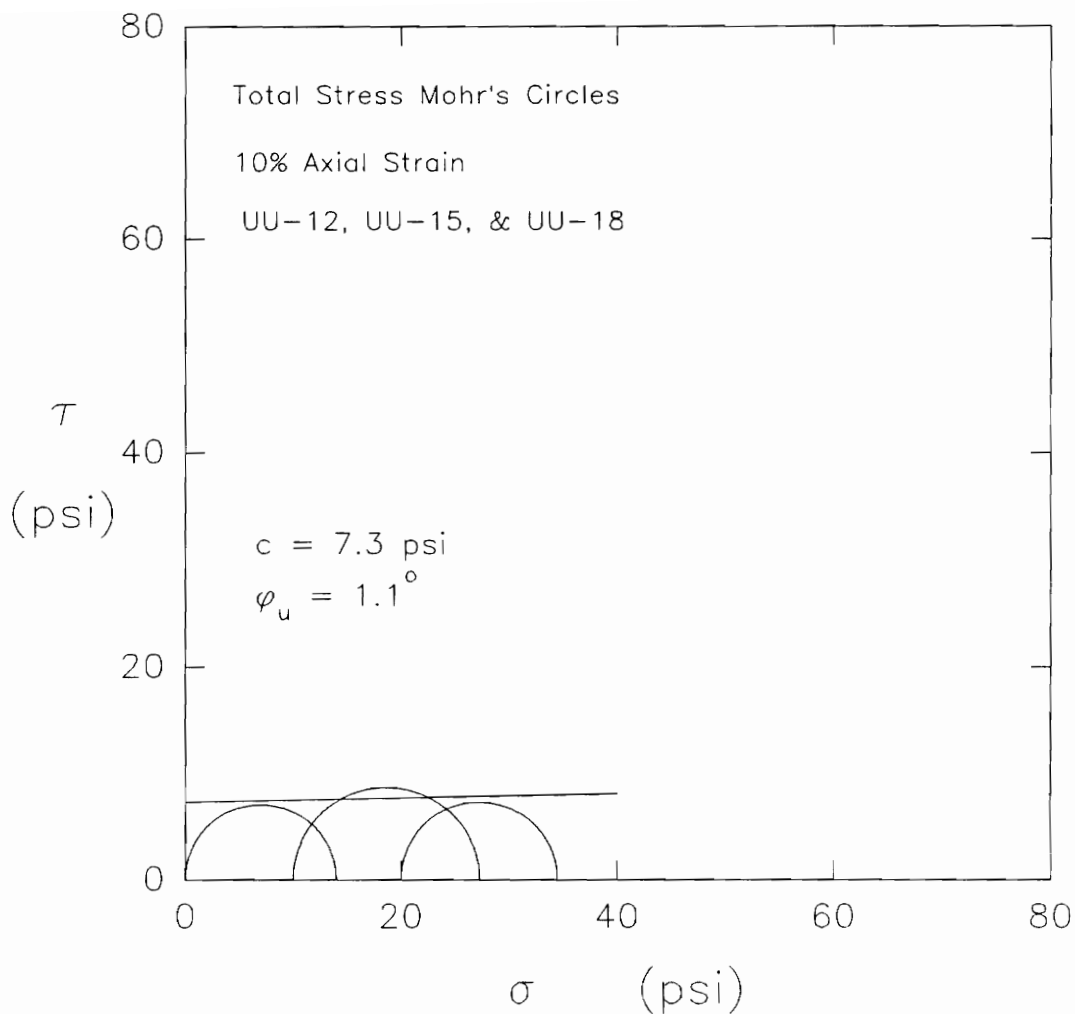


**Figure 6.4. Total stress Mohr's circles at 10% axial strain for Q tests UU-12, UU-15, and UU-18 performed on remolded old LMVD silt**

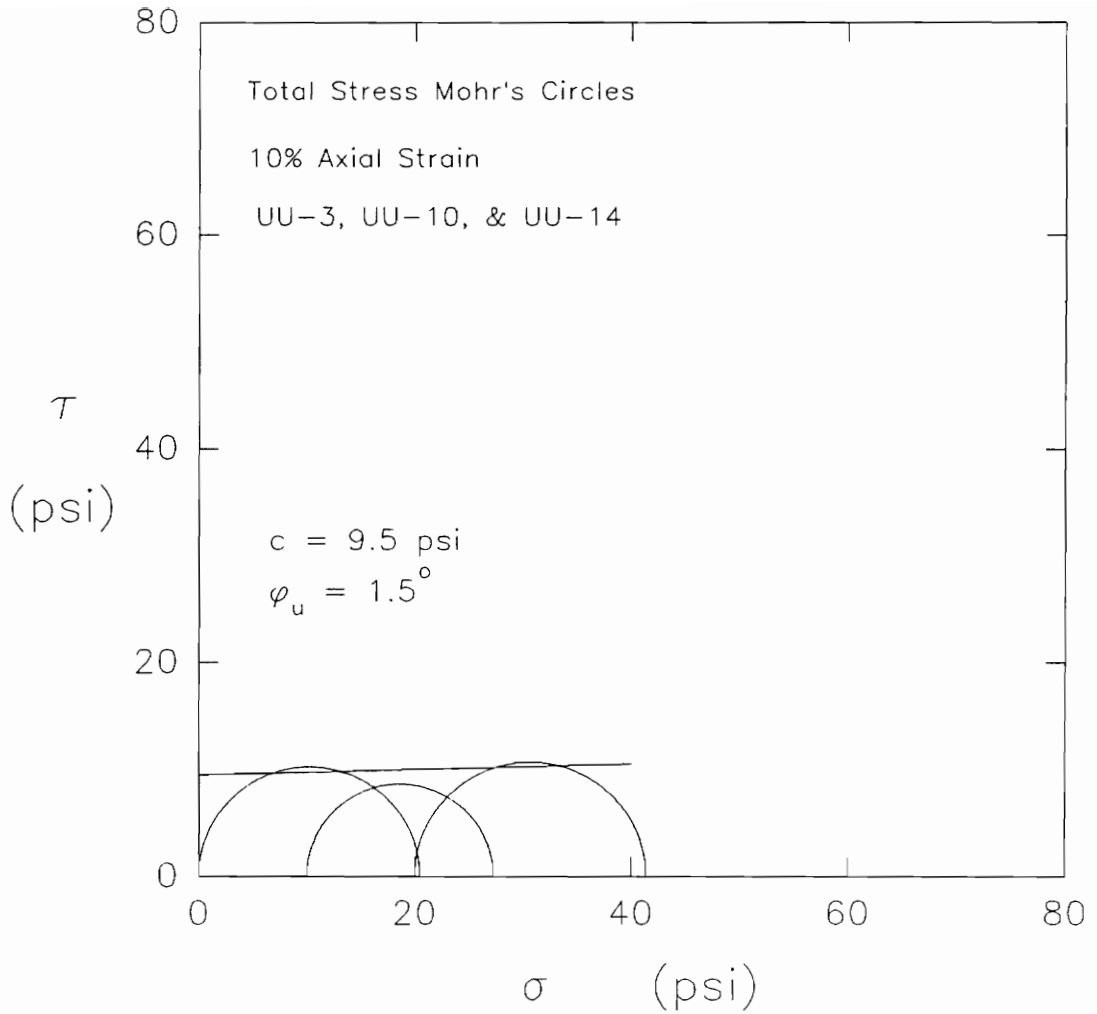


**Figure 6.5. Total stress Mohr's circles at 10% axial strain for  $Q$  tests UU-3, UU-10, and UU-14 performed on remolded old LMVD silt**

should have all had similar void ratios initially. As a result, the pore water pressure responses would have been similar for all of the tests. The density and void ratio of silts are not necessarily a function of the vertical effective consolidation pressure as they are for clays (Fleming and Duncan, 1990). Because of this, the void ratio of these specimens may have varied even though the samples were consolidated under the same vertical effective consolidation pressure. Slight variations in void ratio were measured for these specimens. These variations in void ratio may be the result of both the sensitivity of void ratio measurements to error, as well as disturbance effects on specimen void ratio.

Another possibility is that variable amounts of undissolved air may have been present in the soil specimens or the pore pressure monitoring system. With undissolved air present, the measured pore pressures would have been different from those measured in a fully saturated specimen. Different amounts of undissolved air from one specimen to another could have resulted in the observed variations in the measured pore pressures. Dissolved air coming out of solution from the pore water as pore water pressures decreased may have also lead to the observed variations in pore pressure response.

It is also possible that slight variations in strain rate between the different tests may have resulted in the observed variations in measured pore pressure. These Q tests with midheight pore pressure monitoring were performed over a period of about 8 months. Although the strain rate was set as close as possible to 1%/min for each test, it was not possible to ensure that the strain rate would be the same for all specimens tested. Some of the variations observed in the measured pore water pressures, may have been due to shearing the specimens at slightly different rates.

Review of Figure 6.2 indicates that the specimens which showed the largest ultimate decreases in pore water pressure during shear were the specimens tested at higher cell pressures. In general, the tests performed at a cell pressure of 20 psi had larger maximum decreases in pore water pressure than the specimens tested at 10 psi. Similarly, the maximum decreases in pore water pressure were generally larger in the tests performed at a cell pressure of 10 psi than those performed as unconfined compression tests.

The tests with a higher cell pressure would have had a higher initial pore water pressure at the start of shear. These specimens could have experienced a larger decrease in pore water pressure before the pore water pressure would

have decreased below atmospheric pressure. When the pore water pressure approached atmospheric pressure, gases dissolved in the pore water would have been more likely to exit solution. In addition, small air bubbles were very likely present in the samples when they were first placed in the triaxial cell. The specimens tested at higher cell pressures should have had smaller air bubbles and therefore, have been more fully saturated, giving better pore pressure responses.

The relationship between the measured pore pressure responses and specimen void ratio can also be compared for tests performed at the same cell pressure. Figure 6.6 shows the measured change in pore water pressure vs. axial strain relationships for tests UU-10, UU-11, and UU-12. These tests were all performed as unconfined compression tests. From the results of these tests, it appears that the specimen with the largest void ratio, UU-10, had the greatest measured decrease in pore water pressure during shear. Conversely, the specimen with the smallest void ratio, UU-11, experienced the smallest decrease in pore water pressure of these specimens.

This was not what was expected. The specimen with the smallest void ratio, UU-11, was the densest and would be expected to exhibit a larger decrease in pore water pressure

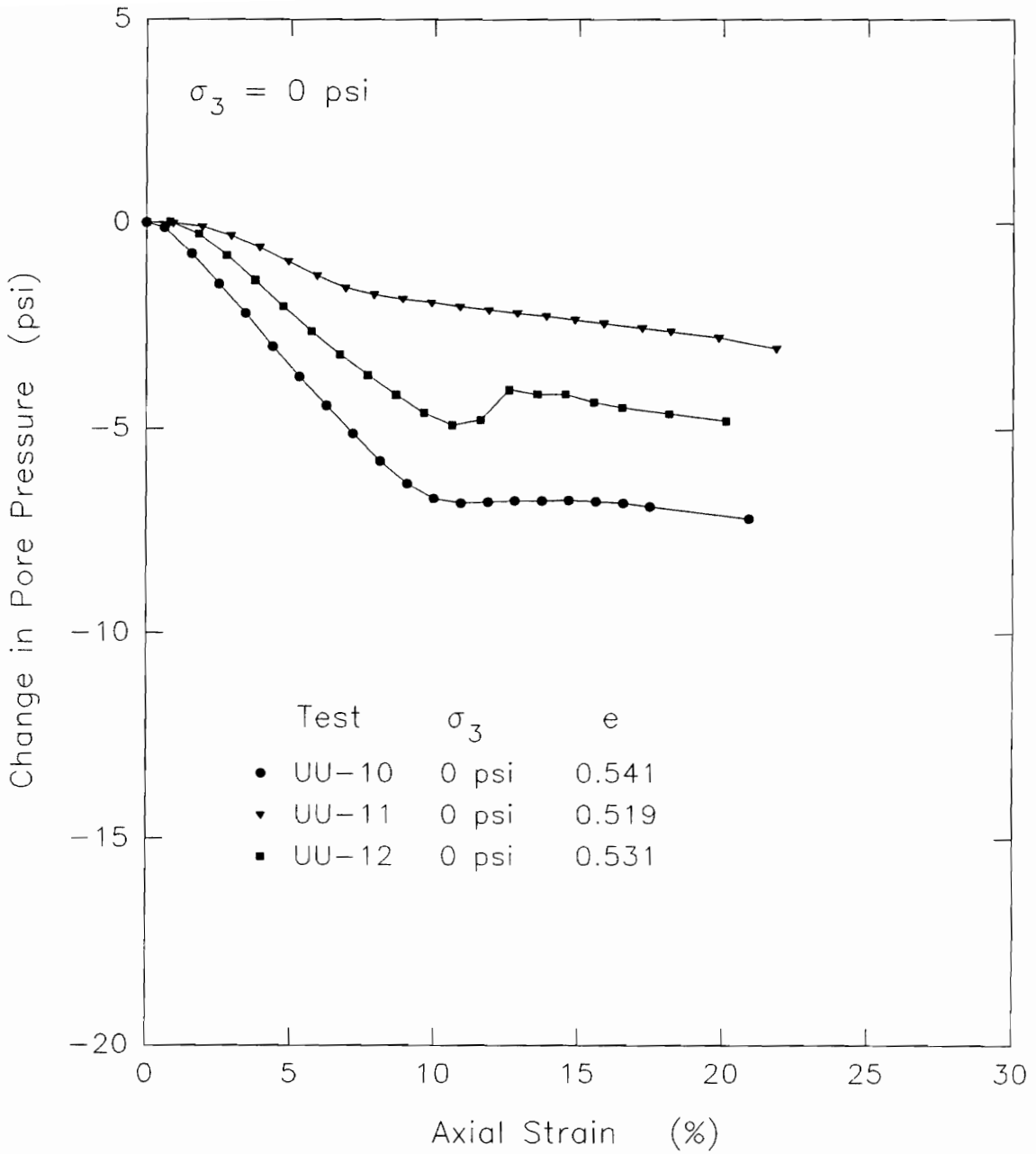


**Figure 6.6.** Change in pore pressure vs. axial strain relationships measured in  $Q$  tests performed as unconfined compression tests on specimens of remolded old LMVD silt

during undrained shear than a looser specimen. This should be true if all other variables within the specimens were equal. As noted previously, the sensitivity of the measurements involved may have lead to variations in specimen void ratios being measured. Variations in degree of saturation, including trapping different amounts of air between the specimen and membrane, may have influenced the measured pore pressures. Slight variations in strain rate may also have caused the observed differences in the measured pore water pressures. Specimen disturbance may have varied as well, leading to different pore pressure responses being observed.

Figure 6.7 shows the measured change in pore water pressure vs. axial strain relationships for tests UU-8, UU-14, and UU-15. These tests were all performed at a cell pressure of 10 psi. The results of these tests indicate that the specimen with the smallest void ratio, UU-15, had an ultimate change in pore water pressure that was between that of the other two tests. The other two specimens, UU-8 and UU-14, had about the same void ratio. Specimen UU-14 experienced a larger decrease in pore water pressure than specimen UU-8, even though the specimens had similar void ratios. The relationships between specimen void ratio and ultimate change in pore water pressure during undrained

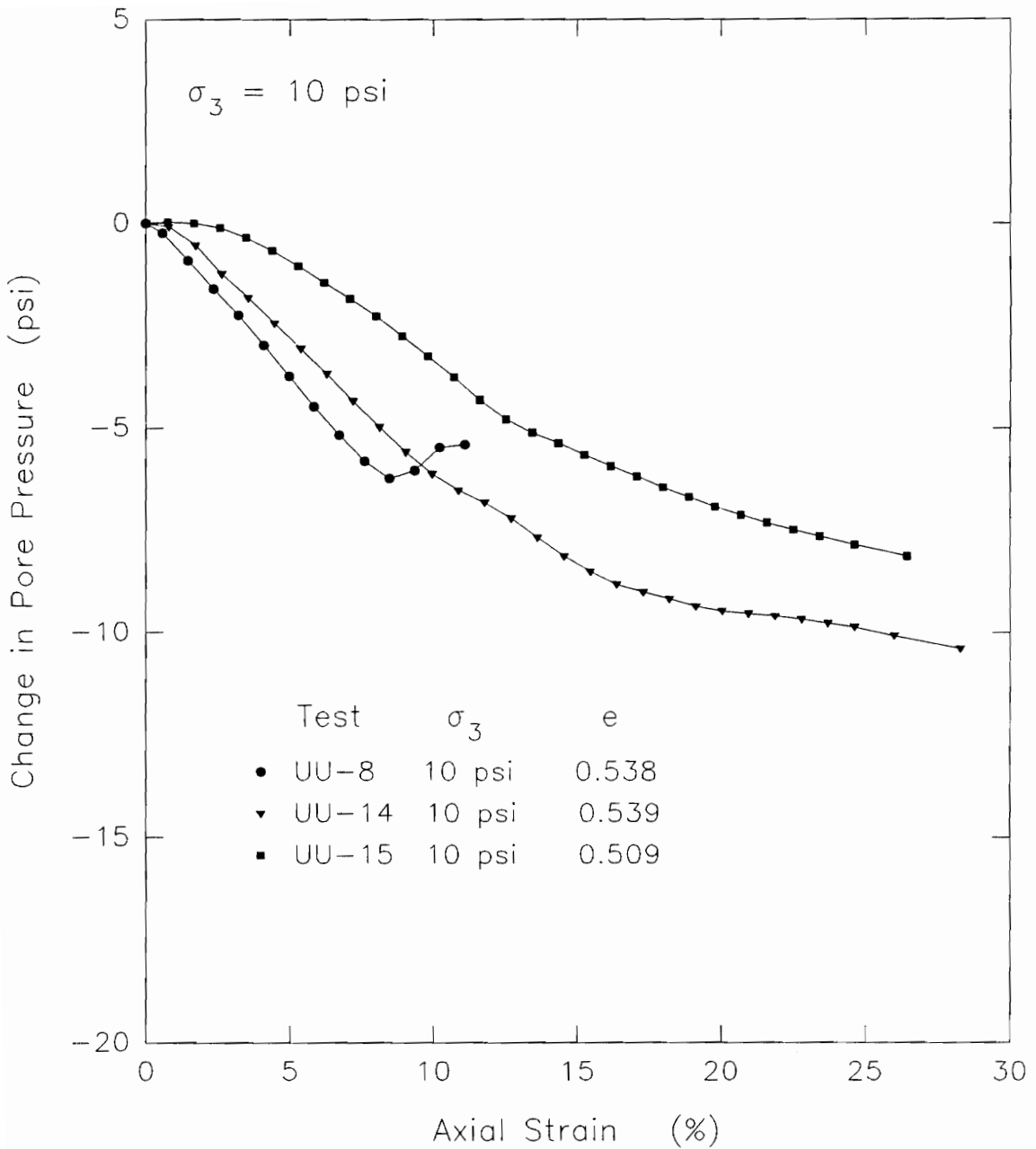


**Figure 6.7.** Change in pore pressure vs. axial strain relationships measured in  $Q$  tests performed at a cell pressure of 10 psi on specimens of remolded old LMVD silt

shear in these tests were not as expected and may be the result of other factors, as discussed above.

Figure 6.8 shows the change in pore water pressure vs. axial strain relationships measured in tests UU-3, UU-6, UU-18, and UU-19. These tests were performed at a cell pressure of 20 psi. In this case, the specimen with the smallest void ratio, UU-6, experienced the largest decrease in pore water pressure of the four specimens. The specimen with the largest void ratio, UU-18, experienced the smallest decrease in pore water pressure during shear. The two other specimens, UU-3 and UU-19, had intermediate values of void ratio. The magnitudes of the change in pore water pressure measured in these two tests were between those of tests UU-6 and UU-18, but did not increase with decreasing void ratio.

Of the three different cell pressures used in these tests, only the tests performed at 20 psi cell pressure tended to show the expected relationship between specimen void ratio and magnitude of change in pore water pressure. As void ratio decreased, the magnitude of the change in pore water pressure tended to increase. The denser specimens tended to experience larger decreases in pore water pressure than looser specimens with higher void ratios. Other factors may have contributed to the inconsistencies in the observed pore pressure responses measured in the Q tests

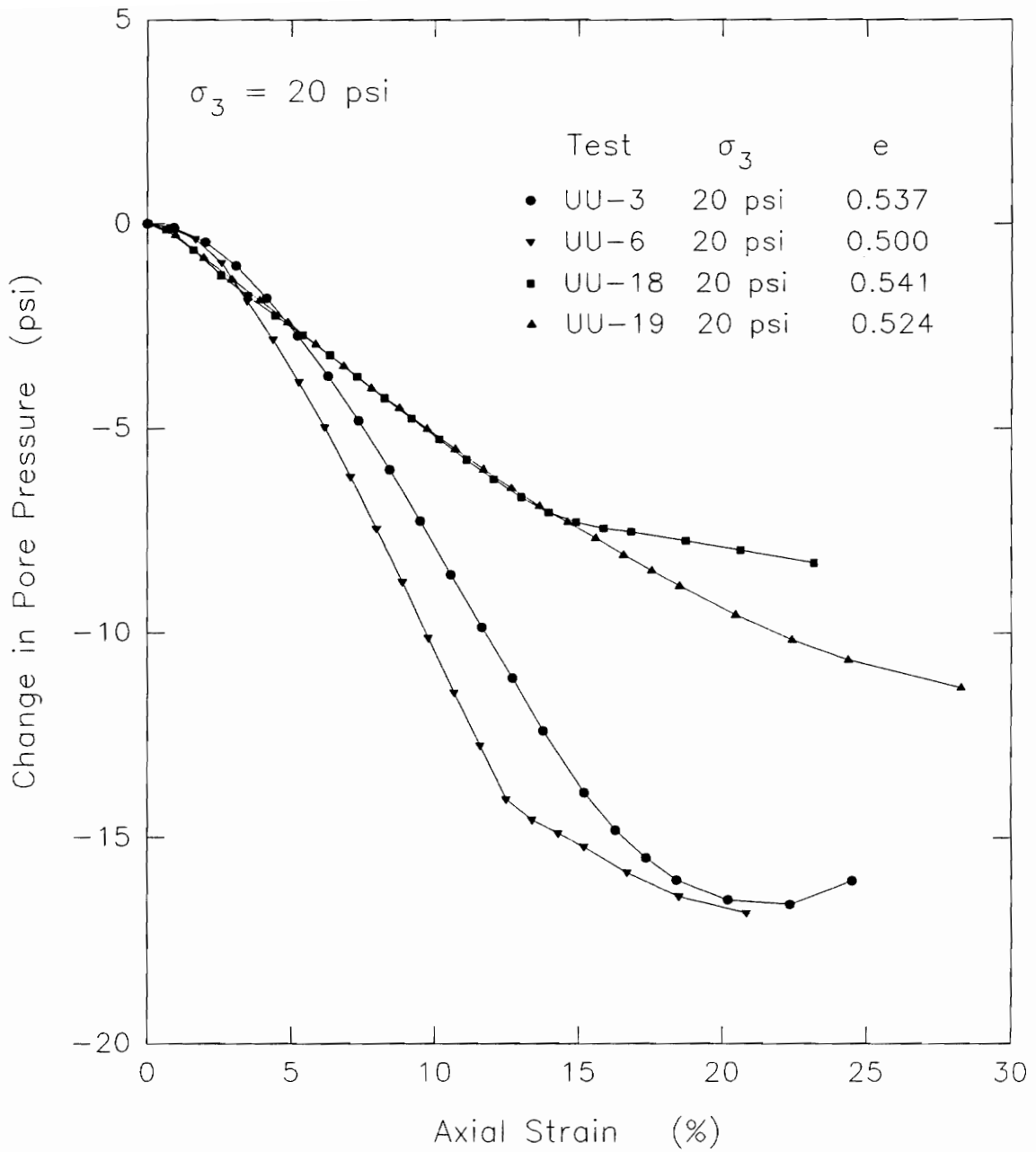


**Figure 6.8.** Change in pore pressure vs. axial strain relationships measured in  $Q$  tests performed at a cell pressure of 20 psi on specimens of remolded old LMVD silt

performed at a cell pressure of 20 psi, compared to those tested at cell pressures of 0 and 10 psi.

These tests were not originally performed to assess the effect of specimen void ratio on the measured pore pressure responses. The consolidation pressures used in remolding the test specimens were not varied to give different void ratios. In addition, the void ratio of low plasticity silts may not be a function of the vertical effective consolidation pressure (Fleming and Duncan, 1990). The void ratios of these specimens did vary, but only over a narrow range of values. This makes the assessment of the effect of void ratio on pore pressure response difficult. Pore pressure measurements in Q tests on silt specimens with a wider range of void ratios may allow for a more meaningful assessment of the relationship between void ratio and pore pressure response in dilatant silts.

As noted previously, variations in the degree of saturation of the specimens may have influenced the pore pressure response of the specimens. The remolding of the silt slurry in the batch consolidometer resulted in soil that was essentially 100 percent saturated. All of the silt specimens tested in these Q tests had degrees of saturation of 100 percent, based on sample measurements. Even though the degree of saturation was measured to be 100%, it is

possible that small amounts of air could have been present in the specimens that the sample measurements used to determine the degree of saturation would not have detected (Bishop and Eldin, 1950).

In addition, in all of the specimens which produced reasonable pore pressure measurements, negative pore water pressures were measured initially. The measurement of a negative pore water pressure or a pore water pressure less than the surrounding air pressure indicates the presence of surface tension forces within the pore water. Surface tension forces act along a water surface in contact with air within the pores of the soil and result in a difference between the pore air and pore water pressure. The relationship between the pore air and pore water pressures in soil was given in Eq. 4-29 as (Williams, 1967):

$$P_a - P_w = \frac{2 T_s}{r} \cos \theta \quad (4-29)$$

where  $P_a$  = the pore air pressure,  
 $P_w$  = the pore water pressure,  
 $T_s$  = the surface tension of the water,  
 $r$  = the radius of curvature of the air-water interface, and  
 $\theta$  = the angle of intersection between the water surface and the soil grains.

Table 6.1 gives the initial air and pore water pressures in these Q test specimens prior to applying the

cell pressure. In this table, the initial air pressure has been assumed to be equal to atmospheric pressure or a gage pressure of 0 psi. The values of pore water pressure were measured at the midheight of the specimens. Also presented are the values of  $r$  which would give the measured difference between pore air and pore water pressure for each of these tests, determined by Eq. 4-29, assuming  $\theta = 0$ . The measurement of negative pore water pressure in these specimens indicates the presence of air-water interfaces and thus, specimens which were not 100% saturated.

**Table 6.1: Initial air and pore water pressure prior to cell pressure application, along with calculated air-water interface radius,  $r$ , for the Q test specimens in which erratic pore pressure measurements were not observed**

Test	$e$	$P_a$ (psig)	$P_w$ (psig)	$P_a - P_w$ (psi)	$r$ (in)
UU-3	0.537	0	-1.45	1.45	0.000575
UU-6	0.500	0	-0.89	0.89	0.000938
UU-8	0.538	0	-1.00	1.00	0.000834
UU-10	0.541	0	-1.62	1.62	0.000512
UU-11	0.519	0	-0.93	0.93	0.000896
UU-12	0.531	0	-1.12	1.12	0.000740
UU-14	0.539	0	-1.06	1.06	0.000788
UU-15	0.509	0	-1.09	1.09	0.000763
UU-18	0.541	0	-1.41	1.41	0.000589
UU-19	0.524	0	-1.11	1.11	0.000751

Figure 6.9 shows a plot of  $P_a - P_w$  or suction vs. void ratio for the ten UU test specimens listed in Table 6.1. From this plot, it appears that the value of  $P_a - P_w$  or the suction initially in the specimens tended to increase with

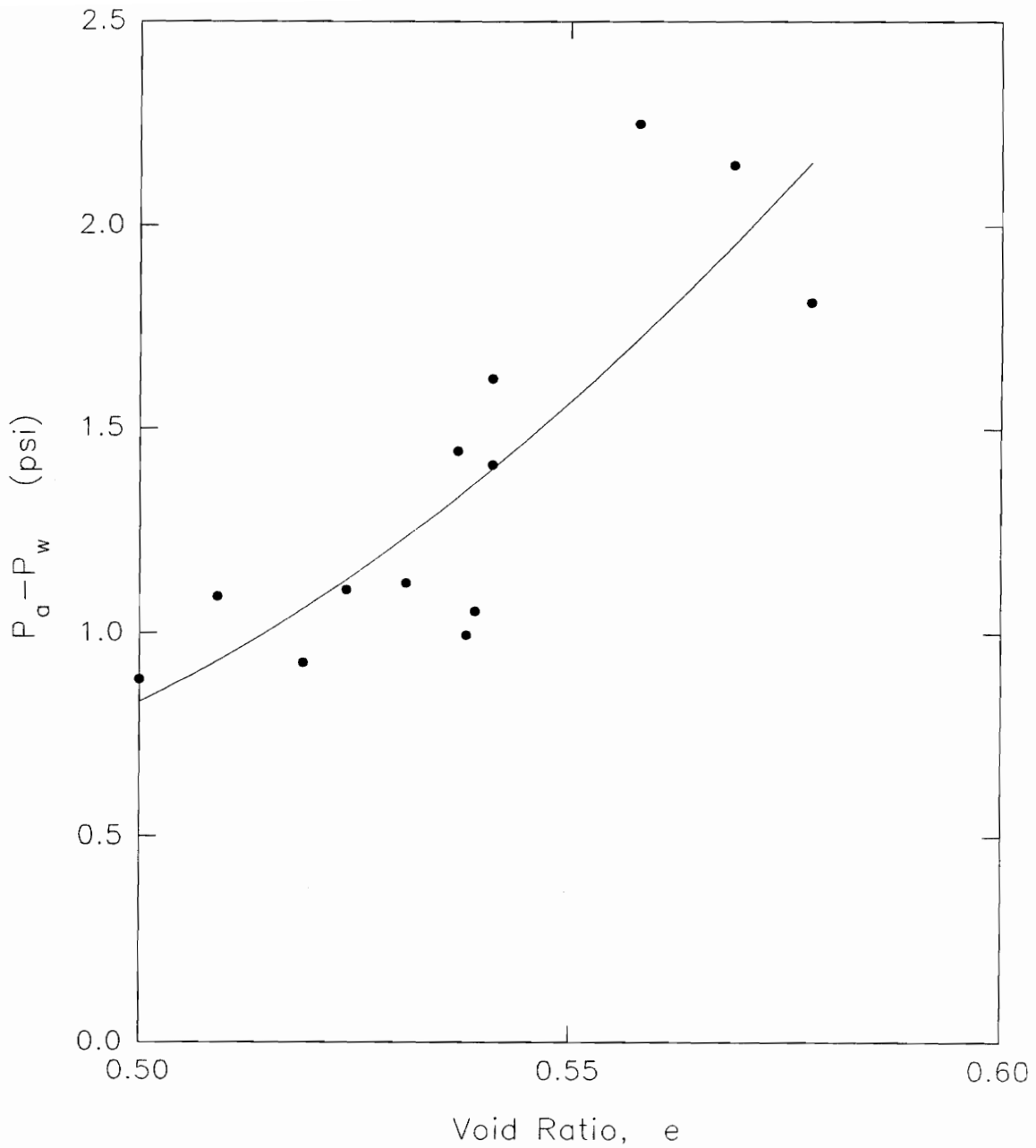


**Figure 6.9.** Variation of  $P_a - P_w$  or suction with specimen void ratio measured prior to application of cell pressure in  $Q$  test specimens with midheight pore pressure monitoring

increasing void ratio. This may indicate that the specimens with higher void ratios had more free air present and lower degrees of saturation initially. As discussed in Section 4.7.1, the value of  $P_a - P_w$  or suction tends to increase as the degree of saturation of the soil decreases (Bishop and Henkel, 1962). The slightly higher void ratios in these specimens may have resulted from more air coming out of solution from the pore water during sample preparation. This would have lead to lower degrees of saturation and higher suctions in the specimens. The range of void ratios in these tests, however, is not felt to be great enough to draw firm conclusions.

The values of  $P_a - P_w$  given for these Q test specimens in Table 6.1, represent the values of residual effective stress,  $\sigma'_r$ , in the soil prior to testing:

$$\sigma'_r = \sigma_3 - u \quad (6-1)$$

where  $\sigma'_r$  = the residual effective stress in the specimen  
 $= P_a - P_w$ ,

$\sigma_3$  = the applied cell pressure:  $\sigma_3 = 0$  psi prior to application of cell pressure, and

$u = P_w$  = the initial value of pore water pressure measured at the midheight of the Q test specimen.

Because  $\sigma_3$  was initially 0 psi, the residual effective stress,  $\sigma'_r = -u$ . The values of residual effective stress for these silt specimens varied from 0.89 to 1.62 psi.

These values are considerably less than the vertical effective consolidation pressure,  $\sigma'_{v0}$ , used in consolidating the slurry to  $K_0$  conditions in the batch consolidometer. During consolidation, the specimens were subjected to a vertical effective consolidation pressure of about 56 psi. The values of residual effective stress in the specimens were only about 1.6 to 2.9% of the initial vertical effective stress used in consolidating the specimens. These values of residual effective stress will be used in further analysis in Section 6.4, where the results from the undrained unloading tests will be used to apply the perfect sampling approach of Ladd and Lambe (1963) to the LMVD silt.

After increasing the cell pressure on a given specimen, the pore air and pore water pressures will have increased. The pore air pressure will be assumed to be equal to the applied cell pressure, although this may not be totally correct. Pore air pressures were not measured within the specimens. The cell pressure applied to the specimens was measured using a calibration quality pressure gage, so that the values of cell pressure applied are felt to be accurate. Table 6.2 presents the assumed pore air pressures and measured pore water pressures in the Q test specimens, after applying the cell pressure to the specimens but prior to

shear. Also given are the values of interface radius,  $r$ , calculated for the given values of air and water pressure.

**Table 6.2: Initial air and pore water pressure and air-water interface radius,  $r$ , after application of cell pressure for the Q test specimens in which erratic pore pressure measurements were not observed**

Test	$\sigma_3$ (psig)	$P_a$ (psig)	$P_w$ (psig)	$P_a - P_w$ (psi)	$r$ (in)
UU-3	20	20	18.28	1.72	0.000482
UU-6	20	20	19.43	0.57	0.001447
UU-8	10	10	8.92	1.08	0.000770
UU-10	0	0	-1.62	1.62	0.000513
UU-11	0	0	-0.93	0.93	0.000896
UU-12	0	0	-1.12	1.12	0.000740
UU-14	10	10	8.75	1.25	0.000663
UU-15	10	10	9.01	0.99	0.000838
UU-18	20	20	18.49	1.51	0.000549
UU-19	20	20	18.63	1.37	0.000606

As can be seen from the values of  $r$  given in Tables 6.1 and 6.2, an air bubble or air-water interface with a very small radius is necessary to yield the negative pore water pressures measured in the Q test specimens. These values of interface radius, however, are up to two orders of magnitude larger than values determined using the approximate diameter of capillary tubes in soils of  $\frac{1}{5}D_{10}$ , suggested for cohesionless soils by Sowers (1979). For the LMVD silt used in these tests,  $D_{10}$  from Figure 5.2 varied from 0.0015 to 0.005 mm (0.000059 to 0.00020 in). A capillary tube diameter of  $\frac{1}{5}D_{10}$  ranges from 0.00001 to 0.00004 in. This would give an interface radius,  $r$ , ranging from  $6 \times 10^{-6}$  in.

to  $2 \times 10^{-5}$  in. The approximate capillary tube radius of  $\frac{1}{5}D_{10}$  does not account for density variations within the soil. The capillary tube diameter can vary with density and pore size, as well as soil grain size. In addition to these factors, the air-water interface radius,  $r$ , can vary due to the degree of saturation of the soil and the size of trapped air bubbles.

Although the remolded silt specimens used in these tests were consolidated from a slurry with a high initial water content, the trimming process resulted in the cylindrical surface of the triaxial specimens being exposed to the atmosphere. On this surface, numerous menisci could have developed in the soil pores at the interface between the soil pore water and atmospheric air (Lambe and Whitman, 1969; Sowers, 1979).

Variations from test specimen to test specimen in factors such as the temperature and relative humidity of the air surrounding the trimmed specimens, as well as the time between completion of trimming and placing the rubber membrane around the specimen in the triaxial cell, could have lead to different amounts of evaporation from the exposed pore water surface. This would have resulted in air-water interfaces of different radii and different negative pore water pressures within the different

specimens. Variations in the level of specimen disturbance may have altered the soil structure, thus influencing the initial pore water pressures and the radii of the air-water interfaces.

It is easy to visualize that air-water interfaces could exist on the exterior cylindrical surface of a triaxial specimen after trimming but prior to placing the membrane around the specimen. Placing the membrane around the specimen will undoubtedly trap some air. Bishop and Henkel (1962) stated that the volume of air typically trapped between the membrane and specimen is about 0.2% of the specimen volume. For 1.4-inch diameter by 3-inch high specimens, this results in a volume of trapped air on the order of  $0.009 \text{ in}^3$ . It could very well be that this small volume of air trapped between the specimen and the rubber membrane provides the nuclei necessary for air to come out of solution from the pore water of saturated, dilatant silt specimens as the pore pressure decreases during undrained shear.

Initially the specimens may have had air bubbles of similar size trapped between the surface of the specimen and the membrane. For the tests which were performed at cell pressures of 10 and 20 psi, the applied cell pressure would have decreased the size of the bubbles and forced some of

the free air into solution. This would have also decreased the void ratio and increased the degree of saturation of the specimens tested at 10 psi and 20 psi over those tested as unconfined compression tests. This may then have resulted in higher quality pore pressure measurements for the tests performed at higher cell pressures.

In these Q tests, the pore pressure measuring needle was inserted through the rubber membrane and into the specimen. The needle-membrane interface was sealed with rubber cement. The cell pressure was then increased and the pore pressure showed some change over time. After applying the cell pressure and waiting until little to no change in pore pressure was observed, the specimen was sheared undrained at a strain rate of about 1%/min. The variation in pore pressure which occurred after applying the cell pressure could have been due to pore pressure equalization effects within the sample. It could also be the result of the minute trapped air pockets compressing and air going into solution due to the increase in cell pressure. When all or most of the air had gone into solution to reestablish equilibrium due to the applied cell pressure, the noticeable variation in measured pore pressure ceased and the Q test was performed.

It is also worth noting that for a number of the tests shown in Figure 6.2, the plots of change in pore pressure vs. axial strain show a change in the slope of the curves at some point during the tests. At low values of axial strain, the pore pressure tended to decrease more rapidly than it did at higher strains. Throughout most of the tests, however, to strains greater than 25 percent, the specimens generally appear to have continued to experience a decrease in pore water pressure during the tests.

The change in slope of the pore pressure-strain curves can also be related to the deviator stress-strain behavior of the samples. At the start of a test, the more rapid decrease in pore water pressure resulted in increased strain-hardening so that the deviator stress increased more rapidly with increasing strain. As the tests progressed, however, the smaller decreases in pore water pressure lead to a decrease in the rate of increase of the deviator stress with increasing strain.

Several of the tests, after experiencing a decrease in pore water pressure, underwent a slight but gradual increase in pore water pressure. Tests UU-3, UU-8, UU-10, and UU-12 in Figure 6.2 show this behavior.

It is not certain what this increase in pore water pressure indicates. It could possibly be the result of a

failure plane forming in the specimen and the silt particles along that plane moving into a more compact orientation, yielding an increase in pore pressure. Because this increase in pore pressure was not observed in all tests in which failure planes developed, however, this does not seem like a consistent explanation.

Another possibility is that in these tests, cavitation occurred or air came out of solution and formed bubbles within the specimens adjacent to or within the pore water pressure monitoring system. If bubbles formed, the pore water pressures measured by the transducer may have been affected, giving the observed increases in measured pore water pressure.

#### **6.1.2 Estimation of Final Degree of Saturation of Q Test Specimens**

For the Q tests where reasonable pore pressure measurements occurred, the assumed initial pore air pressure, the initial and final measured pore water pressures, and the maximum change in pore water pressure measured during the tests are presented in Table 6.3. The value of atmospheric pressure has been added to the measured gage pressures to give absolute pressures.

According to Bair (1992), standard atmospheric pressure at sea level is equal to 29.92 inches of mercury or 14.7

psia. Atmospheric pressure decreases at a rate of about 1 inch of mercury for every 1000 ft. increase in altitude. The elevation of Blacksburg, Virginia is 2080 ft above sea level (The United States Dictionary of Places, 1988). At this elevation, atmospheric pressure would therefore be equal to 13.7 psia.

**Table 6.3: Initial pore air pressure, initial and final pore water pressures, and maximum change in pore water pressure measured in Q tests in which erratic pore pressure measurements were not observed ( $P_a=13.7$  psi at Virginia Tech)**

Test	$\sigma_3$ (psig)	Initial Pore Air Pressure, $P_{ai}$ (psia)	Initial Pore Water Pressure, $P_{wi}$ (psia)	Final Pore Water Pressure, $P_{wf}$ (psia)	$\Delta u_w$ (psia)
UU-3	20	33.7	31.98	15.37	-16.61
UU-6	20	33.7	33.13	16.48	-16.65
UU-8	10	23.7	22.62	16.38	-6.24
UU-10	0	13.7	12.08	4.89	-7.19
UU-11	0	13.7	12.77	9.73	-3.04
UU-12	0	13.7	12.58	7.59	-4.99
UU-14	10	23.7	22.45	12.06	-10.39
UU-15	10	23.7	22.71	14.50	-8.21
UU-18	20	33.7	32.19	23.63	-8.56
UU-19	20	33.7	32.33	21.00	-11.33

For these Q test specimens where a decrease in pore water pressure took place, Eq. 4-41, modified from Lowe and Johnson (1960), can be used to estimate the final degree of saturation of the specimens:

$$S_f = \frac{P_f}{H \Delta u_w + P_f} \quad (4-41)$$

where  $S_f$  = the final degree of saturation of the Q test specimen after air came out of solution from the pore water due to a reduction in pressure,

$P_f$  = the final pore air pressure of the free air in the voids of the soil (assumed to be absolute),

$H$  = the coefficient of solubility of air in water = 0.02 at 20°C, and

$\Delta u_w$  = the change in pore water pressure measured during the Q test.

In using this equation, several assumptions must be made. First, the equation assumes that the specimen was initially fully saturated prior to the reduction in pore pressure. This however, was not the case in these tests because negative pore water pressures existed in the specimens initially, indicating less than full saturation. The specimens did, however, have high initial degrees of saturation and the assumption that they were initially fully saturated seems to be a reasonable approximation.

A second assumption involves the value of the final pore air pressure in each specimen. The pore water pressures were measured during the tests but pore air pressures were not. Two options exist for estimating values of the final pore air pressure. Either the final pore air pressure can be assumed to be equal to the final pore water pressure, or it can be assumed to be greater than the final pore water pressure by the same amount that the initial pore

air pressure was greater than the initial pore water pressure. Because the second possibility is felt to be a more realistic assumption of the actual conditions in the soil, it will be used here in this analysis.

A third assumption that must be made is that the soil pore water was saturated with dissolved air at the initial pore air pressure. This may be a reasonable assumption for the tests performed as unconfined compression tests but it may be unrealistic for the tests performed at cell pressures of 10 and 20 psi. It is uncertain whether the pore water would be saturated with dissolved air at the higher cell pressures. The decrease in pore water pressure during undrained shear may have to negate the positive pore pressure resulting from the applied cell pressure before any gases dissolved in the pore water will come out of solution.

A fourth assumption is that the entire volume of soil pore water was subjected to the pore pressure reduction measured at the midheight of the specimen during the test. This assumes that full equalization of pore water pressure had occurred within the specimens during the tests. This is unlikely, however, because shearing the specimens at a strain rate of 1%/min in a Q test is considerably faster than the strain rate used in CU tests, in which 95 percent equalization of pore pressure is assumed to take place. The

pore pressure reductions measured at the midheight of the specimens near the failure plane, would likely be the largest pore pressure reduction within the sample. Applying this pore pressure reduction to the entire volume of soil pore water would therefore yield a maximum amount of air which would come out of solution from the pore water.

The final assumption is that enough time was available for the air dissolved in the pore water to come out of solution during a Q test, due to the measured reduction in pressure.

Based on these assumptions, the final degrees of saturation,  $S_f$ , of the Q test specimens listed in Table 6.3 have been estimated using Eq. 4-41 and are presented in Table 6.4.

As can be seen from Table 6.4, the reductions in pore water pressure measured in the saturated silt Q test specimens during shear could have resulted in the specimens experiencing a decrease in their degree of saturation of up to 2.2 percent. Specimen UU-10 could have gone from being 100% saturated initially, down to a minimum of 97.8 percent. Even though this specimen had the lowest estimated final degree of saturation of the ten specimens, it did not experience the largest decrease in pore water pressure,  $\Delta u_w$ . The estimated final degree of saturation of this

specimen was lowest because the specimen had the lowest value of final air pressure,  $P_f$ , of the ten specimens.

**Table 6.4: Final degree of saturation of Q test specimens in which erratic pore pressure measurements were not observed, estimated using Eq. 4-41 ( $S_i=100\%$ ,  $H=0.02$  @  $20^\circ\text{C}$ )**

Test	$P_{ai}-P_{wi}$ (psi)	Final Pore Water Pressure, $P_{wf}$ (psia)	Final Pore Air Pressure, $P_f$ (psia)	Decrease in Pore Water Pressure, $\Delta u_w$ (psi)	$S_f$ (%)
UU-3	1.73	15.37	17.09	16.61	98.1
UU-6	0.57	16.48	17.05	16.95	98.1
UU-8	1.08	16.38	17.46	6.24	99.3
UU-10	1.62	4.89	6.51	7.19	97.8
UU-11	0.93	9.73	10.66	3.04	99.4
UU-12	1.12	7.59	8.71	4.99	98.9
UU-14	1.25	12.06	13.31	10.39	98.5
UU-15	0.99	14.50	15.49	8.21	99.0
UU-18	1.51	23.63	25.14	8.56	99.3
UU-19	1.37	21.00	22.37	11.33	99.0

It is stressed that the values of final degree of saturation given in Table 6.4 are estimates based on several simplifying assumptions. It is not certain whether the assumptions made are entirely reasonable. The values given in Table 6.4, however, are felt to give a good idea of the amount of desaturation which could have possibly occurred during the Q tests, and should be considered upper bound values on the magnitude of the desaturation possible.

Another example will now be given of the amount of desaturation which could possibly occur in a saturated silt

Q test specimen using the equations presented in Section 4.5. These equations allow for the estimation of the amount of air which could come out of solution from the pore water of a soil due to a reduction in pressure. In this case, however, the initial degree of saturation of the Q test specimen will be considered in the analysis.

As an example of the amount of air which could potentially come out of solution from the pore water of a saturated silt specimen due to a reduction in pore pressure, consider Q test specimen UU-10 which was tested in an unconfined compression test. In this test the cell pressure was equal to atmospheric pressure, or 13.7 psia.

The Q test specimen UU-10 had a void ratio,  $e$ , of 0.541 and a total specimen volume,  $V_T$ , of 5.090 in<sup>3</sup>. For an assumed laboratory temperature of 20°C, the coefficient of solubility of air in water,  $H$ , is 0.02. In this test the initial pore air pressure has been assumed to be equal to atmospheric pressure,  $P_{ai} = 13.7$  psia. The initial and final pore water pressures were measured with a midheight pore pressure monitoring probe and transducer to be  $P_{wi} = 12.08$  psia and  $P_{wf} = 4.89$  psia.

Because the initial pore water pressure was less than the initial pore air pressure, the sample was not fully saturated at the start of the test as had been indicated by

the measurement of specimen dimensions, specific gravity of solids and specimen water content. The specimen however, can be assumed to have had a very high initial degree of saturation. Using Eq. 4-29 with  $P_a = 13.7$  psia,  $P_w = 12.08$  psia and  $T_g = 0.0004154$  lbf/in; the initial radius of curvature,  $r$ , of air bubbles in the voids of the soil was calculated in Table 6.2 to be 0.000513 inches or 0.01303 mm.

According to Schuurman (1966), for soils with a degree of saturation greater than 85 percent, the air present in the pores of the soil can be assumed to exist as individual bubbles located throughout the pore water of the soil. If the soil is less than 85 percent saturated, the air present in the pores of the soil is believed to exist in larger pockets of air located randomly throughout the soil pores.

Hilf (1956) and Schuurman (1966) assumed that because pore sizes are small in most soils, the radius of individual air bubbles,  $r$ , can be assumed to be the same throughout the entire sample. Under this condition, the difference between the pore air and pore water pressures will also be the same everywhere in the soil. The small variations which may occur in bubble radius may only be significant when the bubbles reach the stage of collapse (Schuurman, 1966).

For Q test specimen UU-10, the radius of the air bubbles initially present in the pore water was estimated to

be 0.000513 inches. The number of bubbles and the corresponding total volume of undissolved air is more difficult to estimate. If the degree of saturation determined by specimen dimensions, specific gravity of solids and specimen water content had been less than 100 percent, the volume of free air present in bubbles in the pore water could have been easily estimated. Because the degree of saturation was found to be 100 percent however, this approach will not work.

Considering that the silt specimen was consolidated from a slurry with a high water content and then trimmed into a triaxial specimen, it is plausible that few air bubbles existed in the pores within the interior of the specimen and that almost all of the air-water interfaces were located at the surface of the triaxial specimen exposed to atmospheric air. The total surface area of this triaxial specimen, neglecting the two ends of the cylinder, was equal to 14.32 in<sup>2</sup>. Knowing that the void ratio of the specimen was 0.541, its porosity was equal to 0.351.

Assuming that 35 percent of the surface area of the cylinder consisted of soil pores exposed to the atmosphere, the area of the exposed pores on the surface of the cylinder was equal to 5.01 in<sup>2</sup>. If it is assumed that the air pockets present on the cylindrical surface existed at each

pore in the form of a hemisphere of radius  $r = 0.000513$  inches, the cylindrical area exposed can be divided by the area of a circle with radius  $r$  to give 5,800,000 hemispheres of radius  $r = 0.000513$  inches. The total volume of free air initially in the specimen can therefore be estimated as the total volume of 5,800,000 hemispheres of radius  $r = 0.000513$  inches:

$$V_{gi} = 5,800,000 \frac{2}{3} \pi (0.000513 \text{ in})^3 = 0.00164 \text{ in}^3 \quad (6-2)$$

This value is smaller than 0.2% of the total specimen volume, or  $0.01 \text{ in}^3$ , suggested by Bishop and Henkel (1962). Using the value of free air calculated by Eq. 6-2, the total volume of the triaxial specimen could possibly have been  $0.00164 \text{ in}^3$  larger than the measured value of  $5.090 \text{ in}^3$ , or  $5.09164 \text{ in}^3$ . Assuming that the volume of solids,  $3.304 \text{ in}^3$ , is correct, the volume of water,  $V_w$ , and volume of voids,  $V_v$ , are:

$$V_w = 5.090 \text{ in}^3 - 3.304 \text{ in}^3 = 1.786 \text{ in}^3 \quad (6-3)$$

$$V_v = 5.09164 \text{ in}^3 - 3.304 \text{ in}^3 = 1.78764 \text{ in}^3 \quad (6-4)$$

The initial degree of saturation,  $S_i$ , of the specimen can then be calculated as:

$$S_i = \frac{V_{wi}}{V_{vi}} 100\% = \left( \frac{1.786 \text{ in}^3}{1.78764 \text{ in}^3} \right) 100\% = 99.9\% \quad (6-5)$$

Thus, specimen UU-10 may have possibly had an initial degree of saturation,  $S_i$ , of 99.9 percent, rather than the value of 100 percent, as determined by laboratory measurements.

If the volume of trapped air was equal to 0.2% of the specimen volume, or  $0.01 \text{ in}^3$ , the total specimen volume may have been  $5.100 \text{ in}^3$ . Assuming the same volume of solids as above, the initial degree of saturation of the specimen may have been as low as:

$$S_i = \frac{5.090 \text{ in}^3 - 3.304 \text{ in}^3}{5.100 \text{ in}^3 - 3.304 \text{ in}^3} \times 100\% = 99.4\% \quad (6-6)$$

These two estimates of the initial degree of saturation indicate that the specimen was probably slightly less than fully saturated. It did have a very high degree of saturation and the slight amount of air possibly in the specimen initially, would have been very difficult to detect using normal measurement techniques.

The final pore air pressure is much more difficult to estimate. Because the test was performed as an unconfined compression test, the initial pore air pressure can be assumed to be equal to atmospheric pressure, 13.7 psia. The pore water pressure measured with the midheight pore water pressure probe and transducer decreased from 12.08 psia initially to a minimum of 4.89 psia.

As the pore water pressure decreased during the test, the pore air pressure would also have decreased, although not necessarily at the same rate. It can be seen from Eq. 4-29, that if  $\theta$  is assumed to be 0, the difference between the pore air and pore water pressure,  $P_a - P_w$ , would still equal  $\frac{2 T_s}{r}$  throughout the pressure reduction and the pore air pressure would be greater than the pore water pressure by this difference. The value of surface tension,  $T_s$ , is essentially independent of pressure (Schuurman, 1966) and can be assumed to be constant. The difference between the pore air pressure and pore water pressure therefore is dependent only on the radius of curvature,  $r$ , of the air-water interfaces.

When the pore water pressure decreases within a silt specimen during undrained shear, the pore water tends to be pulled toward the failure plane within the triaxial specimen and away from the cylindrical surface of the specimen. As this occurs, pores of different dimensions may cause the radius of curvature,  $r$ , of air-water interfaces to change and therefore, the difference between the pore air and pore water pressure would also change.

In a smaller pore, the radius of curvature of the air-water interface would decrease and the difference between pore air and pore water pressures would increase. In a

larger pore, the radius of curvature of the air-water interface would increase and the difference in the pore air and pore water pressures would decrease. As the silt tends to dilate due to the soil grains rising up over each other, some pores would be expected to increase in size.

Furthermore, as the pore water pressure decreases and air comes out of solution in accordance with Henry's law, new air bubbles may form and the existing bubbles could grow in size such that their radii would increase as well. This tends to imply that the difference between the final pore air and pore water pressures would be less than the difference between the initial pore air and pore water pressures. This however, seems questionable when considering that the difference between pore air and pore water pressure increases as the degree of saturation of the soil decreases, as was shown in Figure 4.2 (Bishop and Henkel, 1962).

The determination of the radius of curvature of the pore air bubbles at the lower pore water pressure is difficult and therefore estimation of the final pore air pressure can not be easily accomplished using this procedure. A better method was thought to be direct measurement of both the pore air and pore water pressures in Q test specimens during shear, to observe directly the

difference between the two pressures. This was attempted in this research, but was not successful because in soils with a high degree of saturation, accurate pore air pressure measurements tend to be very difficult (Bishop, 1960; Bishop and Henkel, 1962).

As a simplifying assumption, the radius of curvature of the air-water interface has been assumed to be constant throughout the test. In this case, the difference between the final pore air pressure and pore water pressure will be equal to the difference between the initial values. The final pore air pressure in specimen UU-10 would therefore be:

$$P_{gf} = 4.89\text{psia} + (13.7\text{psia} - 12.08\text{psia}) = 6.51\text{ psia} \quad (6-7)$$

Using the above information, Eq. 4-25 can be used to determine the volume of air which could potentially come out of solution from the pore water of Q test specimen UU-10:

$$V_{gf} = \frac{T_f P_{gi}}{T_i P_{gf}} \left( V_{gi} + H_i V_T \left( \frac{e}{1+e} \right) \right) - H_f V_T \left( \frac{e}{1+e} \right) \quad (4-25)$$

Assuming that the initial volume of free gas,  $V_{gi}$ , was  $0.00164\text{ in}^3$  and that the laboratory temperature remained constant throughout the duration of the Q test ( $T_i = T_f =$

20°C;  $H_i = H_f = 0.02$ ), the final volume of free gas in the specimen can be calculated as:

$$V_{gf} = \left( \frac{20+273}{20+273} \right) \frac{13.7}{6.51} \left( 0.00164 + 0.02(5.09164) \left( \frac{0.541}{1+0.541} \right) \right) - 0.02(5.09164) \left( \frac{0.541}{1+0.541} \right) = 0.04294 \text{ in}^3 \quad (6-8)$$

The maximum potential change in volume of triaxial specimen UU-10,  $\Delta V_g$ , due to air coming out of solution during shear, is therefore equal to  $V_{gf} - V_{gi}$ :

$$\Delta V_g = 0.04294 \text{ in}^3 - 0.00164 \text{ in}^3 = 0.0413 \text{ in}^3 \quad (6-9)$$

This indicates that the volume of the triaxial specimen could have potentially increased by a maximum of  $0.0413 \text{ in}^3$  or from a total volume of  $5.09164 \text{ in}^3$  to  $5.13130 \text{ in}^3$ . From this, the possible final degree of saturation,  $S_f$ , can be calculated. The volume of water,  $V_w$ , is still the same as at the start of the test,  $1.786 \text{ in}^3$ . The volume of voids,  $V_v$ , however, has increased by  $0.0413 \text{ in}^3$  to  $1.82730 \text{ in}^3$ . The final degree of saturation,  $S_f$ , can then be calculated as:

$$S_f = \frac{V_{wf}}{V_{vf}} 100\% = \left( \frac{1.786 \text{ in}^3}{1.82730 \text{ in}^3} \right) 100\% = 97.74\% \quad (6-10)$$

Comparing this final degree of saturation with that given for specimen UU-10 in Table 6.4 ( $S_f=97.8\%$ ), the two values are found to be in fairly close agreement. This shows that for a specimen with a very high initial degree of

saturation, there is little difference between the estimated final degrees of saturation using the two different methods. Including the small volume of air that might possibly be present in the voids of the soil initially, did not result in a value of final degree of saturation substantially different from that estimated assuming the specimen was truly 100 percent saturated initially.

Although the air that could possibly come out of solution only results in an increase in sample volume of 0.81%, the sample void ratio increases by 2.2% from 0.541 to 0.553 and the degree of saturation falls from 99.9 percent to 97.7 percent. The increase in sample volume and void ratio, and the corresponding decrease in the degree of saturation of the specimen resulting from the formation and growth of air bubbles within the voids of the soil, especially near the zone of shear, could have a significant influence on the stress-strain behavior of the soil. The change from an undrained to a partially drained condition could have a significant effect on sample strength and behavior.

The results of test UU-10 can be further analyzed considering the gradual nature of the pore pressure reduction during undrained shear. This analysis was presented in Section 4.7.3 and follows the work of Esrig and

Kirby (1977). It was also discussed by Roscoe, Schofield and Wroth (1958).

The deviator stress-strain and pore pressure-strain curves for specimen UU-10 are reproduced in Figure 6.10. Because the silt specimen had a tendency to dilate during undrained shear, its pore water pressure decreased while its deviator stress increased to a peak value and then began to decrease toward a residual strength value. As the sample was sheared, the pore pressure reduction caused the minor principal effective stress,  $\sigma'_3$ , to increase, as expected for a dilatant soil during undrained shear. The pore pressure reduction resulting from the attempted dilation, however, could have allowed air to come out of solution from the pore water and form bubbles within the voids of the specimen.

The formation of air bubbles would have increased the volume and void ratio of the specimen. This can be illustrated in a plot of  $e$  vs.  $\log \sigma'_3$ , as shown in Figure 6.11. In this figure, the initial conditions for specimen UU-10 are given by point 1, where  $e_i = 0.541$  and  $\sigma'_{3i} = 1.62$  psi. If the specimen maintained a constant volume as the pore water pressure decreased,  $\sigma'_3$  would have increased along the line from point 1 toward point 2. Point 2 could possibly represent a point on an assumed critical state line for the soil. If dissolved air came out of solution from

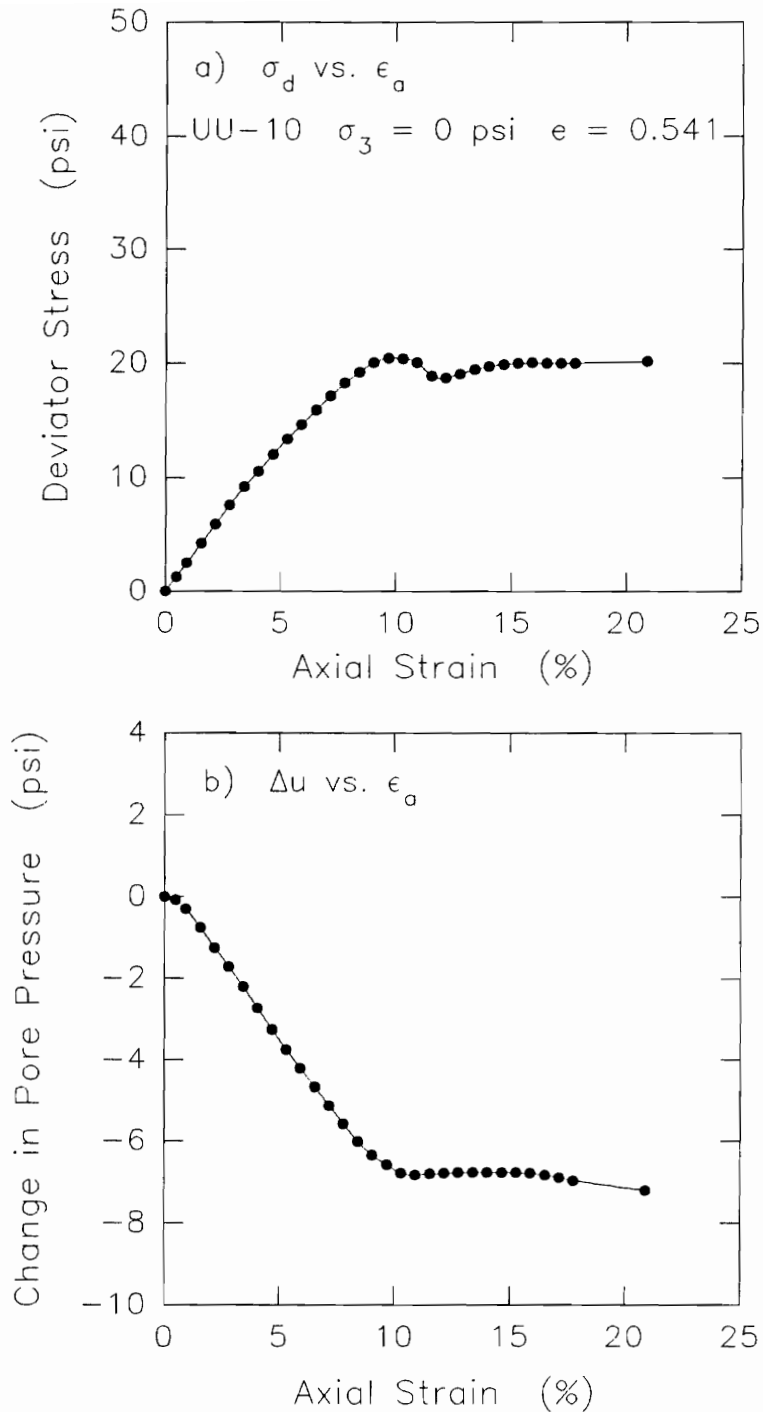


**Figure 6.10. Deviator stress vs. axial strain and change in pore pressure vs. axial strain relationships measured in Q test UU-10 performed as an unconfined compression test, on remolded old LMVD silt**

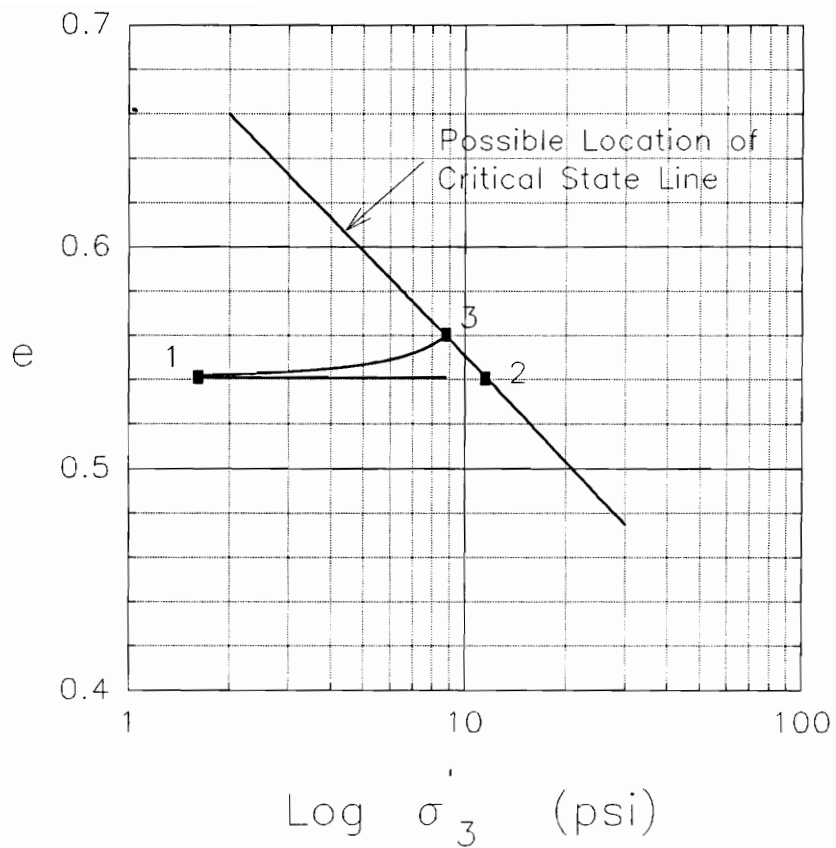


**Figure 6.11. Void ratio vs. minor principal effective stress for Q test specimen UU-10 (Note: location of critical state line is assumed and is presented for illustrative purposes only. The actual location of the critical state line was not determined for the old LMVD silt in this research.)**

the pore water as a result of the decreasing pore water pressure, the void ratio,  $e$ , of the specimen would have increased as  $\sigma'_3$  increased. In this case, the specimen may have followed the path from point 1 to point 3. If at point 3, the specimen had reached the assumed critical state line for the soil, the value of  $\sigma'_{3crit}$  would have been lower and the value of  $e$  would have been higher, than if no dissolved air had come out of solution from the pore water.

It should be noted that the estimated maximum volume of air which could come out of solution from the pore water of Q test specimen UU-10,  $0.0413 \text{ in}^3$ , due to the reduction in pore water pressure measured during the test, was based on several assumptions. These included that the soil pore water was saturated with dissolved air initially, the entire volume of pore water was subjected to the pore water pressure reduction measured at the midheight of the specimen and that the system of air and water was in equilibrium with Henry's law at both the initial and final pressures. Although it can be reasonably assumed that the system was in equilibrium at the initial pressure (atmospheric) prior to running the test, a question arises as to whether or not equilibrium conditions were reached in the system at the final pressure.

With the duration of the Q test being only about 20 minutes and the pore pressure within the specimen decreasing gradually throughout the 20 minute period to the final value used in the above example, the time available may not have been sufficient for equilibrium conditions to be reached at the lower pressure. As will be discussed in Section 6.1.3, the rate at which air can come out of solution from the pore water of a saturated silt Q test specimen may or may not be rapid enough for equilibrium to be reached in 20 minutes for the given change in pressure and its gradual rather than instantaneous application. The major variable involved is the area across which the air can diffuse to come out of solution. Thus, the volume of air which actually came out of solution may have been less than 0.0413 in<sup>3</sup> and the corresponding increases in sample volume and void ratio and decrease in degree of saturation would also have been less. The above example does however, provide a relative measure of the amount of air which may possibly come out of solution from the pore water of a saturated silt Q test specimen during undrained shear and may be considered an upper bound in this situation.

### **6.1.3 Estimation of the Rate at which Air Comes Out of Solution from Soil Pore Water**

In Section 4.8, a review of the literature on the rate at which air goes into and comes out of solution in water

was presented. The following equation was given by Dorsey (1940) for determining the change in dissolved air content of a liquid over time, due to a reduction in pressure:

$$(c - c_0) = (c_\infty - c_0)(1 - e^{-\beta \frac{At}{V_w}}) \quad (4-60)$$

where

- $c$  = concentration of the gas in water at time  $t$ ,
- $c_0$  = concentration of the gas in water at time  $t = 0$  (equilibrium dissolved gas concentration at higher pressure),
- $c_\infty$  = concentration of the gas in water at time  $t = \infty$  (equilibrium dissolved gas concentration at lower pressure),
- $e$  = exponential function,
- $\beta$  = the exit coefficient from water of a given gas at a given temperature; when the gases are those in atmospheric air,  $\beta = 0.0099(T - 239)$  where  $T = ^\circ\text{C} + 273$ , and  $\beta$  is in units of cm/minute,
- $A$  = the surface area across which the gas comes out of solution from the water,  $\text{cm}^2$ ,
- $V_w$  = the volume of the water,  $\text{cm}^3$ , and
- $t$  = time in minutes.

This equation presented by Dorsey (1940), based on the experiments of Adeney and Becker (1919), presents several problems in being applied to saturated silt specimens. First is the difficulty in determining the initial dissolved air content of the pore water. For the remolded silt specimens used in this study, distilled water was used to mix the slurry from which the samples were formed. It can be reasonably assumed that the mixing of the slurry with

distilled water at atmospheric pressure resulted in pore water which was saturated with air at room temperature and atmospheric pressure. The final dissolved air content of the pore water is more difficult to determine. If the pore water is assumed to be initially saturated with air at atmospheric pressure, the final percent saturation that could exist in the pore water can be estimated using Henry's law from the pore pressure reductions measured in the specimens during the Q tests.

Another uncertainty in the applicability of Adeney and Becker's work to the pore water of triaxial specimens is the mixing of the water. In their experiments, the liquid was thoroughly mixed. The water molecules were free to move about within the container due to density variations which developed due to the solution and evolution of air in the water. This allowed portions of the fluid with different levels of saturation to move toward or away from the air-water interface.

It is feasible that the water present in the pores of a soil will be able to move toward or away from the air-water interfaces as dilation occurs along the shear plane and hydraulic gradients are established due to variations in pore pressure throughout the specimen. The actual degree to which mixing of the water will occur is unknown and its

ultimate effect on the rate at which air will come out of solution is uncertain. It would appear that the movement of soil pore water in a Q test specimen and the rate at which dissolved air would come out of solution would be dependent on the permeability of the soil.

The final uncertainty involved in the use of Adeney and Becker's equations is the determination of the surface area, A, across which the gas will diffuse into or out of solution. For a saturated Q test specimen with no air bubbles or free air surface in contact with the pore water, there should be no surface across which air can diffuse and come out of solution.

The review of the literature on cavitation, however, revealed that tiny pockets of trapped gas can exist stably in cracks and crevices on surfaces and solid particles. It is likely that a number of gas pockets of this type could exist in a theoretically saturated silt specimen. Air bubbles may also be trapped between the specimen and rubber membrane. If gas pockets are present in a saturated Q test specimen, they could provide the initial surface area across which the dissolved air could diffuse out of solution. The difficulty comes in determining or estimating the size of this surface area to use in Eq. 4-60.

In addition, as air comes out of solution and enters the existing gas pockets, the gas pockets will grow larger and the surface area across which the air diffuses will change with time. This variation in the area across which diffusion occurs is not considered by Eq. 4-60, even though Adeney and Becker's (1918, 1919) experiments involved a bubble with a surface area which changed as the air in the bubble went into solution. This constant cross sectional area in Eq. 4-60 complicates the problem even more and makes the applicability of Adeney and Becker's work and Dorsey's equation to the problem of air coming out of solution from the pore water of Q test specimens of saturated silt seem questionable.

Neglecting these limitations, an example of the application of Eq. 4-60 has been applied to saturated silt Q test specimen UU-10. In this case the total volume of water in the saturated specimen was 29.27 cm<sup>3</sup>. The initial air-water interface was previously estimated to consist of 5,800,000 hemispheres of radius  $r = 0.000513$  inches. The surface area of these hemispheres is equal to 9.59 in<sup>2</sup> or 61.87 cm<sup>2</sup>. For the change in pore air pressure considered previously in Section 6.1.2, using Henry's law, if the water subjected to an air pressure of  $P_{ai} = 13.7$  psia was initially 100 percent saturated with dissolved air, at the final pore air pressure of  $P_{af} = 6.51$  psia, the equilibrium

air content would be 47.5 percent of the initial dissolved air content ( $P_{af} = 0.475P_{ai}$ ). Considering that the minimum pore pressure was measured at 21 percent axial strain and the test was performed at a strain rate of about 1 percent per minute, at a temperature of 20°C, the decrease in the dissolved air content of the liquid which would have occurred in 21 minutes due to the measured pressure reduction, can be calculated using Eq. 4-40 as follows:

$$(c-100\%) = (47.5\% - 100\%) \left( 1 - e^{-0.0099 (20+273-239) \frac{61.87}{29.27} 21} \right) \quad (6-11)$$

$$c = 100\% - 52.5(1 - e^{-24.66}) = 47.5\% \quad (6-12)$$

This indicates that for the conditions assumed in this analysis, all of the air that could possibly have come out of solution from the pore water, would have done so during the duration of the test.

On the other hand, if the surface area across which gas could diffuse was only 1 cm<sup>2</sup>, the final dissolved air content is calculated to be 83.3 percent of the initial dissolved air content of the pore water. Similarly, if the surface area was only 0.1 cm<sup>2</sup>, the final dissolved air content is calculated to be 98.0 percent of the initial dissolved air content of the pore water. In these last two examples, the pore pressure reduction in test specimen UU-10

would not have resulted in the maximum amount of dissolved gas exiting from solution in the 21 minutes over which the test was performed. This emphasizes the significance in Eq. 4-60 of the area across which air can diffuse to come out of solution. It also highlights the uncertainty involved in determining a reasonable area to use for highly saturated silt specimens.

Again, it should be noted that the actual area through which the air will diffuse will vary as air comes out of solution and the air bubbles grow larger. In addition, the pressure reduction in the pore water occurs gradually over a period of 21 minutes, whereas the example presented above assumes that the entire pressure reduction occurs instantaneously at which point air begins to come out of solution over a 21 minute time period.

Finally, the water in the pores of the soil may or may not be as thoroughly mixed as Adeney and Becker's work assumes. If little to no mixing of the water occurs, the pore water will be much more stationary within the pores of the soil and the equations of Adeney and Becker and Dorsey may not be applicable. If however, mixing of the water occurs due to hydraulic gradients resulting from pore pressure variations throughout the specimen, then the above example provides a reasonable bound on the rate at which air

would come out of solution from the pore water of a saturated silt specimen due to a reduction in pore water pressure. It also emphasizes the influence of the area of the air-water interface across which air can come out of solution on the time for equilibrium conditions to be achieved.

It may very well be that for air coming out of solution from the pore water of a saturated silt specimen, the diffusion process is much more dominant than the streaming effect assumed by Eq. 4-60. The equations of Epstein and Plesset (1950) presented in Section 4.8.1 are based on the diffusion process and as a result, may be more applicable to the growth of air bubbles within the pores of a saturated soil.

The equations of Epstein and Plesset can be applied to Q test UU-10, to estimate the time required for bubbles to grow larger within the specimen. In this test, the initial size of an air bubble in the pores of the soil can be estimated by the radius,  $r$ , given in Table 6.2, as 0.000513 in. Assuming that the pore water was saturated with dissolved air at the initial pore air pressure of 13.7 psia, the approximate reduction in pore air pressure to 6.51 psia would give a degree of oversaturation,  $f$ , of the pore water with dissolved air equal to:

$$f = \frac{13.7 \text{ psia}}{6.51 \text{ psia}} = 2.1 \quad (6-13)$$

Using the equations of Epstein and Plesset (1950) for these conditions, the times required for an existing air bubble with a radius,  $R_0 = 0.000513$  in, to grow in size to radii,  $R = 10R_0$  and  $100R_0$ , are tabulated in Table 6.5.

**Table 6.5:** Approximate times for an existing air bubble with a radius of  $R_0 = 0.000513$  in = 0.01303 cm, to grow to a size of  $10R_0$  and  $100R_0$ , using the equations of Epstein and Plesset (1950) ( $t_A$  = time required neglecting surface tension effects,  $t_g$  = time required including surface tension effects)

Final Size of Bubble	$t_A$ (min)	$t_g$ (min)
$R = 10R_0$	3.2	3.3
$R = 100R_0$	322	323

The times presented in Table 6.5 show that a bubble with an initial radius of 0.000513 in. can grow 10 times as large in less than 3.5 minutes. This is well within the time over which the test was performed. In the 21 minutes over which this specimen was sheared, the bubble could have grown over 10 times larger than it was initially.

The equations of Epstein and Plesset can also be used to estimate the possible increase in bubble size that could have occurred in 21 minutes, due to the pore pressure reduction which was measured in the specimen. By trial and error, it was estimated that the bubble could have grown to

about 25 times its initial radius, or to a radius of about 0.0128 inches.

It is not certain if a bubble growing to a size such as this would have a significant effect on the strength of the soil. It is expected that bubble growth and especially multiple bubble growth, would have some influence on the undrained behavior of the soil, and could be a major source of the erratic behavior observed in Q tests on saturated, dilatant silts. This analysis and the literature on the rate of solubility of air in water tend to support the idea that dissolved gases can exit from solution in water during the time over which a Q test is performed.

The above calculations use the pore pressure reduction measured in Q test UU-10 but do not account for the fact that the water was present and bubble growth would have occurred within the pores of a soil. The equations given by Epstein and Plesset (1950) are for open water. No consideration is given to the water being within the confined spaces of soil pores. It could be that the rate of bubble growth would be affected to some extent by the soil pore size and soil structure.

The work of Black and Lee (1973) indicated that the time for air to go into solution in soil pore water during the back pressure saturation process is quite long. Even

though this process is slightly different because water can flow into the specimen to further increase the degree of saturation as air dissolves, it would be expected that the rate at which air came out of solution would be similarly long. Chace (1975, 1985), in fact, found that the time for air to come out of solution was longer than the time required for air to go into solution in soil pore water. This tends to indicate that the rate at which air comes out of solution from soil pore water may very likely be slower than the rate at which it goes into solution in soil pore water.

The times for air to come out of solution from water or for bubbles to grow larger, due to the confined condition of soil pore water, may be longer than estimated above. For this reason, it is difficult to make any definite conclusions on the rate at which air comes out of solution from soil pore water, as well as the amount of air which came out of solution from the soil pore water during the Q tests performed in this research. It is reasonable, however, to expect that some amount of air will come out of solution due to the reductions in pore pressure which occur in saturated, dilatant silts. Existing bubbles will also tend to grow larger as pore pressures decrease during Q tests on saturated, dilatant silts. The influence of bubble formation and growth within the pores of a saturated,

dilatant soil specimen will be discussed in detail in Section 6.12.

## 6.2 Effect of Sampling on Pore Pressure Changes

As discussed in Section 4.3.1, during sampling of a saturated silt, a reduction in the pore water pressure of the soil will occur as the total stress acting on the soil is reduced and the soil tries to maintain its effective stress (Ladd and Lambe, 1963). According to Skempton (1954), the change in pore water pressure which occurs due to a change in total stress is equal to:

$$\Delta u_w = B\Delta\sigma_3 + \bar{A}_u (\Delta\sigma_1 - \Delta\sigma_3) \quad (6-14)$$

where  $\Delta u_w$  = the change in pore water pressure resulting from a change in total stress,

$B$  = pore pressure parameter relating the change in pore water pressure to the change in cell pressure;  $B$  is approximately equal to 1.0 for a degree of saturation of 100%,

$\Delta\sigma_3$  = the change in minor principal total stress,

$\bar{A}_u$  = the pore pressure parameter relating the change in pore water pressure to the change in deviator stress during unloading, and

$\Delta\sigma_1$  = the change in major principal total stress.

For a saturated soil sample located at some depth below the ground water surface, as shown in Figure 6.12, the in-situ total stresses acting on the soil will be reduced to zero when the soil is sampled and brought to the ground

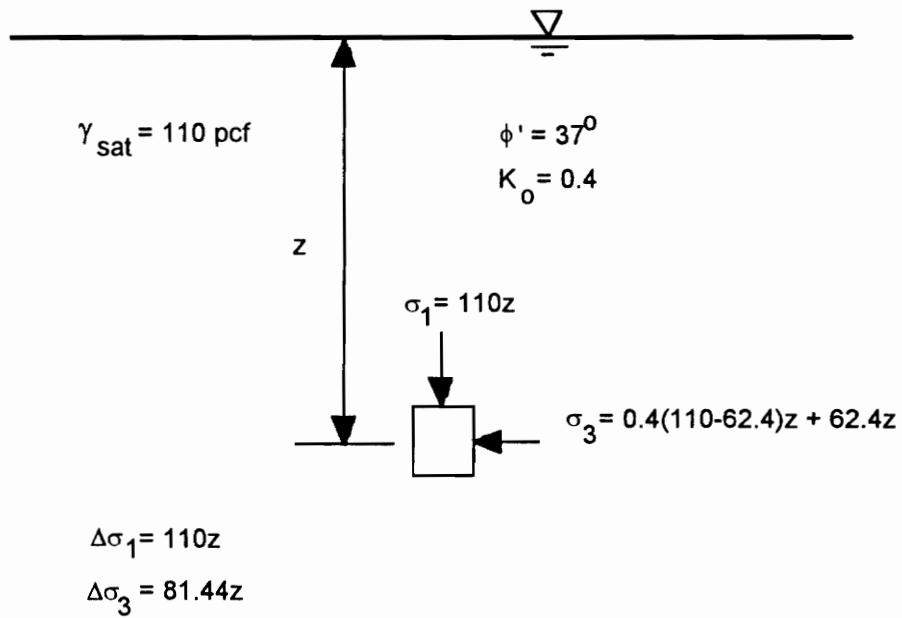


Figure 6.12. Soil conditions considered in sampling analysis of saturated silts

surface. The values of  $\bar{A}_u$  determined in the experimental study and presented in Table 5.9, along with the soil conditions shown in Figure 6.12, can be used to estimate the change in pore water pressure resulting from a soil being sampled from various depths. Table 6.6 presents the calculated values of change in pore water pressure due to sampling, for the values of  $\bar{A}_u$  reported in Section 5.5.

**Table 6.6: Change in pore water pressure associated with sampling, calculated using the values of  $\bar{A}_u$  determined in the undrained unloading tests, for the conditions shown in Figure 6.12**

Depth (ft)	$\Delta u_w$ for $\bar{A}_u=0$ (psi)	$\Delta u_w$ for $\bar{A}_u=-0.1$ (psi)	$\Delta u_w$ for $\bar{A}_u=-0.2$ (psi)
5	2.83	2.73	2.63
10	5.65	5.46	5.26
15	8.48	8.19	7.89
20	11.31	10.91	10.52
30	16.97	16.37	15.78
40	22.62	21.83	21.04
50	28.28	27.29	26.29

Assuming that the pore water was initially saturated with dissolved air at the in-situ hydrostatic pore water pressure, the reduction in pore pressure due to sampling would result in air coming out of solution from the pore water to reestablish equilibrium, in accordance with Henry's law. For the decreases in pore water pressure and pore air pressure which occur during sampling, the final degree of saturation of the soil can be estimated using Eq. 4-41:

$$S_f = \frac{P_f}{H \Delta u_w + P_f} \quad (4-41)$$

Values of the final degree of saturation for the reductions in pore water pressure given in Table 6.6, have been estimated using Eq. 4-41 and are presented in Table 6.7.

**Table 6.7: Possible final degree of saturation of soil sampled from various depths below the ground water surface estimated using Eq. 4-41, for the pore pressure reductions presented in Table 6.6 (H=0.02, P<sub>f</sub>=14.7 psi)**

Depth (ft)	$S_f$ for $\bar{A}_u=0$ (%)	$S_f$ for $\bar{A}_u=-0.1$ (%)	$S_f$ for $\bar{A}_u=-0.2$ (%)
5	99.6	99.6	99.6
10	99.2	99.3	99.3
15	98.9	99.0	98.9
20	98.5	98.5	98.6
30	97.7	97.8	97.9
40	97.0	97.1	97.2
50	96.3	96.4	96.5

As can be seen from the results given in Table 6.7, the pore pressure reductions which could occur during the sampling of a saturated silt from depths of up to 50 feet below the ground water surface, could possibly cause the degree of saturation of the soil to be reduced by up to 3.7 percent. Depending on the conditions of the problem, the final degree of saturation of the soil has been estimated to vary between 96.3 and 99.6 percent.

The values given in Table 6.7 are based on the assumption that the pore water at any depth below the ground water surface is saturated with dissolved air for the given value of hydrostatic pressure. As noted in Section 4.2.2, this may be unrealistic and would very likely be a worst case situation. The soil pore water probably would not be saturated with dissolved air at a pressure equal to the hydrostatic pore water pressure associated with its depth below the ground water surface. In actuality, the dissolved gas content of ground water at all depths should only be dependent on the pressure of the soil gas above the ground water surface. If the pressure of the soil gas is close to atmospheric pressure, a reduction in pore water pressure should have little effect on the amount of air that would come out of solution. This is because it is the pressure of the gas in contact with the water which influences the amount of dissolved gas in the water and not the water pressure.

Another consideration is the difference between the final pore air and pore water pressures after sampling. For a saturated soil in the ground, the pore air and pore water pressures are initially both equal to the hydrostatic pressure in the pore water (Sowers, 1979). The sampling of the soil leads to changes in pore water pressure, as given in Table 6.6. The pore air pressure in the soil decreases

from the hydrostatic water pressure at any given depth down to atmospheric pressure. Comparison of the changes in pore air pressure with the changes in pore water pressure, shows that the final pore air pressure is greater than the final pore water pressure. This suggests that air-water interfaces of radius  $r$ , as calculated by Eq. 4-29, may be present within the sampled soil.

The maximum change in pore water pressure at each depth occurred for the case of  $\bar{A}_u = 0$  in Table 6.6. These values for change in pore water pressure have been used along with the values of the initial hydrostatic pressure to calculate the change in pore air pressure, and the final pore air and pore water pressures for each depth. The results are presented in Table 6.8. Because the values of final pore air pressure were greater than the values of final pore water pressure, the values of interface radius,  $r$ , have been determined by Eq. 4-29, and are presented in Table 6.8, as well.

The presence of negative pore water pressures in the soil after sampling suggests that air-water interfaces must have been formed in the soil during sampling. In order for this to occur, some amount of air must have come out of solution from the soil pore water during the sampling process, leading to an increase in the void ratio of the

soil and a decrease in the degree of saturation of the soil below 100 percent. It is not certain how much air must come out of solution to create the negative pore water pressures given in Table 6.8. It could be that only a few air bubbles of radius  $r$  form in the soil pore water during sampling. On the other hand, if a number of bubbles with the same radius form, they would cause the same negative pore water pressure, but would make the degree of saturation of the soil lower.

**Table 6.8: Final pore air and pore water pressures and air-water interface radii,  $r$ , for saturated soil sampled from various depths**

Depth Below GWT (ft)	Initial Hydrostatic Pressure (psig)	$\Delta u_w$ for $\bar{A}_u=0$ (psi)	Final Pore Air Pressure (psig)	Final Pore Water Pressure (psig)	$r$ (in)
5	2.17	2.83	0	-0.66	0.001259
10	4.33	5.56	0	-1.23	0.000676
15	6.50	8.48	0	-1.98	0.000420
20	8.67	11.31	0	-2.64	0.000315
30	13.00	16.97	0	-3.97	0.000209
40	17.33	22.62	0	-5.29	0.000157
50	21.67	28.28	0	-6.61	0.000126

It should be noted that the values presented in Tables 6.6 through 6.8 neglect the effects of temperature change. During the sampling of the soil and trimming a specimen in the laboratory, the pore water could experience changes in temperature. Typical soil pore water temperatures would have the potential to increase from about 11°C to 20°C (U.S.

EPA, 1990). According to Duncan and Campanella (1965), changes in temperature lead to changes in pore water pressure in undrained triaxial test specimens. Temperature changes during sampling saturated soils may also lead to variations in pore water pressure. Temperature changes would also result in a corresponding change in the coefficient of solubility,  $H$ , of air in the pore water. The solubility of air in water is greater at 11°C than it is at 20°C. Because of this, in addition to the possibility of air coming out of solution due to the pressure reduction, it is very likely that air would have been able to come out of solution due to the increase in temperature.

As was shown in Section 4.5.1, for a saturated soil specimen undergoing a temperature increase from 11°C to 20°C, if the pore water was saturated with dissolved air at the initial temperature, the change in the value of  $H$  could lead to the degree of saturation of the soil decreasing from 100 percent to 99.7 percent, due to air coming out of solution. The air which exits solution due to the increase in temperature during sampling will expand its volume due to the decrease in pressure which occurs as the soil is sampled. This will result in the degree of saturation potentially being lower than 99.7%, as was discussed in Section 4.5.2.

### 6.3 Discussion of Q Tests Performed on Specimens Trimmed from Quarters of 4-inch Diameter Unloading Test Specimens

Two sets of Q tests were performed on 1.4-inch diameter specimens trimmed from the two remolded 4-inch diameter consolidated-undrained unloading test specimens. Each set of Q tests showed different stress-strain behavior.

The first set of tests was performed with midheight pore pressure monitoring on specimens of old LMVD silt. The deviator stress-strain behavior measured in these tests, shown in Figure 5.50, was similar for the three different confining pressures used, up to strains of 5.5 or 6 percent. A Mohr-Coulomb strength envelope for these three tests was given in Figure 5.51 and showed that for 5 percent axial strain at failure, the strength of the soil was characterized by a  $\phi_u = 0$ ,  $S_u = c = 12$  psi condition.

The pore pressure responses measured for these three tests were presented in Figure 5.50. Some erratic pore pressure measurements took place in two of the tests. All three tests tended to show a measured pore pressure which at some point in the tests became and remained relatively constant at higher strains. Two of the three tests reached a relatively constant value of measured pore pressure at strains above 5 percent. The third test, UU-24, showed an initial decrease in pore pressure until about 3.5 percent

strain, at which point erratic pore pressure measurements began and persisted until the end of the test. Even though these erratic pore pressure measurements occurred, the test showed a somewhat constant value of pore pressure after about 5 percent strain.

Considering the deviator stress-strain curve for test UU-24 in Figure 5.50 and the corresponding Mohr's circle in Figure 5.51, it can be seen that the strength of this specimen was slightly less than that of the other two specimens at 5 percent strain. This may be the result of the initiation of the erratic pore pressure measurements at about 3.5 percent strain.

The change in slope of the pore pressure-strain curves from an initially decreasing pore pressure to a relatively constant pore pressure with increasing strain, for all three of these tests, may possibly be an indication that some type of limiting pore pressure was reached. This limiting pore pressure may have corresponded with cavitation or degassing of the pore water. This may have resulted in the observed variations in deviator stress at higher strains. All three specimens appear to have reached a limiting negative change in pore pressure. Table 5.12, however, indicates that the minimum absolute pore pressure in all three specimens was greater than 0 psi absolute, suggesting that vaporous

cavitation did not occur. Gaseous cavitation, however, may have occurred in these tests and resulted in the observed stress-strain and pore pressure-strain behaviors.

At all three cell pressures used in this series of tests, the pore water could have very likely contained high amounts of dissolved air. As indicated by Table 5.8, the 4-inch diameter unloading test specimen (No. 3) from which these Q test specimens were trimmed, had an initial degree of saturation which was determined approximately to be only 86 percent. This specimen was remolded from a slurry, however, and it is felt that the initial degree of saturation was greater than 86%. The degree of saturation of 86% is probably inaccurate due to the approximate nature of the specimen measurements. The back pressure saturation process used on the 4-inch diameter specimen would have increased the degree of saturation closer to 100 percent. In doing so, however, it would have forced a considerable amount of free air into solution in the pore water of the specimen, in order to achieve full saturation.

When the unloading tests had been completed, the specimen was removed from the triaxial cell, split and trimmed into 1.4-inch diameter specimens. For the Q tests performed on these smaller specimens at cell pressures of 0, 10, and 20 psi, the pore water was likely supersaturated

with dissolved air. Some of this dissolved air may have been able to come out of solution during unloading, removal from the triaxial cell, and trimming the smaller specimens from the 4-inch diameter specimen. The similarity of the stress-strain curves from the Q tests at low axial strains, seems to contradict this. The Q tests were then performed as soon as possible after the unloading test, all on the same day. The test at 0 psi was performed first whereas that at 20 psi was performed last. This procedure was used so that if air came out of solution during the time between the first Q test and subsequent tests, the higher cell pressures used in the subsequent tests could possibly force this air back into solution.

All three of these Q test specimens could have had pore water saturated or supersaturated with dissolved air at the cell pressure of the particular test. As pore pressure decreased, air would have tended to come out of solution to maintain equilibrium in accordance with Henry's law.

If conditions were the same in all three specimens, it would be expected that air would come out of solution first from the specimen tested at 0 psi cell pressure and last from the specimen tested at 20 psi cell pressure. The limitation of only being able to perform one test at a time, however, may have resulted in the first two tests performed

at 0 and 10 psi, exhibiting more consistent stress-strain behavior. The test performed at 20 psi cell pressure was the last of the group of three tests to be performed. Even though a higher cell pressure was used in this test, the additional time which elapsed before this test was performed, may have allowed more air to come out of solution prior to beginning the test. This could have resulted in the stress-strain behavior observed in this test being slightly different than that observed in the other two tests which had been performed soon after the unloading test had been completed.

The second set of Q tests were performed on specimens of new LMVD silt. Unlike the stress-strain behavior observed for the other set of Q tests, this group showed a variation in the deviator stress-axial strain curves for the three different tests, as shown in Figure 5.53. In these tests, the deviator stress or strength of the soil at any value of axial strain increased with increasing confining pressure. This was illustrated in Figure 5.54, where the Mohr's circles for the three tests yielded an undrained strength envelope characterized by a cohesion intercept of 7 psi and an undrained friction angle,  $\phi_u$ , of  $12^\circ$ , for a failure criterion of 5 percent axial strain.

In this group of tests, pore pressures were not measured. The 4-inch diameter unloading test specimen (No. 4) from which these specimens were obtained had an approximate initial degree of saturation of 100 percent, as given in Table 5.8. The stress-strain behavior of the three Q test specimens suggests that the samples may have contained different amounts of free air in the pores of the soil, prior to testing. The stress-strain curves show that from the beginning to the end of the tests, at any given strain, the value of deviator stress increased with increasing cell pressure.

It may be that more air came out of solution from the pore water during this undrained unloading test than in the other 4-inch diameter specimen. The approximate initial degrees of saturation of the two specimens, however, would suggest that the opposite should be true. The values of  $\bar{A}_u$  measured in the two tests may help explain somewhat, the possible differences in the amount of air which could have come out of solution in the two samples during undrained unloading.

For the 4-inch diameter specimen of old LMVD silt from which the first set of Q test specimens was obtained, the value of  $\bar{A}_u$  measured was -0.2. For the 4-inch diameter specimen of new LMVD silt which provided the second set of Q

test specimens, the value of  $\bar{A}_u$  measured was -0.1. In the sampling analysis presented in Section 6.2, Table 6.6 indicates that for soil sampled from the same depth, a value of  $\bar{A}_u$  of -0.1 would give a larger change in pore water pressure,  $\Delta u_w$ , than would a value of  $\bar{A}_u$  of -0.2. This, in turn, would correspond to a slightly lower final degree of saturation,  $S_f$ , for the unloading test specimen with a value of  $\bar{A}_u$  of -0.1 (No. 4), than for the specimen where the value of  $\bar{A}_u$  was -0.2 (No. 3), as indicated in Table 6.7.

The larger value of  $\Delta u_w$  can also be related to a larger negative pore water pressure in the soil, indicating a lower degree of saturation after sampling. Because of this, the unloading test specimen from which the second set of Q test specimens were obtained may have had more air come out of solution during unloading than the other unloading test specimen. This may be the reason that the second set of Q tests gave the observed stress-strain behavior.

#### **6.4 Perfect Sampling of LMVD Silt**

The results of the undrained unloading tests can also be used in applying the perfect sampling approach of Ladd and Lambe (1963) to the tests on LMVD silt. According to Ladd and Lambe (1963), perfect sampling of the soil occurs when the in-situ shear stresses due to anisotropic conditions are removed during sampling, without subjecting

the soil to any other disturbance. If the soil could be sampled perfectly without disturbance, the effective stress in the soil after perfect sampling would be:

$$\sigma'_{ps} = \sigma'_{vo} [K_o + \bar{A}_u (1 - K_o)] \quad (6-15)$$

where  $\sigma'_{ps}$  = the effective stress in the soil after perfect sampling,  
 $\sigma'_{vo}$  = the initial in-situ vertical effective stress,  
 $K_o$  = the ratio of the effective horizontal consolidation pressure to the effective vertical consolidation pressure, and  
 $\bar{A}_u$  = the pore pressure parameter for unloading.

For the Q tests performed with midheight pore pressure monitoring, the remolded specimens had been consolidated to  $\sigma'_{vo} = 56$  psi in the batch consolidometer. The value of  $K_o$  for the LMVD silt was assumed to be 0.4, based upon the effective stress friction angle measured in the CU tests. For the range of values of  $\bar{A}_u$  determined in the undrained unloading tests, the values of  $\sigma'_{ps}$  have been calculated for the remolded batch consolidometer specimens of old LMVD silt and are presented in Table 6.9. Also presented in Table 6.9 are the ratios between  $\sigma'_{ps}$  and  $\sigma'_{vo}$  calculated for LMVD silt.

**Table 6.9: Perfect sampling effective stress for batch consolidometer specimens of old LMVD silt calculated using the values of  $\bar{A}_u$  from the undrained unloading tests ( $\sigma'_{v0} = 56$  psi,  $K_0 = 0.4$ )**

$\bar{A}_u$	$\sigma'_{ps}$ (psi)	$\sigma'_{ps}/\sigma'_{v0}$
0	22.4	0.40
-0.1	19.0	0.34
-0.2	15.7	0.28

The values  $\sigma'_{ps}$  given in Table 6.9 represent the values of effective stress that should have existed in the specimens after sampling, if no disturbance occurred. Disturbance of the soil during sampling, trimming, and sample preparation, however, is unavoidable. As a result of disturbance, the pore water pressure in the soil will increase and the initial effective stress in the specimens will be below the perfect sampling effective stress. This, in turn, will affect the measured strength of the soil, which is dependent on effective stress.

Ladd and Lambe (1963) reported that the ratio between the perfect sampling effective stress,  $\sigma'_{ps}$ , and the in-situ vertical effective stress,  $\sigma'_{v0}$ , ranged from 0.35 to 0.5 for normally consolidated clayey silt. For the LMVD silt used in this research, the ratio between the value of perfect sampling effective stress,  $\sigma'_{ps}$ , and the effective vertical consolidation pressure,  $\sigma'_{v0}$ , ranged from 0.28 to 0.40. These values of  $\sigma'_{ps}/\sigma'_{v0}$  calculated for low-plasticity LMVD

silt have a slightly lower range than the values reported by Ladd and Lambe (1963) for clayey silt.

For the Q tests with midheight pore pressure monitoring, the difference between the initial pore air and pore water pressure,  $P_a - P_w$ , corresponds to the residual effective stress,  $\sigma'_r$ , in the soil specimens. The residual effective stress is the effective stress in the soil after sampling, specimen trimming, and placement in the triaxial cell. The residual effective stress is less than the perfect sampling effective stress due to disturbance.

For the ten Q tests discussed in Section 6.1, the values of  $P_a - P_w$ , or  $\sigma'_r$ , were given in Table 6.1. For the three Q tests performed with midheight pore pressure monitoring on specimens obtained from the 4-inch diameter unloading test specimen of old LMVD silt, the values of  $P_a - P_w$ , or  $\sigma'_r$ , are presented in Table 6.10.

**Table 6.10: Initial pore air and pore water pressures prior to cell pressure application for the three Q test specimens obtained from the 4-inch diameter unloading test specimen of old LMVD silt**

Test	e	$P_a$ (psig)	$P_w$ (psig)	$P_a - P_w$ (psi)
UU-22	0.569	0	-2.15	2.15
UU-23	0.558	0	-2.25	2.25
UU-24	0.578	0	-1.81	1.81

The values of  $P_a - P_w$  or residual effective stress,  $\sigma'_r$ , for the thirteen Q test specimens included in Tables 6.1 and

6.10 range from 0.89 to 2.25 psi. These are considerably less than the values of perfect sampling effective stress,  $\sigma'_{ps}$ , given in Table 6.9, which range from 15.7 to 22.4 psi.

According to Ladd and Lambe (1963), the ratio between the values of residual effective stress and perfect sampling effective stress can be used as an indication of the level of disturbance in the specimens, with the ratio decreasing with increasing disturbance. The ratio,  $\sigma'_r/\sigma'_{ps}$ , for the ten Q tests listed in Table 6.1, have been calculated for the three different values of  $\sigma'_{ps}$ , and are presented in Table 6.11.

**Table 6.11: Ratio of  $\sigma'_r$  to  $\sigma'_{ps}$  for Q tests with midheight pore pressure monitoring**

Test	$\sigma'_r$ (psi)	$\sigma'_r/\sigma'_{ps}$ for $\sigma'_{ps} =$ 22.4 psi	$\sigma'_r/\sigma'_{ps}$ for $\sigma'_{ps} =$ 19.0 psi	$\sigma'_r/\sigma'_{ps}$ for $\sigma'_{ps} =$ 15.7 psi
UU-3	1.45	0.065	0.076	0.092
UU-6	0.89	0.040	0.047	0.057
UU-8	1.00	0.045	0.053	0.064
UU-10	1.62	0.072	0.085	0.103
UU-11	0.93	0.042	0.049	0.059
UU-12	1.12	0.050	0.059	0.071
UU-14	1.06	0.047	0.056	0.068
UU-15	1.09	0.049	0.057	0.069
UU-18	1.41	0.063	0.074	0.090
UU-19	1.11	0.050	0.058	0.071

For the ten Q tests listed in Table 6.11, the ratios between the residual effective stresses measured in the Q test specimens and the calculated values of perfect sampling effective stress, indicate that the values of residual

effective stress are only about 4 to 10% of the perfect sampling values. This tends to indicate that the level of disturbance of these specimens was considerable. Because the residual effective stress was much lower than the values of perfect sampling effective stress, as well as the in-situ vertical effective stress, the strengths measured for these test specimens are probably lower than the actual perfect sampling and in-situ strengths would be, with all other factors being equal.

The three Q tests listed in Table 6.10 were obtained from the 4-inch diameter consolidated, undrained unloading test specimen of old LMVD silt. This specimen was consolidated anisotropically to  $\sigma'_{v0} = 65$  psi with  $K_0$  estimated to be equal to 0.4. The perfect sampling effective stress,  $\sigma'_{ps}$ , calculated by Eq. 6-15, was 18.2 psi. In this unloading test, the value of  $\bar{A}_u$  was measured to be -0.2. The ratios of  $\sigma'_r/\sigma'_{ps}$  for these tests, based on  $\sigma'_{ps} = 18.2$  psi, are presented in Table 6.12.

**Table 6.12: Ratio of  $\sigma'_r$  to  $\sigma'_{ps}$  for Q tests with midheight pore pressure monitoring obtained from the 4-inch diameter unloading test specimen**

Test	$\sigma'_r$ (psi)	$\sigma'_r/\sigma'_{ps}$ for $\sigma'_{ps} =$ 18.2 psi
UU-22	2.15	0.118
UU-23	2.25	0.124
UU-24	1.81	0.099

For the three Q tests listed in Table 6.12, the values of residual effective stress are about 10 to 12% of the perfect sampling effective stress. The residual effective stress was higher in these three specimens than in the other ten specimens discussed above. The values of residual effective stress in these three specimens are still considerably below the values of perfect sampling effective stress. This suggests that the strengths measured in these Q tests are less than the perfect sampling strength, as well as the in-situ strength of the soil.

The values of residual effective stress were lower for the ten Q test specimens in Table 6.11 than for the three specimens in Table 6.12. This suggests that the ten specimens in Table 6.11 had a slightly higher level of disturbance than the three test specimens in Table 6.12.

Considering the three Q tests listed in Table 6.12, tests UU-22 and UU-23 had similar values of residual effective stress. These two tests were observed to have similar stress-strain behavior, as shown in Figure 5.50. Test UU-24 had a value of residual effective stress that was less than the other two specimens. The stress-strain behavior of this test specimen tended to show a lower strength for the soil than the other two specimens in the group, as shown in Figure 5.50. The results of this one

group of tests suggests that the higher the value of residual effective stress initially in the specimen, the larger the measured strength of the soil. In order to develop more definitive conclusions, additional Q tests with midheight pore pressure monitoring on specimens obtained from 4-inch diameter unloading test specimens would be needed. More accurate methods of measuring  $\sigma'_r$  may also provide an improved means of assessing the level of disturbance of saturated silt Q test specimens. This would allow the behavior suggested by this one set of tests to be more fully explored.

#### **6.5 Discussion of Effective Stress Strength Parameters of LMVD Silt**

The effective stress strength parameters were determined for LMVD silt from CU and CD tests. After completing the unloading tests, the two 1.4-inch diameter undrained unloading test specimens were tested in CU tests. The specimen of remolded old LMVD silt was consolidated to 20 psi and showed dilative tendencies in the CU test, as expected. The behavior of this silt specimen in the CU test, when plotted in terms of its effective stress path, defined the  $K_f$  line for the soil. Based on the  $K_f$  line, this test yielded an effective stress friction angle,  $\phi'$ , of  $36^\circ$  for the silt.

The undisturbed specimen of new LMVD silt was consolidated to 19.7 psi and showed strain softening behavior and compressive tendencies throughout the CU test. The specimen had a very low dry density, contained numerous fissures, and was only partly saturated initially. These factors may have contributed to the observed behavior. The behavior of this silt specimen in this one CU test, when plotted in terms of its effective stress path, defined the  $K_f$  line for the soil. Based on the  $K_f$  line, this test yielded a cohesion intercept,  $c'$ , of 1.21 psi and an effective stress friction angle,  $\phi'$ , of  $31^\circ$  for the silt. No other values of the effective stress strength parameters were determined for new LMVD silt.

One of the quarters obtained from the first 4-inch diameter undrained unloading test specimen was tested in a CU test. This CU test specimen was consolidated to 10.5 psi. The effective stress path for this test defined the  $K_f$  line for the soil. The orientation of the  $K_f$  line yielded an effective stress friction angle,  $\phi'$ , of  $35^\circ$ .

The series of CU tests performed with  $\sigma'_{3con} = 10$  psi and different values of back pressure, also gave effective stress paths which clearly defined the  $K_f$  line for the soil. The orientation of the  $K_f$  line for these tests corresponded with an effective stress friction angle,  $\phi'$ , of  $34^\circ$ .

A series of CD tests performed on old LMVD silt gave an effective stress friction angle,  $\phi'$ , of  $38^\circ$  for the soil.

The values of  $\phi'$  determined in these tests on old LMVD silt are similar to the values of effective stress friction angle reported by Brandon, Duncan, and Huffman (1990) for old LMVD silt.

## **6.6 Discussion of the Prepressurization Study**

As noted in Section 5.6, the results of the prepressurization study were inconclusive due to the inability to confirm whether or not the specimens were initially fully saturated. This is especially significant because the majority of the Q tests with midheight pore pressure monitoring discussed in Section 6.1, had negative pore water pressures initially, suggesting that the specimens were somewhat less than fully saturated. If the Q test specimens used in the prepressurization study were less than fully saturated, which is highly likely, then the specimens subjected to the high cell pressure prior to testing, would have probably had smaller void ratios and thus higher strengths than the non-prepressurized specimens, to which they were later compared.

The presence of even the smallest amount of free air in a Q test specimen, when subjected to a high cell pressure on

the order of 200 to 260 psi, would have lead to the specimens experiencing an increase in the degree of saturation as the free air was forced into solution by the high pressure. Similar Q test specimens from the same batch consolidometer sample should have had about the same amount of free air present as the prepressurized specimens did initially. These specimens, however, would not have had the free air forced into solution prior to performing the Q test. They would have had a slightly lower degree of saturation and slightly higher void ratio at the start of the Q test than the prepressurized specimens.

Based on this, the two prepressurized specimens should have had higher strengths than the two non-prepressurized specimens tested from each batch at a given cell pressure. Review of Figures 5.55 through 5.61, however, indicates that this was not always the case. The group of tests performed at a cell pressure of 20 psi were the only ones for which the two prepressurized specimens were consistently stronger than the two non-prepressurized specimens. The other sets of Q tests showed stress-strain behavior which was somewhat inconsistent with this theory.

An explanation for this inconsistency may be that different amounts of free air were initially present in the four specimens in the other groups. This may have lead to

the prepressurization having different effects on sample behavior. Different amounts of free air in the specimens may have resulted from variations in the level of specimen disturbance. Membrane leakage may also have occurred due to the high pressure in some tests but not in others, leading to different behavior being observed in the tests. Overall, it is difficult to draw firm conclusions from the prepressurization study because no pore pressure measurements were performed to enable consideration of the initial degree of saturation, whether membrane leakage occurred, and what changes in pore pressure took place during the Q tests.

One interesting thing to note about the prepressurized Q tests is that the tests performed at 0 psi and 20 psi each showed consistent stress-strain results, whereas the tests performed at 10 psi did not. This may be an indication that for the tests at 0 psi and 20 psi, the specimens contained similar amounts of free air initially. The prepressurization would then have had similar effects on the void ratios of both specimens at each cell pressure, resulting in similar stress-strain curves.

The variation in the stress-strain behavior of the prepressurized specimens tested at 10 psi may be an indication that these specimens contained different amounts

of free air initially. This would have lead to different void ratios and strengths. Different amounts of free air in the specimens could have resulted from different levels of disturbance during trimming, or perhaps the two tests were performed at considerably different times after the soil had been removed from the batch consolidometer, so that one sample could have possibly had more free air present than the other specimen.

Further research on prepressurized Q test specimens is of limited value. The prepressurization of Q test specimens was used in this research to study the influence of prepressurization on the pore pressure response and associated stress-strain behavior of saturated dilatant silts. These tests were performed based on similar procedures discussed in the cavitation literature. Prepressurization of Q test specimens is not considered a reasonable procedure for determining the undrained strength of saturated silts because it can not be applied to field conditions. Under normal field loading conditions, the pore water of saturated silts will be subjected to pressures considerably less than those used in the prepressurized Q tests performed in this research.

Comparison of prepressurized Q test specimens to non-prepressurized specimens with pore pressure measurements

during the Q tests as well as during the high pressure application may still be of some use. Pore pressure measurements during the application of the prepressurization pressure would allow for the assessment of whether or not the specimens were fully saturated. The most useful information could be gained by measuring pore water pressures during undrained shear. This would make it possible to evaluate whether the decrease in pore water pressure was greater in the prepressurized specimens than in the non-prepressurized specimens. If this were found to be the case, it would possibly indicate that the application of the prepressurization pressure, lead to the pore water being stronger in tension and more resistant to cavitation.

#### **6.7 Discussion of Q Tests with Pore Air and Pore Water Pressure Measurements**

The Q tests performed on compacted specimens of new LMVD silt were tested while attempting to measure pore air and pore water pressures within the specimens. The specimens tested were partially saturated because the measurement of pore air pressures is extremely difficult, if not impossible at high degrees of saturation.

The results of these tests were presented in Section 5.7. In the presentation of the results of these tests, it was noted that the results were felt to be questionable.

The tests showed that the pore air and pore water pressures decreased in the specimens during undrained shear. The rate of decrease of pore air pressure tended to be greater than the rate of decrease of the pore water pressure.

Although it is felt to be reasonable that the pore air and pore water pressures both would decrease during undrained shear of specimens with dilatant tendencies, the magnitudes of the measured pressures may be incorrect. The actual values of pressure measured in these tests are felt to be questionable do to the nature of the measured pressures and the uncertainties presented in the calibration and measurement of the pressures with the available equipment.

This is true for the tests with high degrees of saturation where pore air pressures were not consistently greater than pore water pressures, as expected for partially saturated soils. The high degree of saturation may have prevented accurate pore air pressure measurements. The tests performed at 0 psi cell pressure showed unusual pore water pressure responses. These pore water pressures are felt to be incorrect. The other tests performed at a cell pressure of 10 psi had measured values of pore air and pore water pressure which did not always appear to be consistent with the pressures expected within a specimen subjected to

10 psi cell pressure. In some cases, the specimens had measured pore air pressures considerably greater than the applied cell pressure of 10 psi. In other tests, the measured pore air pressure was considerably below 10 psi. Too few tests were performed to assess which of these pore pressure responses, if any, represent the actual pore pressure behavior in the soil.

The inconsistencies in the pore pressures measured in these tests make the results unreliable. These tests have not provided any information that is useful in studying the behavior of saturated silts in Q tests. The performance of these tests emphasized the difficulties and uncertainties associated with the measurement of pore air pressures in soils, as has been observed by other researchers (Bishop, 1960; Bishop and Henkel, 1962).

#### **6.8 Discussion of Q Tests Performed at Different Strain Rates**

The results of the Q tests performed on saturated silt specimens at different strain rates tended to show inconsistencies which make it difficult to develop firm conclusions. The inconsistencies observed may possibly be the result of specimen disturbance. This disturbance can not be quantified and its influence on the observed behavior is uncertain.

One result of the Q tests performed at different strain rates worth noting is the relationship between the rate of shear and the frequency of abrupt strain-softening in the stress-strain behavior of the specimens. The Q test specimens sheared at the faster strain rates tended to have stress-strain behavior in which noticeably abrupt strain-softening occurred. Specimens sheared at the slowest strain rates did not exhibit abrupt strain-softening to the same extent.

This suggests that in the rapidly sheared specimens, where larger decreases in pore water pressure would be expected along the location of the failure plane, cavitation of the pore water and abrupt yielding may have occurred. The slowly sheared specimens would have been expected to experience smaller decreases in pore water pressure. As a result, the pore water in these specimens may not have experienced cavitation or gases coming out of solution to the extent that abrupt yielding of the specimens occurred. The relationship between cavitation and bubble growth in soil pore water, yielding along a shear plane, and abrupt strain-softening will be discussed in detail in Section 6.12.

## **6.9 Discussion of Results of CU Tests with Different Back Pressures**

A set of four CU tests were performed on remolded specimens of old LMVD silt. The test specimens were all consolidated to the same consolidation pressure, but different values of back pressure were used in the specimens. The variation of the back pressure in these tests resulted in the undrained specimens experiencing desaturation at different points during the tests, due to the pore pressure reductions which occurred during shear.

The dilatant tendencies of the silt specimens lead to reductions in pore water pressure during undrained shear. When the back pressure initially in the specimens was negated due to the decrease in pore water pressure, the pore water pressure went below atmospheric pressure and reached a relatively constant, limiting value. Reaching a limiting pore water pressure less than atmospheric pressure is associated with the desaturation of the specimens. Desaturation of the specimens corresponded with the stress-strain curves of the CU test specimens reaching their peak values, followed by strain-softening behavior.

During undrained shear, the pore water pressure in three of these specimens decreased below atmospheric pressure. The pore water pressure never decreased as low as -13.7 psi, at which point vaporous cavitation would have

occurred. The pore water pressure decreasing below atmospheric pressure resulted in desaturation or gaseous cavitation at pressures considerably greater than -13.7 psi. Dissolved gases coming out of solution from the soil pore water would have increased the volume of the specimens and lead to peak strengths being reached in the tests.

Consolidated-drained triaxial tests on remolded specimens of old LMVD silt also show that when the volume of the specimens increased above the initial specimen volume, a corresponding peak in the deviator stress-strain curve occurred. The occurrence of peak strength values in CD tests when volume increase takes place suggests that the peak values of deviator stress in CU and Q tests may correspond with volume increase in the undrained test specimens.

One of the most plausible ways that an undrained test specimen of saturated, dilatant silt could experience an increase in volume is by gases dissolved in the pore water coming out of solution due to the pore water pressure reduction during shear. In addition, any existing air bubbles present in the specimen would grow larger as a result of pore pressure reductions, leading to increases in specimen volume.

## **6.10 Discussion of Undrained Strength of LMVD Silt**

Numerous Q tests were performed in this research on remolded, saturated specimens of old and new LMVD silt. Most of the tests performed are felt to have given fairly reasonable, although sometimes erratic, undrained behavior. Some tests with midheight pore pressure monitoring may have experienced leakage giving undrained behavior which is questionable. The stress-strain behavior measured in the Q tests was used to determine the undrained shear strength for the soil throughout Chapter 5. In many cases, the stress-strain behavior varied from test to test such that the values of undrained shear strength of the soil varied considerably for different groups of tests. In other groups of tests, similar stress-strain behavior was observed for the specimens, especially at low strains. The variation in the measured undrained strengths tended to increase with increasing axial strain.

Mohr-Coulomb failure envelopes were presented throughout Chapter 5 for the Q tests on remolded specimens of LMVD silt. In some cases, these failure envelopes were based on a limiting axial strain as a failure criterion. In other cases, the values of peak deviator stress were used as the failure criterion to develop the undrained strength envelopes for the soil.

When a limiting axial strain was used as the failure criterion, the value of axial strain selected to develop the Mohr-Coulomb envelope, was based on the observed stress-strain behavior of the specimens. The axial strain chosen was influenced by the point at which the stress-strain curves began to vary from each other or where peaks began to occur in the stress-strain curves. The values of axial strain used as a failure criterion varied from 4.5% to 10%.

In engineering practice, the value of limiting axial strain chosen as a failure criterion for Q tests on saturated silts is determined based on the field loading conditions for a given project. Values of axial strain on the order of 10% (Brandon, Duncan, and Huffman, 1990) to 15% (Fleming and Duncan, 1990) have been suggested as appropriate failure criteria for Q tests on saturated silts for most engineering projects.

A summary of the undrained strengths determined from the Q tests on old and new LMVD silt will be presented in several tables. Some of the Q tests presented in these tables were those which are believed to have experienced problems with the midheight pore pressure monitoring system. These tests are noted in the tables.

For the cases where a limiting axial strain was used as the failure criterion, the problems in midheight pore

pressure monitoring typically occurred at a higher axial strain than that used in developing the strength envelope. Where values of peak deviator stress were used to develop the failure envelope, problems with the midheight pore pressure monitoring system tended to coincide with the occurrence of a peak value of deviator stress. It is felt that in these cases, the peak value of deviator stress was influenced by the occurrence of the problems with the midheight pore pressure measurements. Because of this, the undrained strength envelopes determined using these tests are felt to be questionable.

The undrained strength parameters for the Q tests on old LMVD silt, based on a failure criterion of 9 or 10% axial strain, are summarized in Table 6.13. The undrained strength parameters given in Table 6.13 show noticeable variations. The values of undrained cohesion intercept,  $c$ , varied from 3.5 psi to 11.5 psi. The undrained friction angles,  $\phi_u$ , measured for the strength envelopes varied from  $0^\circ$  to  $19^\circ$ . The strength envelopes given in Table 6.13 for old LMVD silt have been plotted together in Figure 6.13.

The variation of the undrained strength envelopes for old LMVD silt plotted in Figure 6.13 illustrates the difficulty encountered in selecting undrained strengths for saturated, dilatant silts, for use in engineering analysis

**Table 6.13: Undrained strength parameters determined from Q tests on remolded old LMVD silt, based on a failure criterion of 9 or 10% axial strain**

Figure Number	Tests	$\sigma'_v$ (psi)	$e_{ave}$	$\epsilon_{af}$ (%)	$c$ (psi)	$\phi_u$	$S_u/\sigma'_v$
5.24	UU-13+ UU-14	56	0.541	10	9.2	0°	0.16
5.27	UU-6 UU-11 UU-15 UU-16+	56	0.508	10	3.5	19°	-
5.31	UU-3 UU-13+ UU-14	56	0.539	10	8.1	5.4°	-
6.4	UU-12 UU-15 UU-18	56	0.527	10	7.3	1.1°	0.13
6.5	UU-3 UU-10 UU-14	56	0.539	10	9.5	1.5°	0.17
5.88	B9-1 B9-2 B9-4	67	0.512	10	9.1	1.5°	0.14
5.91	B11-1 B11-2 B11-3 B11-4	67	0.479	9	8.1	0.3°	0.12
5.100	B4-4 B9-1 B9-2 B9-4	67	0.517	10	9.7	1.1°	0.14
5.103	B8-1 B8-2 B8-4 B7-1 B7-2	67	0.493	9	11.5	1.9°	0.17
5.106	B9-1 B9-2 B9-4 B10-1	67	0.509	10	8.5	1.9°	0.13
5.111	B9-1 B9-2 B9-4 B11-1 B11-2 B11-3	67	0.491	9	7.9	1.5°	0.12

+ Tests in which midheight pore pressure monitoring problems occurred

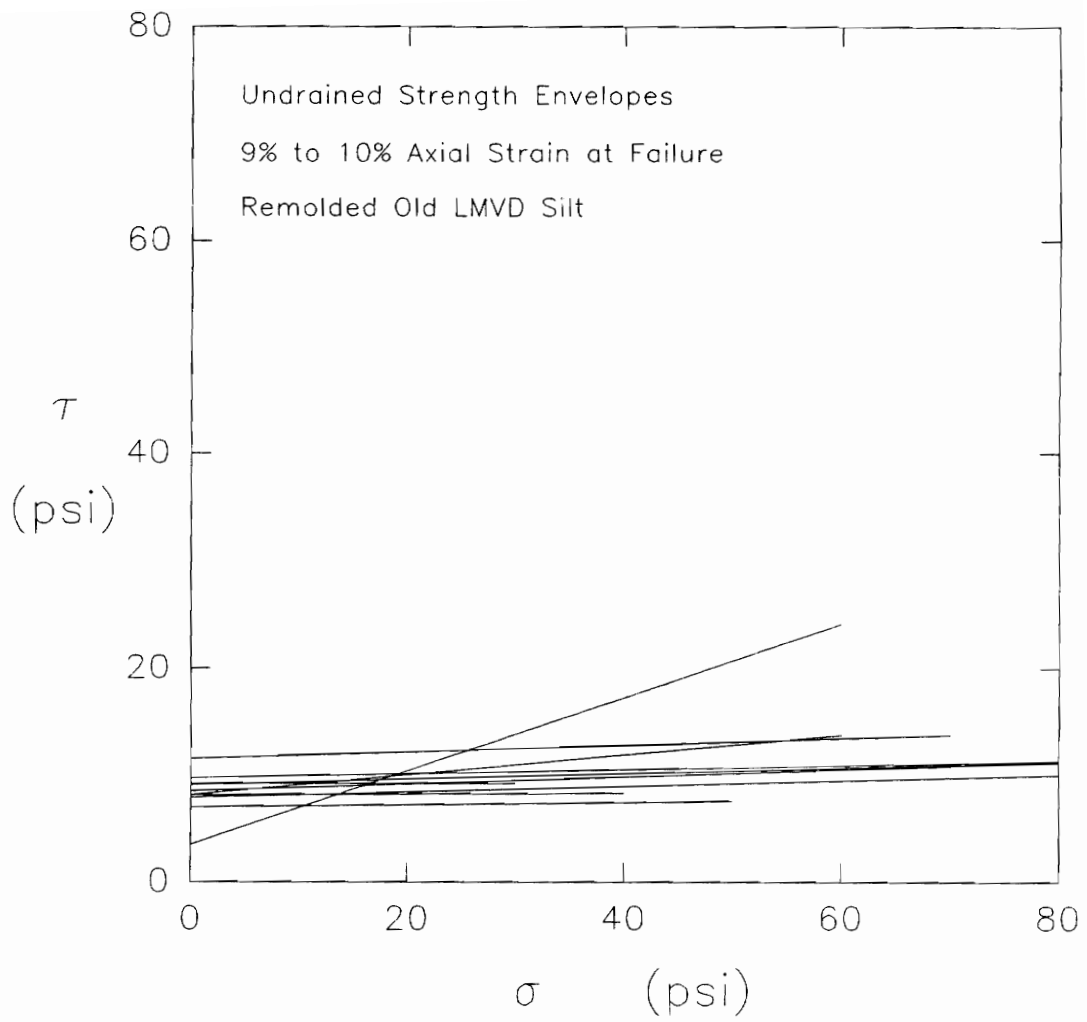


**Figure 6.13. Undrained strength envelopes for remolded old LMVD silt, based on 9% to 10% axial strain at failure**

and design. The strength envelope with  $c = 3.5$  psi and  $\phi_u = 19^\circ$  appears to be inconsistent with the other envelopes. If this strength envelope is neglected, the average values of void ratio and the undrained strength parameters for old LMVD silt at 9 to 10% axial strain are:  $e = 0.513$ ,  $c = 8.8$  psi, and  $\phi_u = 1.6^\circ$ .

The averaging of the undrained strengths of the soil from nine different undrained strength plots may not be a viable procedure. This is especially true considering that many of the strength envelopes given in Table 6.13 were developed using the same  $Q$  tests, which would weight the average values toward certain  $Q$  test results. In addition, some of the batch consolidometer samples from which the test specimens were obtained were  $K_0$  consolidated to  $\sigma'_{vcon} = 56$  psi, whereas, others were  $K_0$  consolidated to  $\sigma'_{vcon} = 67$  psi. This averaging does tend to provide an increased level of confidence in the range of values of the undrained strength parameters to use in engineering analysis and design. The number of tests needed to obtain these values may be considered excessive and uneconomical.

The ratios  $S_u/\sigma'_v$  for the various undrained strength plots are also given in Table 6.13. The value of  $S_u$  used in calculating these ratios was taken at a value of normal stress,  $\sigma$ , equal to zero, or in other words,  $S_u = c$ . The

values of  $S_u/\sigma'_v$  range from 0.12 to 0.17. This range of values of  $S_u/\sigma'_v$  was observed for the two different values of  $\sigma'_v$  used in the Q tests on remolded old LMVD silt.

One point that is worth noting about the strength values given in Table 6.13 is related to the groups of tests where 9% axial strain was chosen as the failure criterion. These groups of Q tests had lower average void ratios than the groups of specimens where 10% axial strain was used as the failure criterion. In the specimens with lower average void ratios, the tendency for dilation was greater. As a result, the negative pore water pressures developed during undrained shear were larger and the stress-strain behavior of these groups of specimens began to vary or became erratic at an axial strain of about 9%, rather than 10%.

This suggests that in the specimens with lower average void ratios, the decrease in pore water pressure at which erratic stress-strain behavior began occurred at a slightly smaller axial strain than it did in the specimens with higher void ratios. The erratic stress-strain behavior may be the result of cavitation or gases exiting solution from the soil pore water as pore pressures decreased during undrained shear.

Although the value of limiting axial strain chosen as a failure criteria will depend on the type of engineering

project, the occurrence of erratic stress-strain behavior at different values of axial strain highlights the difficulty in using a consistent value of limiting axial strain as a failure criterion for a given project.

For the old LMVD silt used in this research, the undrained strength envelopes obtained for the soil began to become erratic at different values of axial strain. The axial strain at which the undrained strength went from a  $\phi_u = 0$  to a  $\phi_u > 0$  condition appears to be dependent on the void ratio of the soil. The lower the void ratio, the lower the value of axial strain at which the stress-strain behavior begins to exhibit erratic behavior. Other variables, such as the liquidity and plasticity indices of the soil, might be related to the axial strain at which erratic undrained stress-strain behavior begins for a given soil. This makes it difficult to use a consistent value of limiting axial strain as a failure criterion to determine the undrained shear strength of saturated, dilatant silts for a given engineering project.

In some groups of  $Q$  tests, erratic stress-strain behavior began at even lower axial strains. In these cases, limiting axial strains between 5 and 8.5% were used as the necessary failure criteria to achieve  $\phi_u = 0$  undrained strength envelopes for the soil. Table 6.14 presents the

undrained strength parameters for old LMVD silt based on a limiting axial strain of less than 9% as the failure criterion.

**Table 6.14: Undrained strength parameters determined from Q tests on remolded old LMVD silt, based on a failure criterion of less than 9% axial strain at failure**

Figure Number	Tests	$\sigma'_v$ (psi)	$e_{ave}$	$\epsilon_{af}$ (%)	$c$ (psi)	$\phi_u$	$S_u/\sigma'_v$
5.17	UU-1+ UU-2+ UU-3	56	0.549	8.5	9.8	0°	0.18
5.21	UU-8 UU-10	56	0.540	8	9.5	0°	0.17
5.51*	UU-22 UU-23 UU-24	65	0.568	5	12	0°	0.18
5.85	B8-1 B8-2 B8-4	67	0.474	8.5	10.2	4°	0.15
5.94	B12-1 B12-3	67	0.490	7.7	20.5	0°	0.31
5.97	B13-1 B13-2	67	0.475	7	8.1	2.2°	0.12

+ Tests in which midheight pore pressure monitoring problems occurred

\* Q test specimens trimmed from unloading test specimen

The undrained strength parameters given for old LMVD silt in Table 6.14 also show some variation, even though lower values of axial strain were used as the failure criterion. In this table, the values of undrained cohesion intercept,  $c$ , varied from 8.1 psi to 20.5 psi. The measured values of undrained friction angle,  $\phi_u$ , presented in Table 6.14 varied from 0° to 4°. The undrained strength envelopes

for old LMVD silt defined by the parameters given in Table 6.14, are plotted together in Figure 6.14.

The plotted strength envelopes again illustrate the erratic undrained strengths of saturated, dilatant silts. Some of this variation is likely the result of mixing strength data from the tests at a wide variety of axial strains. The one strength envelope plotted for  $c = 20$  psi and  $\phi_u = 0^\circ$  appears to be inconsistent with the other strength envelopes shown and may be incorrect.

The ratios  $S_u/\sigma'_v$  for these undrained strength plots are also given in Table 6.14. The values of  $S_u$  used in calculating these ratios were taken at a value of normal stress,  $\sigma$ , equal to zero, so that  $S_u = c$ . The values of  $S_u/\sigma'_v$  range from 0.12 to 0.31. Other than the value of 0.31, these values of  $S_u/\sigma'_v$  are similar in magnitude to those given in Table 6.13. Several groups of tests had a somewhat consistent value for  $S_u/\sigma'_v$  of about 0.18.

Undrained strength envelopes have also been developed for old LMVD silt based on the peak values of deviator stress measured in the Q tests. In the Q tests with erratic stress-strain behavior, the peak value of deviator stress was taken as the first peak to occur in the stress-strain curve. In some tests, a peak in the stress-strain curve occurred and was followed by a decrease in deviator stress

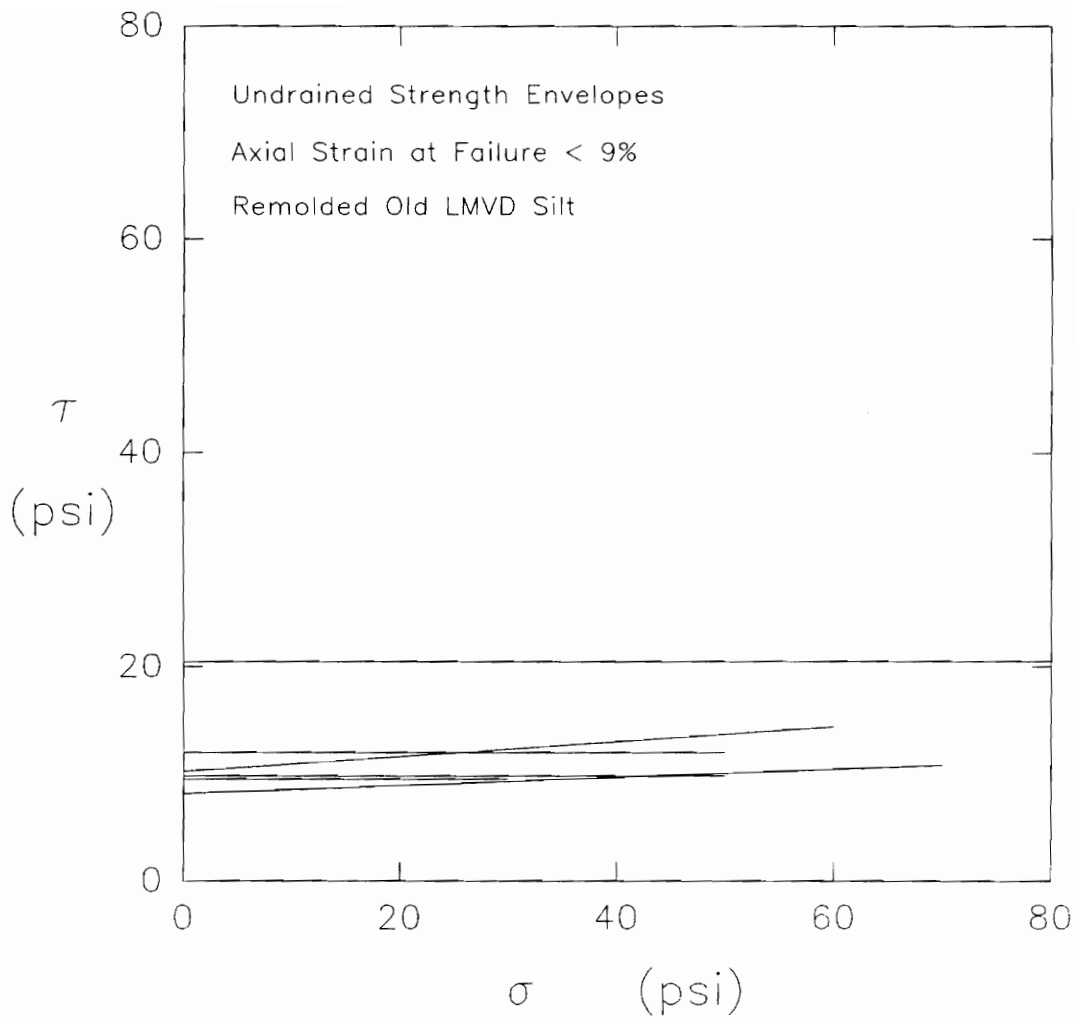


**Figure 6.14** Undrained strength envelopes for remolded old LMVD silt, based on a failure criterion of less than 9% axial strain at failure

and then a subsequent increase in deviator stress. The subsequent increase in deviator stress often lead to a value of deviator stress greater than that at the first peak. In these tests, the higher value of deviator stress at the second peak was ignored and the value of deviator stress at the first peak in the curve was used in developing the strength envelope for the soil.

Some of the groups of Q tests had values of peak deviator stress that resulted in undrained strength envelopes for old LMVD silt defined by a linear strength envelope. Other groups of tests gave bilinear envelopes. Bilinear envelopes tended to occur when the Q tests were performed over a range of cell pressures. The linear envelopes were observed mainly in the cases where the Q tests were performed at low cell pressures. The groups of tests which resulted in linear undrained strength envelopes are presented in Table 6.15.

The linear undrained strength envelopes presented in Table 6.15 can only be taken as linear within the range of normal stresses used in performing the tests. These values of limiting normal pressure are noted in the table. The values of the undrained strength parameters,  $c$  and  $\phi_u$ , given in Table 6.15 vary. The values of  $c$  range from 3.0 psi to 15.5 psi. The values of  $\phi_u$  range from  $14.3^\circ$  to  $25.3^\circ$ .

**Table 6.15: Undrained strength parameters determined from Q tests on remolded old LMVD silt, based on peak deviator stress failure criterion (linear envelopes)**

Figure Number	Tests	$e_{ave}$	Limiting $\sigma$ (psi)*	c (psi)	$\phi_u$
5.86	B8-1 B8-2 B8-4	0.474	60	7.7	22.2°
5.92	B11-1 B11-2 B11-3 B11-4	0.479	35	5.6	14.3°
5.95	B12-1 B12-3	0.490	140	15.5	14.4°
5.98	B13-1 B13-2	0.475	70	3.0	23.7°
5.109	B8-1 B8-2 B8-4 B11-1 B11-2 B11-3	0.472	60	4.6	25.3°

\* Approximate value based on range of cell pressures used in tests.

The values of undrained friction angle,  $\phi_u$ , are below the values of effective stress or drained friction angle,  $\phi'$ , measured in CU and CD tests on old LMVD silt. The values of  $\phi'$  measured for LMVD silt ranged from 34° to 38°. The measurement of undrained friction angles considerably greater than zero suggests that truly undrained conditions may not have existed in these tests. The fact that the undrained friction angles,  $\phi_u$ , were less than the effective stress or drained friction angles,  $\phi'$ , for the same soil, suggests that fully drained conditions were not reached in the Q test specimens. Conditions corresponding to partially

drained conditions, possibly resulting from gases exiting solution during shear leading to specimen volume expansion, may have occurred giving undrained friction angles greater than zero.

Figure 6.15 shows the five linear undrained strength envelopes plotted together over their ranges of applicable normal stress. The erratic variation in the undrained strengths measured for the old LMVD silt is apparent. The undrained strength envelope defined by  $c = 15.5$  psi and  $\phi_u = 14.4^\circ$  appears to be especially inconsistent with the other strength envelopes presented in Figure 6.15. The undrained strength of the soil measured in the two tests used to develop this strength envelope may be incorrect.

Table 6.16 presents the undrained strength parameters for the bilinear undrained strength envelopes for old LMVD silt.

The bilinear envelopes presented in Table 6.16 do not allow for very meaningful comparisons because they were all developed using the B9 group of Q tests. It is worth noting however, that when the results of the B9 tests, which were performed at higher cell pressures, were combined with the results of the B11 tests, which were performed at lower cell pressures, the normal stress at which the  $\phi_u = 0$  portion of the bilinear envelope began, was shifted downward. For the

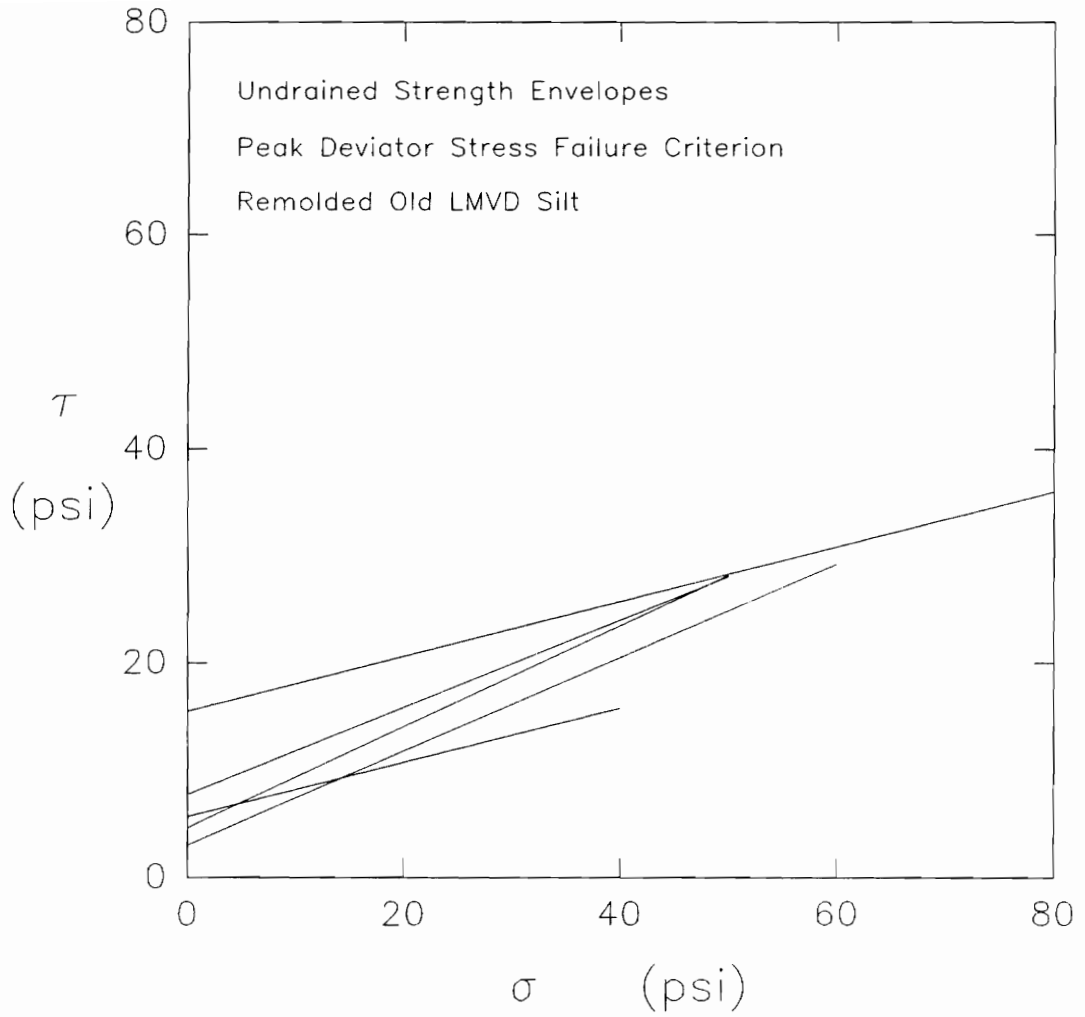


**Figure 6.15** Undrained strength envelopes for remolded old LMVD silt, based on the peak deviator stress failure criterion

B9 tests alone, the  $\phi_u = 0$  portion of the bilinear strength envelope began at about  $\sigma = 70$  psi. When the B11 tests were included as well, the  $\phi_u = 0$  portion of the strength envelope began at about  $\sigma = 55$  psi. This suggests that Q tests should be performed over a wide range of cell pressures when trying to develop the undrained strength envelope for a saturated, dilatant silt with bilinear strength behavior. These two undrained strength envelopes are plotted together in Figure 6.16.

**Table 6.16: Undrained strength parameters determined from Q tests on remolded old LMVD silt, based on peak deviator stress failure criterion (bilinear envelopes)**

Figure Number	Tests	$\sigma'_v$ (psi)	$e_{ave}$	Range of $\sigma$ (psi)	$c$ (psi)	$\phi_u$	$S_u/\sigma'_v$
5.89	B9-1 B9-2 B9-4	67	0.512	0-70	8.6	10.1°	-
	>70			23.74	0°	0.35	
5.101	B4-4 B9-1 B9-2 B9-4	67	0.517	0-70	8.6	10°	-
	>70			19	1.5°	0.28	
5.107	B9-1 B9-2 B9-4 B10-1	67	0.509	0-70	8.6	10.1°	-
	>70			19	1.5°	0.28	
5.112	B9-1 B9-2 B9-4	67	0.491	0-55	5.5	14.6°	-
	B11-1 B11-2 B11-3			>55	19	1.5°	0.28

Bilinear strength envelopes, such as those shown in Figure 6.16, could also result from Q tests on specimens

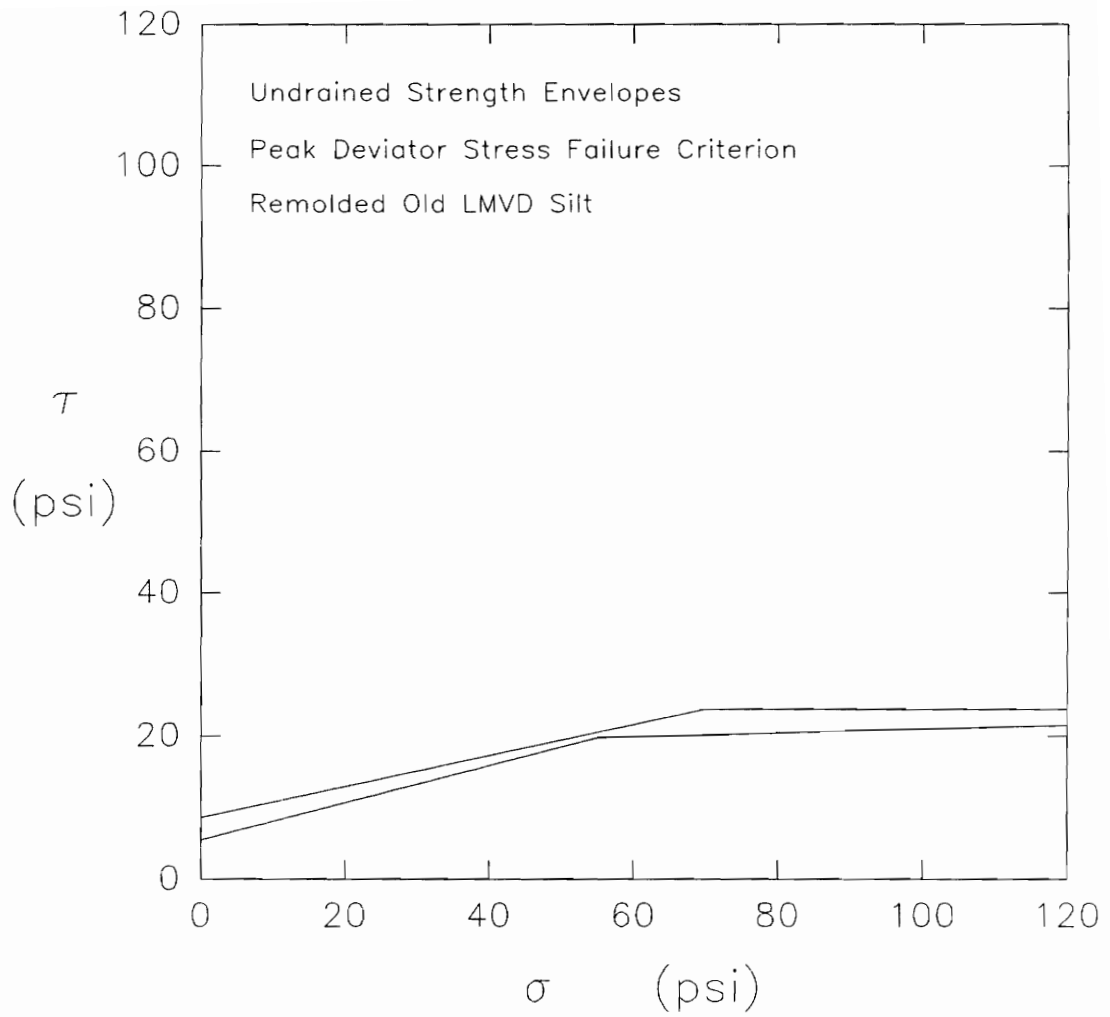


**Figure 6.16. Bilinear undrained strength envelopes for remolded old LMVD silt, based on the peak deviator stress failure criterion**

which were not fully saturated. At low cell pressures, the specimens would have degrees of saturation less than 100%. The tests performed at higher cell pressures would have more of the free air compressed and forced into solution. As a result, they would have a higher degree of saturation and lower void ratio. They therefore, would have higher strengths, resulting in a  $\phi_u > 0$  envelope for the soil. Eventually, at some value of cell pressure, all of the free air will have been forced into solution and the specimen will be fully saturated. At higher cell pressures, the void ratio and degree of saturation of the specimens will be the same so that the undrained strength will be the same, as well. A  $\phi_u = 0$  strength envelope would then be obtained.

If two groups of specimens had the same initial void ratio but different initial degrees of saturation, the transition from  $\phi_u > 0$  to  $\phi_u = 0$  behavior would occur at different cell pressures. The group of specimens with the lower degree of saturation would go from  $\phi_u > 0$  to  $\phi_u = 0$  behavior at a higher cell pressure. This is because a higher cell pressure would be necessary to force the additional free air into solution to reach fully saturated conditions. These specimens should also have a higher undrained shear strength in the  $\phi_u = 0$  region because their void ratio would be lower in the fully saturated condition.

The B9 and B11 specimens for which the bilinear undrained strength envelopes are shown in Figure 6.16, all had measured degrees of saturation of 100%. The actual degrees of saturation of these specimens were likely less than 100% (Bishop and Henkel, 1962) and may have varied from one group to another. As a result, the location of the transition from the  $\phi_u > 0$  to  $\phi_u = 0$  behavior may have been related to variations in the degree of saturation of the two groups of Q test specimens.

For the  $\phi_u = 0$  portion of the bilinear envelopes, the ratios of  $S_u/\sigma'_v$  have been presented in Table 6.16. The values of  $S_u$  used are for  $S_u = c$  at the point where the second linear portion of the envelope began. For the B9 group of tests, the value of  $S_u/\sigma'_v$  is equal to 0.35. When the B9 tests are combined with the results of other tests, the value of  $S_u/\sigma'_v$  is reduced to 0.28. As expected, these values of  $S_u/\sigma'_v$  for peak deviator stress conditions are greater than those calculated for limiting axial strain failure criteria.

The number of Q tests performed on saturated specimens of new LMVD silt were not as numerous as those performed on old LMVD silt. As a result, they will be presented in a more concise form. Two different failure criteria were considered for the new LMVD silt. The first was a limiting

value of axial strain. Limiting axial strains between 4.5 and 10% were used. The value of axial strain selected to determine the strength was based on the initiation of erratic stress-strain behavior in the tests. In engineering practice, the value of axial strain chosen as a failure criterion would depend on the project. The undrained strength parameters determined from Q tests on new LMVD silt, based on a limiting axial strain failure criterion, are presented in Table 6.17.

**Table 6.17: Undrained strength parameters determined from Q tests on remolded new LMVD silt, based on a limiting axial strain failure criterion**

Figure Number	Tests	$\sigma'_v$ (psi)	$e_{ave}$	$\epsilon_{af}$ (%)	$c$ (psi)	$\phi_u$	$s_u/\sigma'_v$
5.54*	UU-25 UU-26 UU-27	65	0.697	5.5%	7	12.2°	-
5.114	B17-1 B17-2 B17-3 B17-4	67	0.626	4.5%	11.9	6.8°	-
5.117	B18-1 B18-2 B18-3 B18-4	67	0.613	10%	18.1	1.4°	0.27

\* Q test specimens trimmed from unloading test specimen

It can be seen from this table that the undrained strength parameters of the new LMVD silt varied considerably. This is as expected due to the variation in the values of axial strain used as failure criteria. The values of undrained cohesion intercept,  $c$ , varied from 7 psi

to 18.1 psi. The values of undrained friction angle,  $\phi_u$ , varied from  $1.4^\circ$  to  $12.2^\circ$ . For the two sets of tests for which failure criteria of 4.5 and 5.5% axial strain were used, the strength envelopes have been plotted in Figure 6.17.

It can be seen from the values given in Table 6.17 and the plots in Figure 6.17, that the undrained strengths of the soil for these two groups of tests were different. Both sets of tests were performed over the same range of cell pressures. The differences in the undrained strength envelopes of these two sets of Q tests may be the result of one group of specimens having been tested in an undrained unloading test prior to performing the Q tests whereas the other group was not. In both of these groups of Q tests, at 4.5% and 5.5% axial strain, undrained friction angles greater than zero were measured for the soil.

For the group of tests where a limiting axial strain of 10% was used as the failure criterion, the undrained strength envelope has been plotted in Figure 6.18. For this group of tests, at 10% axial strain, the undrained friction angle of the soil was close to zero.

For the undrained strength envelope presented in Table 6.17 in which a  $\phi_u = 0$  envelope was approached, the ratio of  $S_u/\sigma'_v$  has been calculated and is also presented in Table

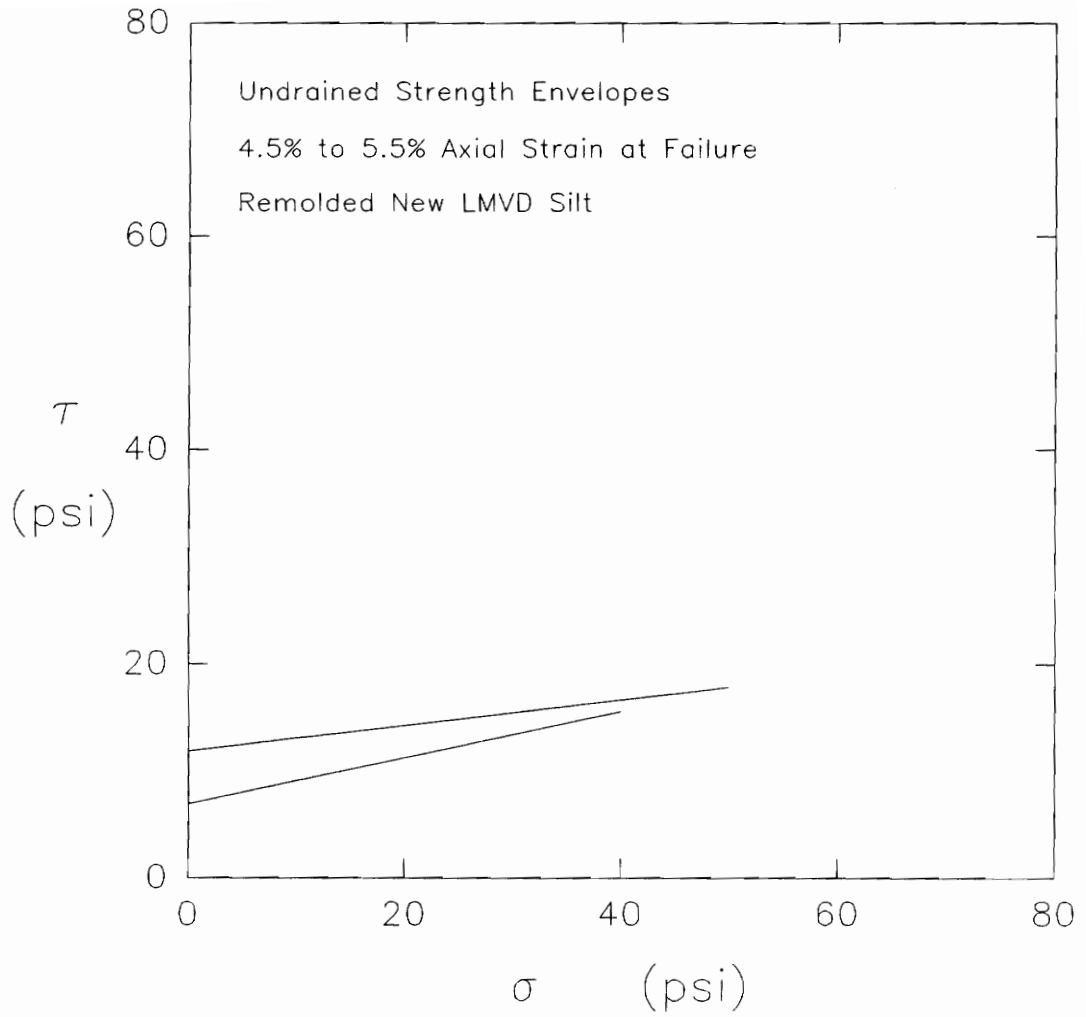


**Figure 6.17** Undrained strength envelopes for remolded new LMVD silt, based on 4.5% and 5.5% axial strain at failure

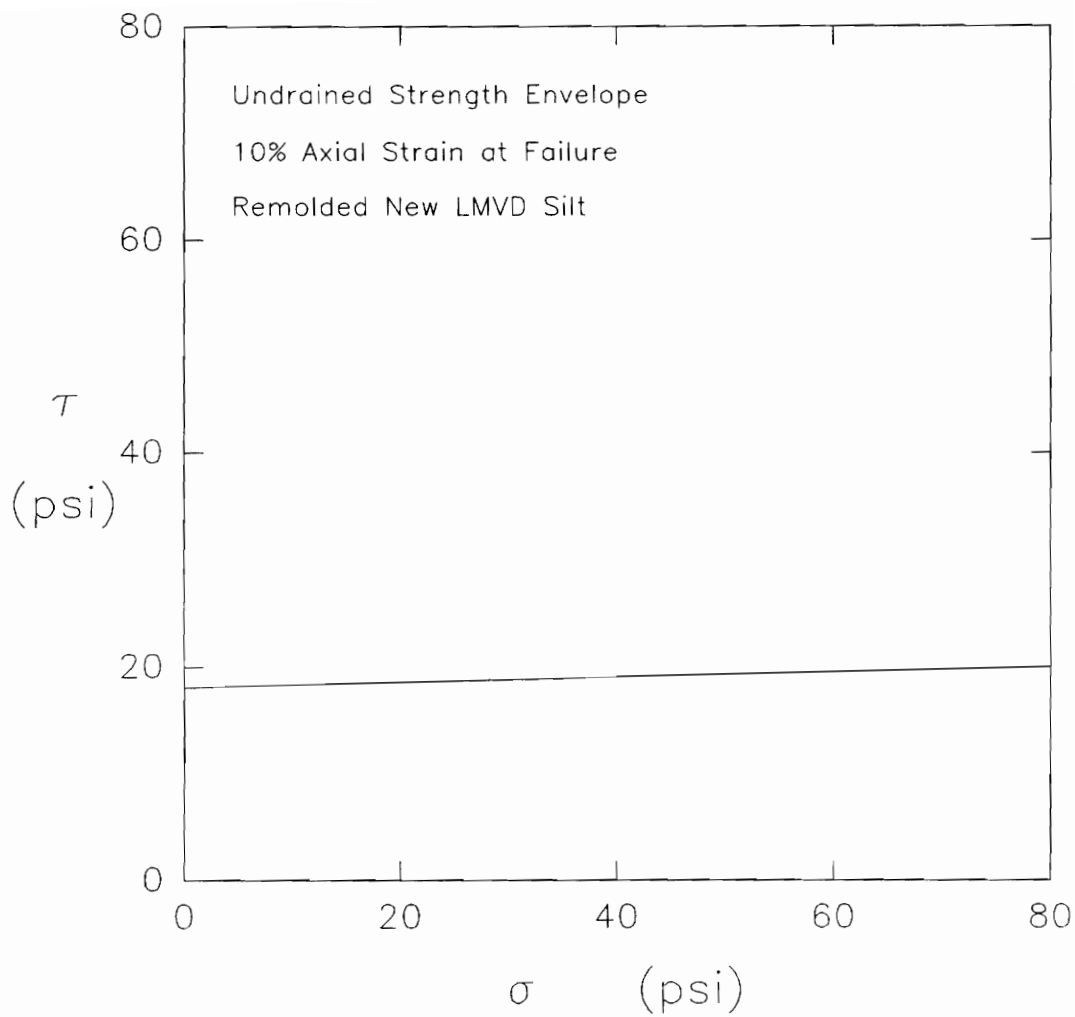


**Figure 6.18. Undrained strength envelope for remolded new LMVD silt, based on 10% axial strain at failure**

6.17. The value of  $S_u$  used is for  $\sigma = 0$  psi, so that  $S_u = c$ . The value of  $S_u/\sigma'_v$  calculated for this one group of tests on remolded new LMVD silt was 0.27.

Undrained strength envelopes were also developed for new LMVD silt based on the peak values of deviator stress measured in the Q tests. Depending on the range of values of cell pressure used, some of the Q tests yielded linear undrained strength envelopes, whereas others gave bilinear envelopes. A summary of both the linear and bilinear undrained strength envelopes for new LMVD silt are presented in Table 6.18.

The values of the undrained strength parameters given in Table 6.18 show some variation. For the linear,  $\phi_u > 0$  envelopes and the  $\phi_u > 0$  portions of the bilinear envelopes, the values of undrained cohesion intercept,  $c$ , varied from 7 psi to 9.9 psi. The values of undrained friction angle,  $\phi_u$ , varied from  $12.2^\circ$  to  $20.8^\circ$ . For the  $\phi_u = 0$  linear envelopes and the  $\phi_u = 0$  portions of the bilinear envelopes, the values of undrained cohesion intercept,  $c$ , varied from 24 psi to 26.5 psi. The undrained friction angles,  $\phi_u$ , for these envelopes varied from  $0^\circ$  to  $1.7^\circ$ .

**Table 6.18: Undrained strength parameters determined from Q tests on remolded new LMVD silt, based on peak deviator stress failure criterion**

Figure Number	Tests	$\sigma'_v$ (psi)	$e_{ave}$	Range of $\sigma$ (psi)	$c$ (psi)	$\phi_u$	$S_u/\sigma'_v$
5.54*	UU-25 UU-26 UU-27	65	0.697	up to 40	7	12.2°	-
5.115	B17-1 B17-2 B17-3 B17-4	67	0.626	0-40 >40	9.9 25.6	20.8° 0°	- 0.38
5.118	B18-1 B18-2 B18-3 B18-4	67	0.613	up to 130	24.7	1.7°	0.37
5.120	B17-1 B17-2 B17-3 B17-4 B18-1 B18-2 B18-3 B18-4	67	0.619	0-45 >45	9.9 26.5	20.8° 0°	- 0.40

\* Q test specimens trimmed from unloading test specimen

For the undrained strength envelopes presented in Table 6.18 in which a  $\phi_u = 0$  envelope was approached, the ratios of  $S_u/\sigma'_v$  have been calculated and are also presented in Table 6.18. The values of  $S_u$  used are for  $\sigma = 0$  psi, so that  $S_u = c$ . The values of  $S_u/\sigma'_v$  for new LMVD silt vary from 0.37 to 0.40. These values of  $S_u/\sigma'_v$  based on peak deviator stress are higher than the value calculated based on 10% axial strain at failure, as expected.

The undrained strength envelopes presented in Table 6.18 for new LMVD silt, based on peak values of deviator

stress, are plotted together in Figure 6.19. From the values of the undrained strength parameters given in Table 6.18 and the plots shown in Figure 6.19, some similarity is apparent between the undrained strengths obtained from the B17 and B18 groups of specimens. The B17 and B18 groups of specimens were performed at cell pressures between 0 and 30 psi whereas the B18 group of specimens were performed at cell pressures between 20 and 80 psi.

The results of several groups of Q tests performed in this research show that up to certain values of axial strain, a  $\phi_u = 0$ ,  $S_u = c$  undrained strength envelope was obtained for the soil. In these same groups of Q tests,  $\phi_u > 0$  undrained strength envelopes were obtained when higher values of axial strain, or the peak value of deviator stress were used as failure criteria.

Figure 6.20 shows the Mohr's circles for Q tests B8-1, B8-2, and B8-4 based on 6% axial strain as the failure criterion. These specimens had an average void ratio of 0.474. In this case, the undrained strength of the soil is defined by the parameters  $c = 7.6$  psi and  $\phi_u = 1.0^\circ$ . When 15% axial strain is used as the failure criterion, the undrained strength envelope shown in Figure 6.21 is obtained. At this level of axial strain, the undrained

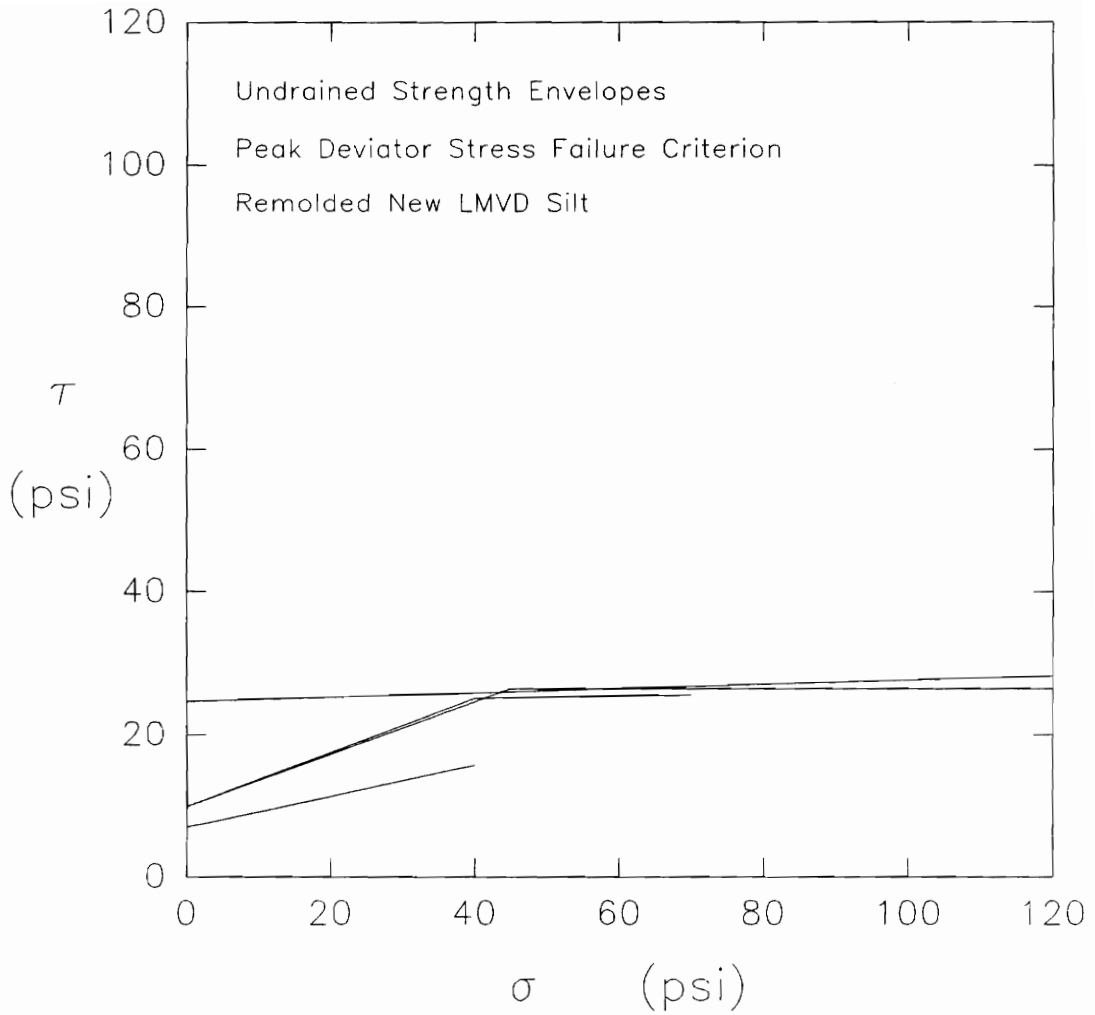


**Figure 6.19. Undrained strength envelopes for remolded new LMVD silt, based on the peak deviator stress failure criterion**

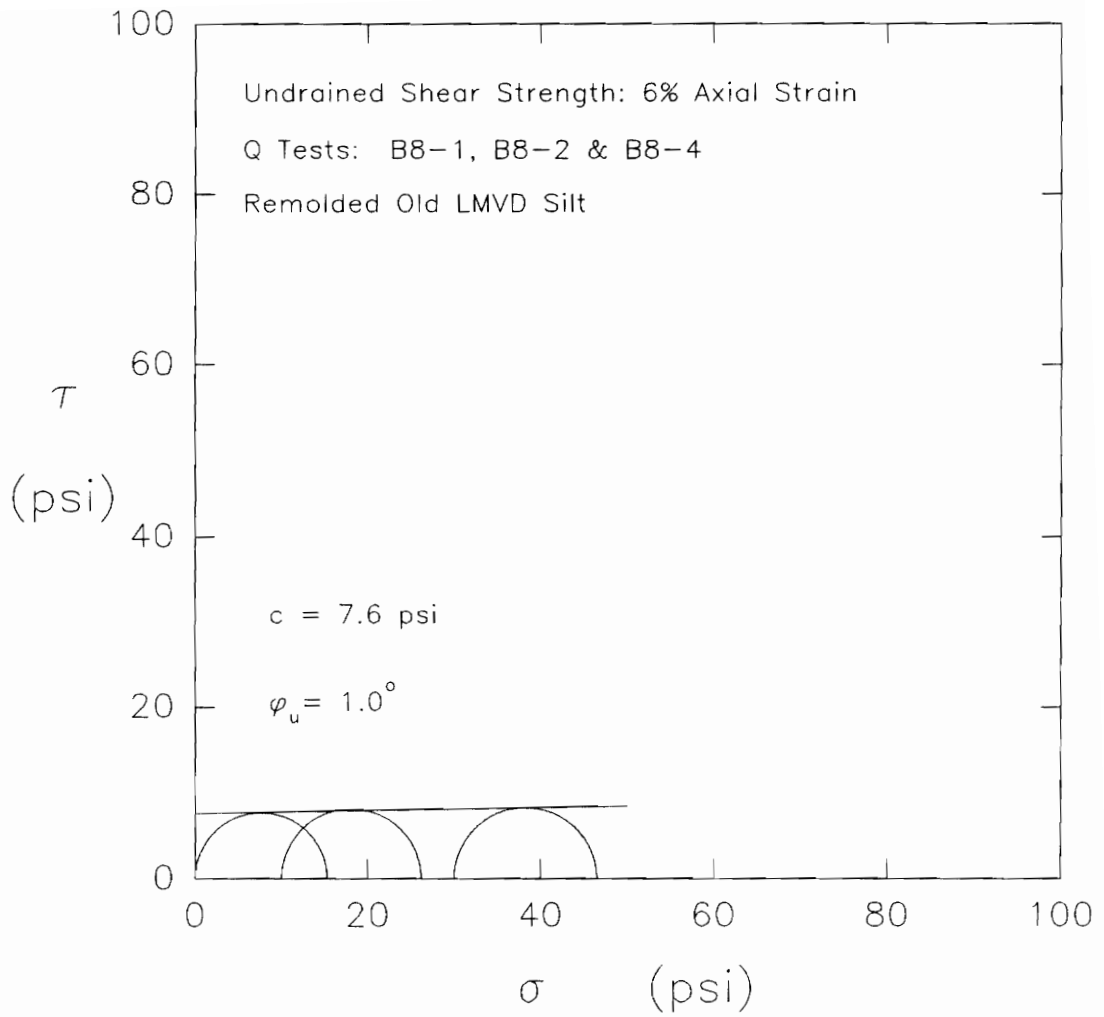


**Figure 6.20. Total stress Mohr's circles for Q tests B8-1, B8-2, and B8-4, based on 6% axial strain as the failure criterion**

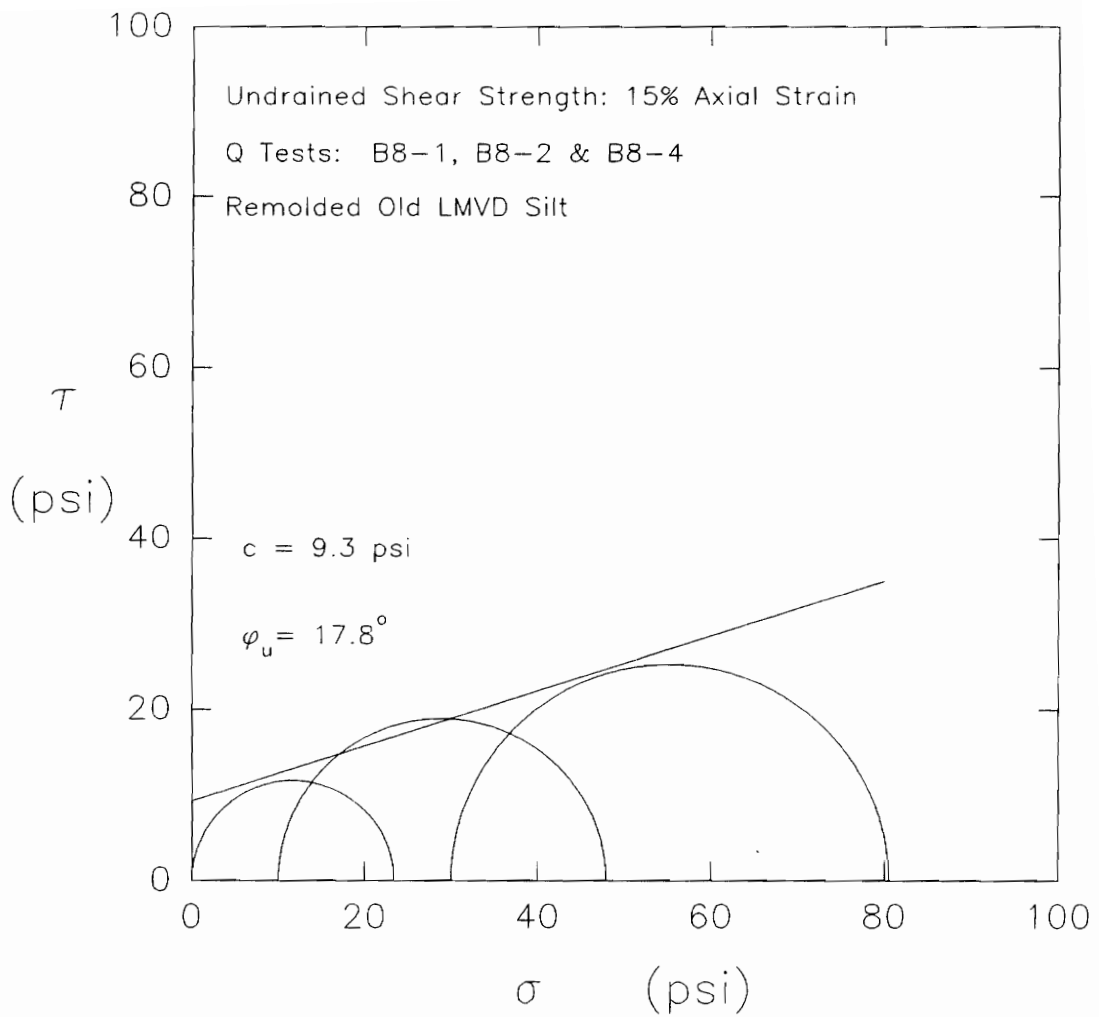


**Figure 6.21. Total stress Mohr's circles for Q tests B8-1, B8-2, and B8-4, based on 15% axial strain as the failure criterion**

strength of the soil is characterized by the parameters  $c = 9.3$  psi and  $\phi_u = 17.8^\circ$ .

For Q tests B9-1, B9-2, and B9-4, at 10% axial strain, the undrained strength of the soil was defined by the parameters  $c = 9.1$  psi and  $\phi_u = 1.5^\circ$ , as was shown in Figure 5.88. The average void ratio of these specimens was 0.512. At 15% axial strain, the undrained strength envelope, shown in Figure 6.22, is defined by the parameters  $c = 12.8$  psi and  $\phi_u = 2.6^\circ$ .

The Q tests B11-1, B11-2, B11-3, and B11-4 gave the undrained strength envelope, for a failure criterion of 9% axial strain, shown in Figure 5.91. In these specimens, the average void ratio was equal to 0.479. The undrained strength parameters of the soil for this failure criterion were  $c = 8.1$  psi and  $\phi_u = 0.3^\circ$ . When 15% axial strain was chosen as the failure criterion, the undrained strength envelope for the soil, plotted in Figure 6.23, gives the strength parameters  $c = 5.1$  psi and  $\phi_u = 15.3^\circ$ .

These comparisons of undrained strength envelopes at different axial strains for LMVD silt, illustrate several important aspects of saturated silt behavior in Q tests. If a series of high quality Q tests are performed on specimens of saturated, dilatant silt, up to a certain value of axial strain, a  $\phi_u = 0$  undrained strength envelope will be

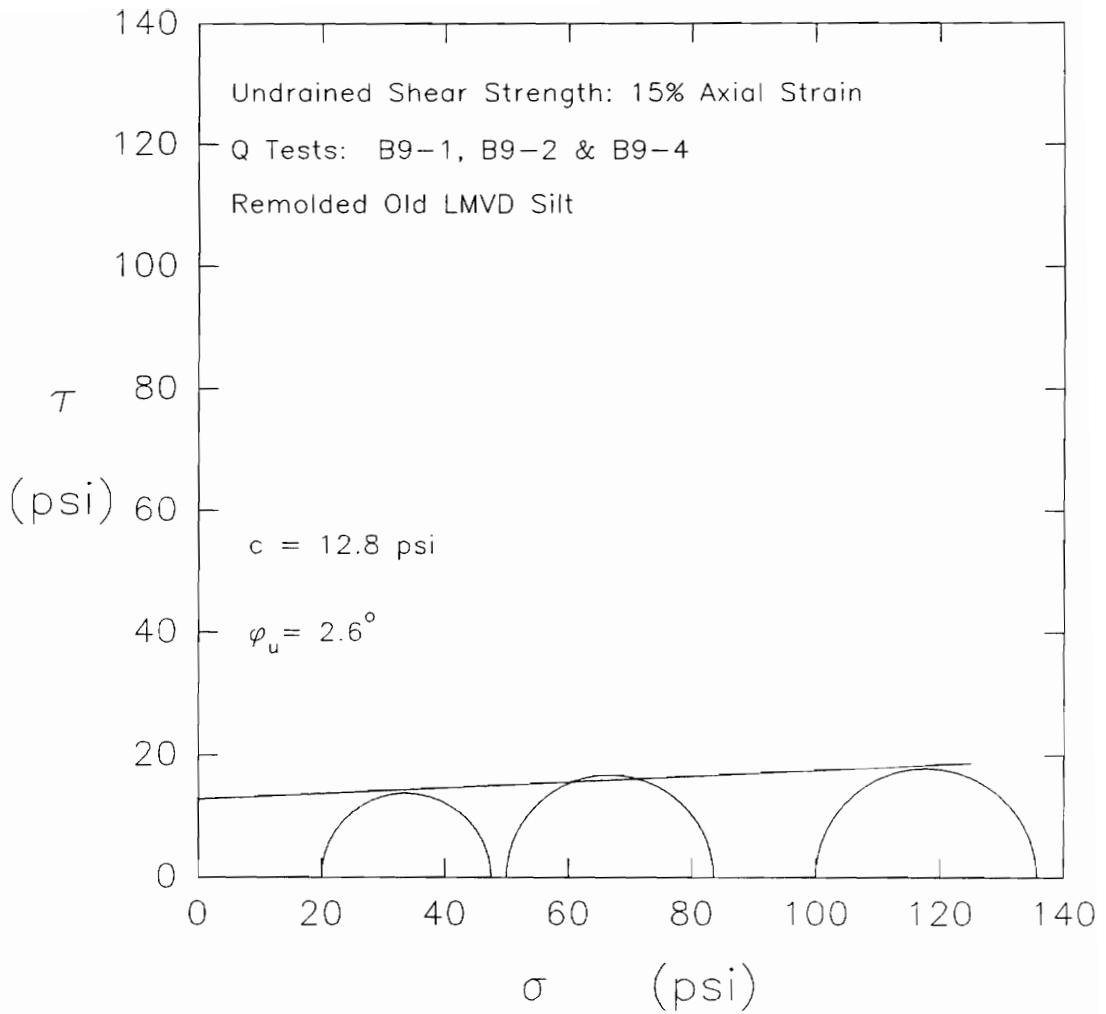


**Figure 6.22. Total stress Mohr's circles for Q tests B9-1, B9-2, and B9-4, based on 15% axial strain as the failure criterion**

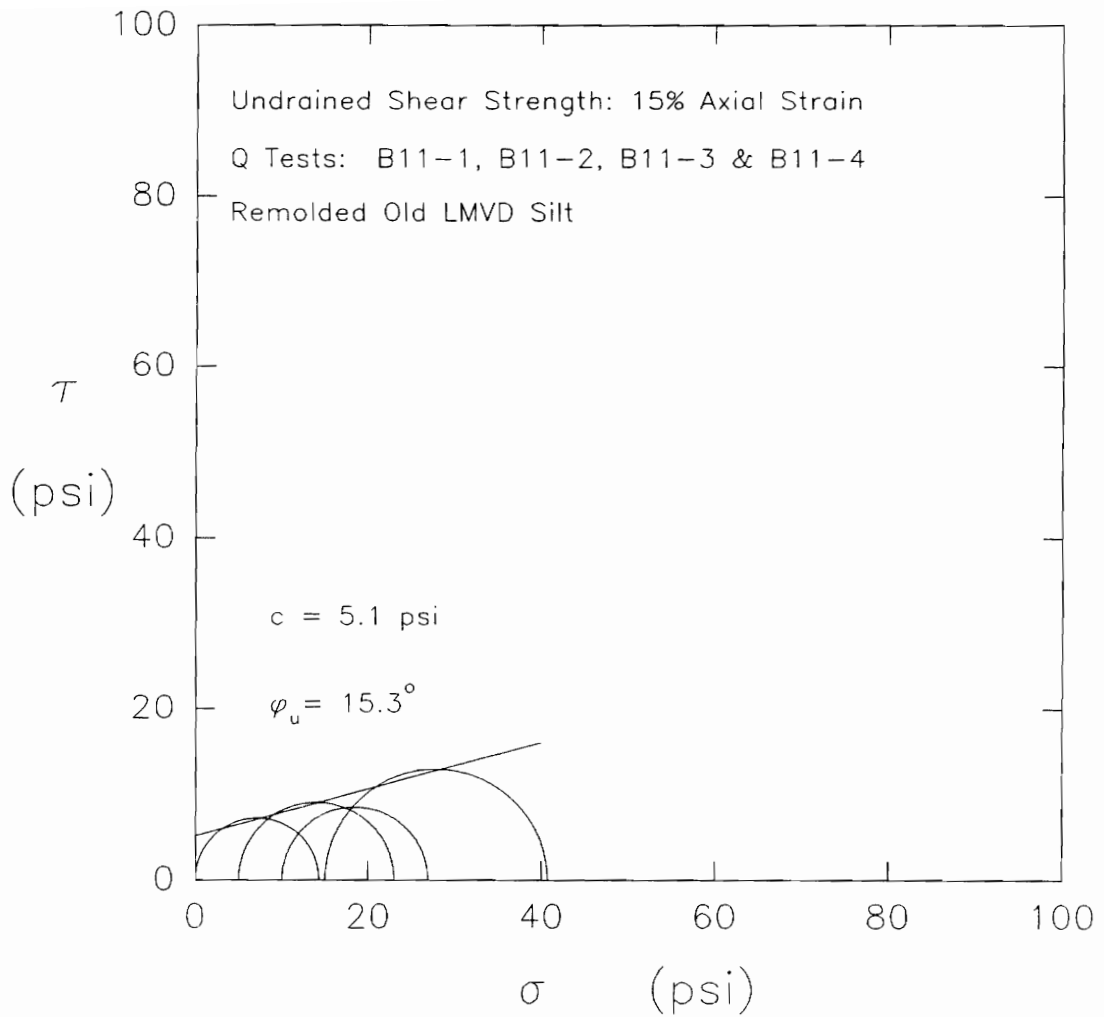


**Figure 6.23. Total stress Mohr's circles for Q tests B11-1, B11-2, B11-3, and B11-4, based on 15% axial strain as the failure criterion**

obtained. The value of limiting axial strain up to which  $\phi_u = 0$  behavior was obtained varied in this research. The variations may be the result of different void ratios and the resulting variation in the dilatant tendencies of the specimens.

The lower average values of void ratio in the B8 specimens resulted in deviations from  $\phi_u = 0$  behavior beginning at about 6% axial strain. For the B9 specimens, the higher value of average void ratio resulted in  $\phi_u = 0$  behavior continuing up through an axial strain of about 10%. Even at 15% axial strain, the B9 group of specimens had an undrained friction angle,  $\phi_u$ , that was only slightly greater than zero. In the case of the B11 specimens, the average void ratio was between that of the B8 and B9 specimens. The average void ratio of the B11 specimens was actually closer to the lower value of average void ratio of the B8 specimens. The B11 specimens tended to show  $\phi_u = 0$  behavior up through about 9% axial strain.

Other factors, such as different levels of specimen disturbance, different amounts of dissolved air in the soil pore water, slightly different strain rates during shear, and even different temperature and humidity conditions in the laboratory, may also have influenced the value of axial

strain at which the undrained strength of the soil began to show increased deviation from  $\phi_u = 0$  behavior.

Fleming and Duncan (1990) suggested that 15% axial strain may be used as a reasonable failure criterion for most engineering projects in the determination of the undrained shear strength of silts. Applying this value of axial strain as a failure criterion to the LMVD silt used in this research would tend to result in  $\phi_u > 0$  undrained strength envelopes for the soil. In addition, for many of the Q tests performed at low cell pressures in this research, peak values of deviator stress were observed at axial strains below 15%. In these cases, the 15% axial strain failure criterion should not be used and peak deviator stresses should be used instead.

The observed variation in the axial strain at which the deviation from  $\phi_u = 0$  behavior began in the Q tests on LMVD silt, further suggests that the use of a consistent value of limiting axial strain at failure for a given engineering project may result in variations in the undrained strength behavior of the soil. The value of limiting axial strain up to which a  $\phi_u = 0$  undrained strength envelope will be obtained may vary for each set of Q tests. The variation may be dependent on factors such as specimen void ratio, disturbance levels, degree of saturation, and dissolved gas

content of the soil pore water. This would be expected to be true for other silts, as well.

For cases where a  $\phi_u = 0$  undrained strength envelope is not obtained at any value of axial strain, or only at very low axial strains, the undrained strength of the soil is difficult to evaluate. The absence of a  $\phi_u = 0$  condition for a given set of Q tests on a saturated, dilatant silt, may be the result of the specimens experiencing different levels of disturbance, giving inconsistent stress-strain behavior.

As with performing all strength tests on soil, disturbance should be minimized in order to get the highest quality and most reliable results. This is especially true for silts, which tend to be more susceptible to disturbance than clays (Fleming and Duncan, 1990). If noticeable disturbance occurs or difficulties are encountered in setting up and performing a given Q test on a silt specimen, the disturbance should be noted and the results of the test discarded or de-emphasized in the analysis and determination of the undrained shear strength of the soil.

#### **6.11 Discussion of Back Pressure Saturated Q Tests**

The use of a back pressure in Q test specimens of saturated silts was investigated and showed some interesting

results. For specimens tested at the same cell pressure, the use of a back pressure in Q test specimens, tended to give higher values of undrained shear strength than measured in specimens without back pressure. The higher the back pressure used in these specimens, the higher the undrained strength. The slopes of the stress-strain curves tended to be similar for specimens tested both with and without back pressure, at the same cell pressure.

In Q tests performed at low values of cell pressure, the specimens with back pressure tended to show less abrupt strain-softening than specimens without back pressure. The specimens with back pressure tended to reach peak values of deviator stress at higher axial strains than specimens without back pressure.

Specimens with similar initial values of pore water pressure, gave peak undrained strengths for the soil which tended to be of a similar order of magnitude, regardless of whether the initial pore water pressure resulted from back pressure, cell pressure, or a combination of back pressure and cell pressure. The undrained strength of a soil with dilatant tendencies appears to depend on the magnitude of the decrease in pore water pressure possible in the specimen, and not on how the initial pore water pressure in the specimen was developed. The slopes of the stress-strain

curves, however, did tend to vary somewhat, which may have resulted from the method by which the initial pore water pressure was developed in the specimen.

The back pressure saturated specimens had increased strengths, relative to the specimens tested without back pressure at the same cell pressure. This increase in strength resulted from two sources. The first source of increased strength was the higher value of initial pore water pressure in the back pressure saturated specimens. This allowed for larger decreases in pore water pressure during undrained shear. As a result, more strain-hardening occurred and higher undrained strengths were measured.

The second source of increased strength was the slight consolidation of the back pressure saturated Q test specimens. During the application of the back pressure, the Q test specimens were subjected to an effective stress of 2 psi. This small value of effective stress would have consolidated the specimens slightly, leading to some increase in the strength of the soil. This small value of effective stress, however, is only slightly greater than the values of residual effective stress measured in some of the Q tests performed in this research, as discussed in Section 6.1. As a result, the increase in strength of these Q test specimens, due to their being consolidated to  $\sigma'_{3con} = 2$

psi, may not be that significant. The increase in strength resulting from the higher initial value of pore water pressure in the back pressure saturated specimens may be much more substantial.

Fleming and Duncan (1990) noted that Q tests on saturated silts tended to give undrained strengths lower than in-situ strengths. They added that reconsolidating the soil to the in-situ consolidation stress conditions resulted in the measurement of undrained strengths that were higher than in-situ strengths. The small consolidation pressure of 2 psi used in the back pressure saturation of the Q test specimens gave measured strengths that were higher than determined in conventional Q tests. The undrained strengths determined in the back pressure saturated specimens, however, are likely below those that would be measured if the specimens had been reconsolidated to the in-situ stress conditions prior to undrained shear. The strengths measured in the back pressure saturated Q tests may therefore be conservative relative to the in-situ strength of the soil.

The use of a back pressure resulted in Q test specimens that were more fully saturated. The back pressure also delayed the onset of cavitation or degassing of the pore water during undrained shear of dilatant specimens until higher axial strains had been reached.

The use of a back pressure in these Q tests is felt to represent field conditions where the in-situ hydrostatic pore water pressure would be greater than the applied undrained loading. The value of initial pore water pressure is significant in Q tests on saturated, dilatant silts and can influence the peak strength of the soil. Using higher cell pressures in Q tests to achieve appropriate values of initial pore water pressure appears to have a similar effect on the undrained strength of the soil and is an easier test procedure than attempting to back pressure saturate the specimens.

Even with the use of a back pressure in Q tests on saturated, dilatant silts, the use of a limiting axial strain would still be necessary to obtain an undrained strength envelope characterized by a  $\phi_u = 0$  condition. This is due to the dilatant tendencies and strain-hardening behavior of the soil during undrained shear. Back pressure saturated Q test specimens of a dilatant silt will still tend to yield a  $\phi_u > 0$  undrained strength envelope for the soil when peak values of deviator stress are used as the failure criterion.

## 6.12 Consideration of Observed Stress-Strain Behavior

This research study has verified that unconsolidated undrained (Q) triaxial tests on saturated, dilatant silts exhibit erratic stress-strain behavior. By considering the behavior that might be expected if dissolved gases were to come out of solution from soil pore water during undrained shear, some insight and explanation may be obtained as to why saturated silts exhibit erratic behavior.

A saturated silt can be thought of as a composite material. According to Dowling (1993), composite materials are generally made by combining two or more materials which are insoluble in each other to create a new material with more desirable properties. Within the composite material, the individual components retain their individual properties.

Although saturated soils do not precisely fit the above definition for a composite material, they can be considered a type of naturally occurring composite material. A saturated soil is composed of a matrix of solid soil grains surrounded by a liquid phase (water). Both the solid soil grains and the water have unique properties. When the two materials are combined, they create a new material with properties which are different and perhaps less desirable than those of the individual components.

The presence of the water in the pores of a fully saturated soil makes the material essentially incompressible under undrained conditions. On the other hand, the water provides no additional shear strength to the soil and the shear strength of the material is governed by the intergranular forces (Bishop and Eldin, 1950).

When a saturated silt is sheared in a triaxial test, it has a tendency to dilate or expand in volume. During undrained shear, this tendency for dilation leads to a reduction in the pore water pressure within the saturated silt specimen. The decrease in pore water pressure which occurs during the tests has a strengthening effect on the soil. It causes an increase in the effective confining pressure on the specimen, leading to stress-strain behavior which is characterized by strain-hardening.

If the pore water pressure is reduced below atmospheric pressure, the pore water will be in tension. Liquid water has some ability to withstand negative pressures or tensile stresses. There will be some limitation on how negative the pore water pressure can become before cavitation occurs. When the limiting negative pressure or tensile strength of the water is reached, the pore water will cavitate and the triaxial specimen will no longer experience strain-hardening.

As was discussed in Chapter 3, the tensile strength of water is influenced by the presence and distribution of cavitation nuclei within the liquid. In addition, the presence of dissolved gases in the pore water could lead to variations in the tensile strength of the water. Variations in the dissolved gas content of the pore water may result in gas bubble formation at different negative pore water pressures within the soil. Pre-existing air bubbles of different sizes, within the pores of the soil, could also facilitate bubble formation and growth at various pressures.

#### **6.12.1 Strain-hardening of Saturated, Dilatant Materials**

Strain-hardening behavior in dense, saturated geologic materials under undrained conditions has been observed and discussed by a number of researchers (Reynolds, 1885, 1886; Mead, 1925; Brace and Martin, 1968; Rice, 1975). Several of these researchers noted or implied that the strain-hardening resulting from the dilatant tendencies of the materials may be limited in some way.

Reynolds (1885) is generally credited as being the first to identify and describe dilatancy in granular materials. Based upon his observations of simple experiments with lead shot, Reynolds concluded that, in general, a granular material subjected to any slight disturbance, will experience some change in volume. If the

material is initially dense, its volume will tend to increase due to dilation. He noted that different parts of a granular material may dilate to different degrees under an applied loading.

Reynolds (1886) also studied the dilatant behavior of saturated granular masses under undrained conditions. He noted that when a saturated dilatant material was placed in a sealed bag and was squeezed between two plates, the mass experienced hardening. He added that the amount of dilatant hardening which could occur was limited by the properties of the water. If a large enough force was applied, a vacuum could be created within the mass. Reynolds (1886) called this the formation of a vacuum. Today this is what is commonly referred to as cavitation of the water.

Reynolds (1886) attached a mercury based pressure measurement gage to a sealed rubber bag filled with a dense sand. The voids of the sand were filled with water and no air was present. He found that upon squeezing the bag, the dilatant tendency of the material resulted in the water pressure decreasing below atmospheric pressure to about -27 inches of mercury (-13.2 psi). Additional squeezing of the bag resulted in only a slight further decrease in water pressure before a vacuum was formed within the bag. The

formation of a vacuum at a gage pressure of about -27 inches of mercury corresponds to vaporous cavitation of the water.

Mead (1925) noted that the tensile strength of the pore fluid may limit the degree of rigidity which can be attained by saturated, granular, geologic materials with dilatant tendencies under undrained conditions. He observed that during undrained deformation, the tendency for dilation lead to failure of the material by fracture along definite shear planes rather than by plastic yielding of the material. Mead's observations suggest that under undrained conditions in a dilatant, granular material, in the zone with the maximum tendency for dilation, the pore fluid may cavitate resulting in the occurrence of an abrupt fracture on a well-defined shear plane. If cavitation does not occur, the material may be more likely to experience plastic deformation and failure.

Brace and Martin (1968) studied the behavior of saturated, crystalline rocks of low porosity in triaxial compression. They found that when the specimens were tested at slow rates of strain, drainage of pore water was able to occur. At higher rates of strain, drainage of the pore water could not take place and negative pore water pressures developed. These negative pore water pressures lead to strain-hardening of the rock mass. They noted, however,

that there was a limit on how negative the pore water pressure could become. They stated that when the pore pressure had decreased to about zero absolute pressure, no further strain-hardening was possible regardless of the rate of loading.

Rice (1975) also studied the hardening behavior of saturated rock masses under undrained conditions. During rapid loading, such as might occur during seismic events, drainage of the rock mass may not be able to occur. The dilatant tendency of the rock material lead to a decrease in the pore water pressure under undrained conditions. This resulted in dilatant hardening of the rock. He noted that there were limitations on the amount of dilatant hardening that the rock mass could experience.

#### **6.12.2 Strain-softening in Saturated, Dilatant Materials**

Brace and Martin (1968), Rice (1975), and Wheeler (1988a, 1988b) indicated that under certain conditions, a geologic material which had experienced strain-hardening due to its dilatant tendencies, may subsequently exhibit strain-softening behavior.

Brace and Martin (1968) observed that saturated porous rock masses tended to fail along definite shear planes, regardless of the strain rate used in the test and the

drainage conditions which resulted. After reaching peak strengths, the failure of the test specimens was characterized by strain-softening. There was a notable difference observed in the strain-softening for the different strain rates used in the tests. Saturated porous rock masses tested at slow strain rates showed much more gradual strain-softening than when the rocks were tested at rapid strain rates. At rapid strain rates, the strain-softening occurred very suddenly and the failure plane in the rock mass formed abruptly.

As previously noted, the slow strain rates lead to drained conditions in the rock while the rapid strain rates resulted in undrained conditions and the development of negative pore pressures. In the slowly sheared specimens, drained conditions lead to volume expansion and failure along well-defined shear planes. This resulted in gradual strain softening behavior. In the rapidly sheared specimens, the formation of a well-defined shear plane was combined with abrupt strain softening. This suggests that cavitation of the pore water occurred along the shear plane leading to an abrupt failure and rapid strain-softening.

Rice (1975) studied the parameters which control the dilatant hardening behavior of saturated rock masses under undrained conditions. He found that the amount of dilatant

hardening that the rock mass could experience was limited. In his model of the behavior, the dilatant hardening that the undrained rock mass experienced became unstable when the drained stress-strain curve was decreasing and strain-softening was occurring.

Rice (1975) noted that significant increases in strength are measured for saturated dilatant rocks in undrained tests, as opposed to during drained tests. He added that even when the drained stress-strain curve showed strain-softening, the undrained curve could still be exhibiting strain-hardening. He stated, however, that continuous hardening can not be achieved in practice. He added that the increased strength resulting from the hardening behavior in undrained tests should only be considered when the drained stress-strain curve is experiencing strain-hardening as well. Once the drained stress-strain curve begins to show strain-softening, the increased strength observed in the undrained behavior should be neglected.

Wheeler (1988a) proposed a model for the behavior of gas bearing marine soils. The model predicts that if the volume of free gas present in bubbles within the sample decreases during shear, the stress-strain curve of the specimen will exhibit strain-hardening. This behavior was

observed in triaxial tests on remolded specimens of normally consolidated soil containing bubbles of methane gas (Wheeler, 1988b).

The measurement of the volume change of the triaxial cell fluid and its relation to specimen volume change in undrained triaxial tests performed by Wheeler (1988b) indicated that the gas bubbles were compressed during undrained shear, forcing gas into solution in the pore water. This resulted in strain-hardening behavior being observed for all of the tests, as predicted by the model (Wheeler, 1988a).

Wheeler (1988a) noted that the model predicted that if the gas bubbles expanded during shear, a decrease in the stress required to cause further deformation would have been observed, resulting in strain-softening behavior. All of Wheeler's (1988b) triaxial tests were on normally consolidated specimens of a gassy clay soil so that bubble shrinkage occurred rather than bubble expansion. If tests had been performed on overconsolidated samples containing bubbles of methane gas, bubble expansion may have resulted, leading to strain-softening during undrained shear.

### 6.12.3 Experimental Studies and Model Predictions of the Behavior of Materials Containing Voids

Stress-strain models for the behavior of solid materials which contain some small pre-existing pores or voids indicate that these materials may also exhibit strain-softening behavior if these voids in the material grow in size due to the applied loading (Berg, 1970; Green, 1972).

Berg (1970) noted that a material with a porous structure can show both hardening and softening behavior with increasing strain. In a solid material containing micro-cavities or voids, if there is negligible cavity growth or if the cavities shrink, the material will show hardening behavior. If the material dilates and the cavities grow and interact with each other, strain-softening will result. As the cavities grow and interact, the actual load carrying area on a section through the material will decrease. With less area available to carry load, the strength of the material will decrease, leading to strain-softening behavior.

Green (1972) presented a plasticity theory for a solid material containing spherical voids. He assumed that the solid material exhibited rigid-perfectly plastic behavior and that the growth or decay of the voids occurred isotropically. His model predicted that the presence of spherical voids within the solid material will cause the

yield stress of the material to be less than if no voids were present.

The model proposed by Green (1972) indicated that the post-yield behavior of the material may be quite different when tensile stresses are present within the material, as opposed to compressive stresses. He stated that the solid portion of the porous material behaves similarly in both tension and compression. The behavior of the whole material of solids and voids in tension, however, is different than it is in compression.

In compression, the voids will shrink leading to a strengthening effect in the material. This strengthening is characterized by strain-hardening of the whole material, even though the solid material itself does not exhibit strain-hardening. If tensile stresses are present within the material surrounding the voids, the voids will tend to grow larger. As the volume of voids within the material increases, the yield stress decreases and strain-softening results.

Other theoretical models and experimental studies of solid materials and composites containing two different materials indicate that cavity formation and growth within the material is possible under certain loading conditions. The presence of these cavities in materials may lead to a

reduction in the strength of the material and failure (Gurson, 1977; Vaandrager and Pharr, 1989; Evans and Rana, 1980; Heuer et al., 1980; Sheikh and Pharr, 1985).

Gurson (1977) developed a constitutive theory, yield criteria, and physical model for ductile porous media. His theory considers the nucleation and growth of voids within the material during ductile fracture. He stated that the *hydrostatic stress* has a significant influence on plastic yield and void growth within the material.

According to Frederick and Chang (1965), under certain conditions, the stresses acting on a material can be decomposed into two parts. One part is called the hydrostatic stress which represents a uniform normal stress acting equally in all directions. The other part gives a stress state of pure shear, otherwise known as the stress deviator.

The principal stresses acting externally on a triaxial specimen ( $\sigma_1$  and  $\sigma_3$ ) are both compressive stresses having the same sign; therefore, they do not meet the requirements necessary for decomposition into a hydrostatic stress and a state of pure shear. The pore water within the specimen is isotropic with respect to stresses. The shear stress in the pore water will be zero and the normal stress will be hydrostatic. This uniform normal stress or pressure in the

pore water will be either positive (compression) or negative (tension) and will act equally in all directions.

Gurson's (1977) theory for plastic dilation requires that some initial porosity be present within the material. He added that when no pores are initially present within the material, the nucleation and growth of spherical voids can result from the failure of the bonds between the different material phases or substances present within the specimen during deformation. Void nucleation can also occur during straining at grain boundaries within the solid material, especially where misfits occur between the solid crystals or grains. He stated that the material can experience an increase in the volume of voids as the hydrostatic stress increases (Gurson assumed that tension was positive).

Vaandrager and Pharr (1989) studied the creep behavior of solid copper with a liquid bismuth intergranular phase. They tested cylinders of the material at high temperatures in compression. After completion of the tests, the specimens were cooled under sustained load and cut open in order to examine their microstructural conditions.

It was found that the creep deformation of the specimens resulted from two different mechanisms. The first mechanism involved the redistribution of the liquid in the voids of the copper. The liquid bismuth flowed out of the

compressed boundaries which were perpendicular to the loading axis, and flowed into the less stressed boundaries, which were parallel to the loading axis. This flow of the liquid bismuth occurred very rapidly as the load was applied, and the initial deformation observed was associated with this mechanism. Under sustained load, the material continued to deform by a second mechanism referred to as "grain boundary sliding."

Vaandrager and Pharr (1989) proposed that the grain boundary sliding was "accommodated" by the nucleation and growth of cavities in the liquid bismuth. The cavities formed in the regions of the intergranular liquid bismuth where hydrostatic tension was developed. Figure 6.24 shows that as grain boundaries which were aligned parallel to the axis of compression moved apart from each other, the liquid bismuth would be subjected to tensile stresses. Eventually, under sufficient tension, cavities would form in the liquid bismuth. These cavities were observed in the solidified bismuth during the microstructural observations. Vaandrager and Pharr (1989) concluded that the creep behavior of the copper-liquid bismuth composite was dominated by the grain boundary sliding mechanism and associated cavitation in the liquid bismuth.

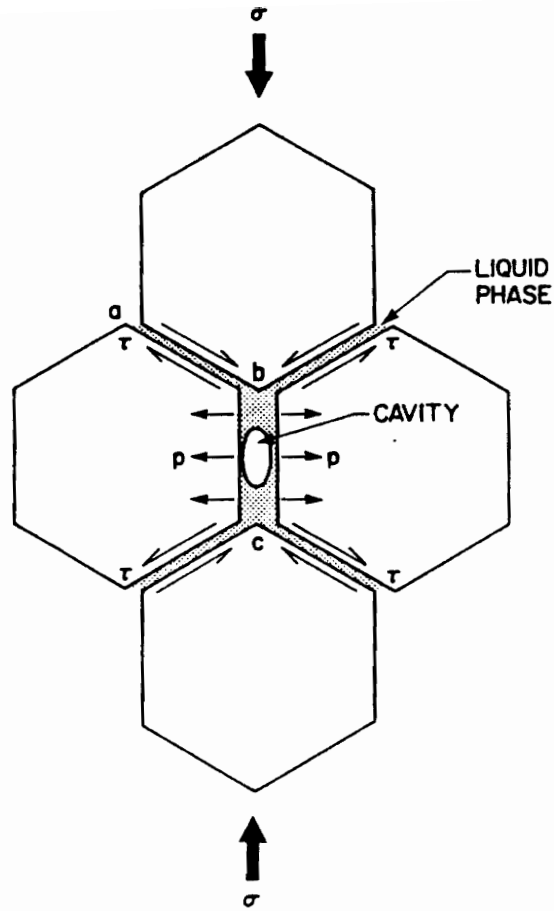


**Figure 6.24.** Schematic diagram of grain boundary sliding model proposed by Vaandrager and Pharr (1989) showing cavity formation in the liquid phase

Evans and Rana (1980) developed a model for predicting the creep failure of ceramic materials at high temperatures due to the nucleation and growth of cavities within the material. They considered three different microstructures for the material in which cavities could grow, as shown in Figure 6.25. In the first microstructure considered, the material would be composed of a single phase or material in which cavities would form and grow along the grain boundaries. The second and third microstructures consider the material to consist of two phases: (1) a solid granular phase, and (2) an amorphous intergranular phase. In the second microstructure, the amorphous second phase is continuous. In the third microstructure considered, the amorphous second phase is isolated, or non-continuous. They noted that in many ceramic materials, the second and third microstructures are more common than the first microstructure.

In their model, cavities form as a result of the viscous flow of a boundary phase or by diffusive processes in response to both external stresses and grain boundary sliding displacements. Individual cavities can grow and intersect with other cavities leading to the formation of a macrocrack, which can propagate and result in failure of the material.

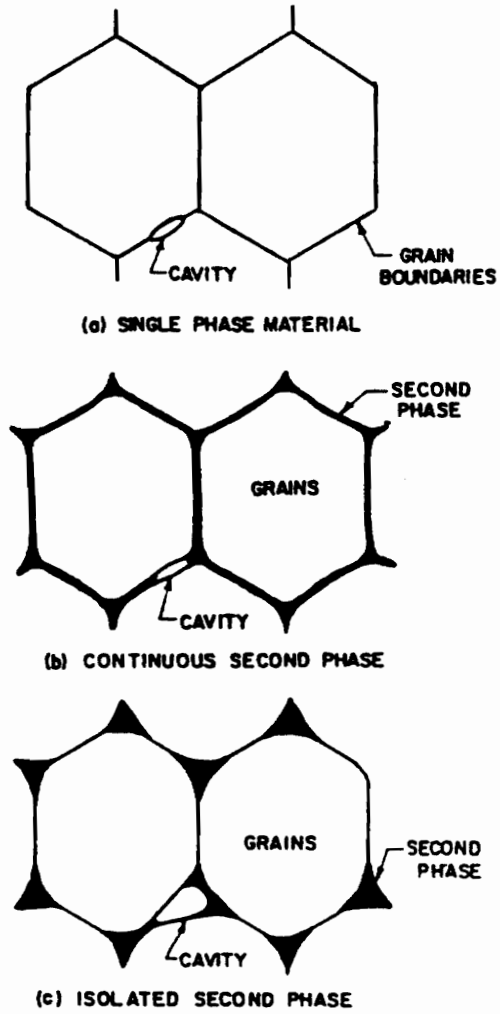


Figure 6.25. Schematic diagram of material microstructures considered by Evans and Rana (1980) for cavity formation and growth within a material

Evans and Rana (1980) noted that most ceramic materials will contain some small voids. These pre-existing voids are even present in materials thought to be made fully dense by hot-pressing. They added that if no pre-existing voids are present, some limiting stress must be exceeded in order for a void to form within the material. They also stated that when a continuous second phase is present in the material, cavitation will likely occur within this second phase.

Heuer et al. (1980) studied the deformation behavior of fine-grained alumina polycrystals with grain sizes between 1 and 5  $\mu\text{m}$ . Compression tests on cylinders machined from high-density, hot-pressed billets of alumina showed that the density of the material decreased due to the formation and growth of cavities within the material at high levels of axial strain. Heuer et al. (1980) found that a compression test specimen of alumina tested to 38 percent axial strain went from being initially at a density of 99 percent of the maximum density (maximum density corresponds to no voids being present) to having a density of only 93.3 percent of the maximum possible density of the material. They indicated that the deformation, volume increase and density decrease occurred as a result of "unaccommodated grain boundary sliding."

Sheikh and Pharr (1985) stated that the term "unaccommodated" was used by Heuer et al. (1980) to indicate that the grain boundary sliding which occurred in the specimen was not accompanied by a mechanism through which a constant volume could be maintained within the specimen. Microstructural observations by Heuer et al. (1980) showed that in the test specimens, the grains of the material had slid past each other along grain boundaries due to the applied load. Adjacent material grains were unable to undergo plastic deformation rapidly enough to keep up with the grain movement, and as a result, a void was produced at the grain boundary.

These references generally indicate that an important aspect of the creep behavior of polycrystalline solid materials and composite materials is the occurrence of grain boundary sliding, and the formation and growth of microscopic cavities or voids within the material where individual grain boundaries move apart from each other. In pure solids, this often occurs at grain boundary triple points within the grain or crystal structure. In composites containing an amorphous intergranular phase, the cavities form within the amorphous phase as the solid grains tend to move apart from each other and the amorphous phase material is placed in tension.

In these materials, as well as in saturated silts, the attempted dilation or grain boundary sliding can lead to the development of tensile stresses within the material. In a pure, solid, polycrystalline material; the individual grains are stronger than the combined grains. If the tensile strength of the bond between individual solid grains is exceeded, a void may form at the grain boundary. For solid-liquid mixtures, the solid particles are more resistant to tensile loading than the liquid, so that the tensile strength of the liquid phase limits the allowable tension which can be developed within the specimen. When the tension exceeds this tensile strength, a cavity will form within the liquid, possibly at the solid-liquid boundary.

During the shearing of saturated, dilatant materials under constant volume conditions, the attempted volume increase is resisted by the development of tensile stresses within the material. Small imperfections within a shear test specimen could possibly serve as nuclei for the formation of cavities when internal tensile forces are developed during shear. Microscopic cracks, air pockets, or unbonded grain boundaries in a single-phase, solid material could lead to concentrations of tensile stresses resulting in the possible nucleation and growth of cavities.

Similarly, in a two-phase material, an undissolved bubble or air pocket, or a solid surface not fully wetted by the liquid or amorphous intergranular phase could serve as a nucleus from which a cavity could grow. Since it is expected that such microscopic imperfections could be quite common in test specimens of many different materials, the failure of materials by grain boundary sliding and internal cavitation is a plausible failure mechanism for numerous materials, as well as for saturated silts.

#### **6.12.4 Consideration of Undrained Behavior of Saturated, Dilatant Silts**

The Q tests performed with midheight pore pressure monitoring in the early stages of this research often had stress-strain curves which showed noticeable strain-softening behavior. These occurrences of strain-softening were originally thought to be the result of disturbance caused by the presence of the midheight pore pressure monitoring probe and transducer adjacent to the specimen. Additional Q tests in which midheight pore pressure monitoring was not used also showed stress-strain behavior in which noticeable strain-softening occurred. It therefore seems possible that an alternative explanation for the observed strain-softening behavior of saturated silts may be obtained by considering the undrained mechanics of dilatant materials.

During the Q tests performed on saturated silts in this research, strain-hardening was observed in the initial stages of the tests. In the early stages of loading, the deviator stress increased with increasing axial strain. Many of the tests continued to show strain-hardening behavior throughout the entire test.

At some point in several of the Q tests, after the initial strain-hardening behavior, a peak deviator stress was reached. After this peak, the deviator stress decreased or remained relatively constant with further increase in strain, as shown in Figure 6.26. Similar behavior was observed in other Q tests, as was shown in Figures 5.50, 5.53, and 5.90. After this strain-softening occurred, in several of the tests, the specimens again began to show strain-hardening behavior, wherein the strength of the specimen again increased with increasing strain.

The strain-softening which occurred in some of the Q tests performed in this research, can possibly be explained by the formation and growth of bubbles of air or water vapor in the specimens. During Q tests on saturated soils, pore pressures will develop within the specimens. A typical section showing silt particles, pore water, and a potential shear plane is given in Figure 6.27.

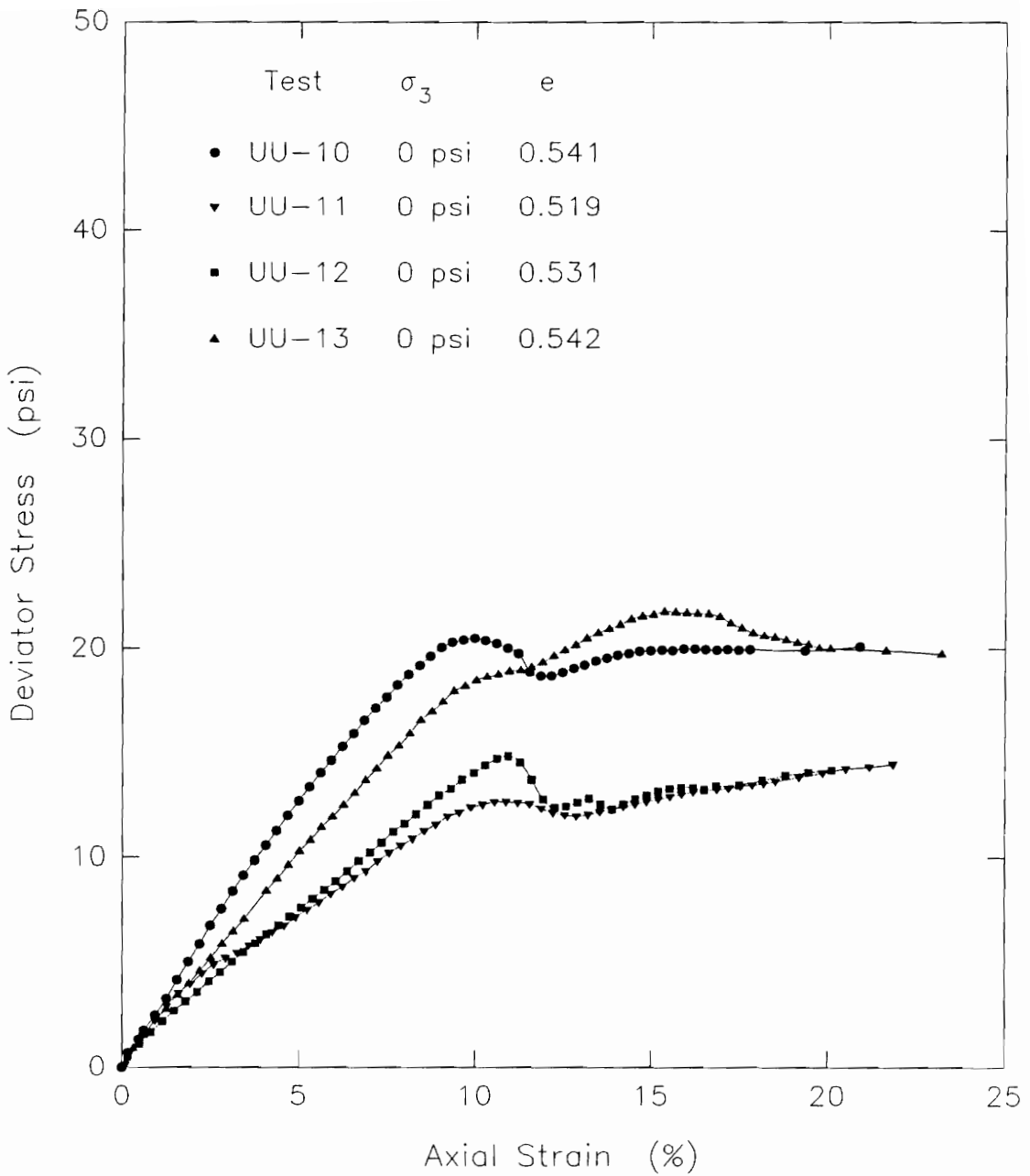


**Figure 6.26. Stress-strain curves for unconfined compression tests performed with midheight pore pressure monitoring on remolded old LMVD silt**

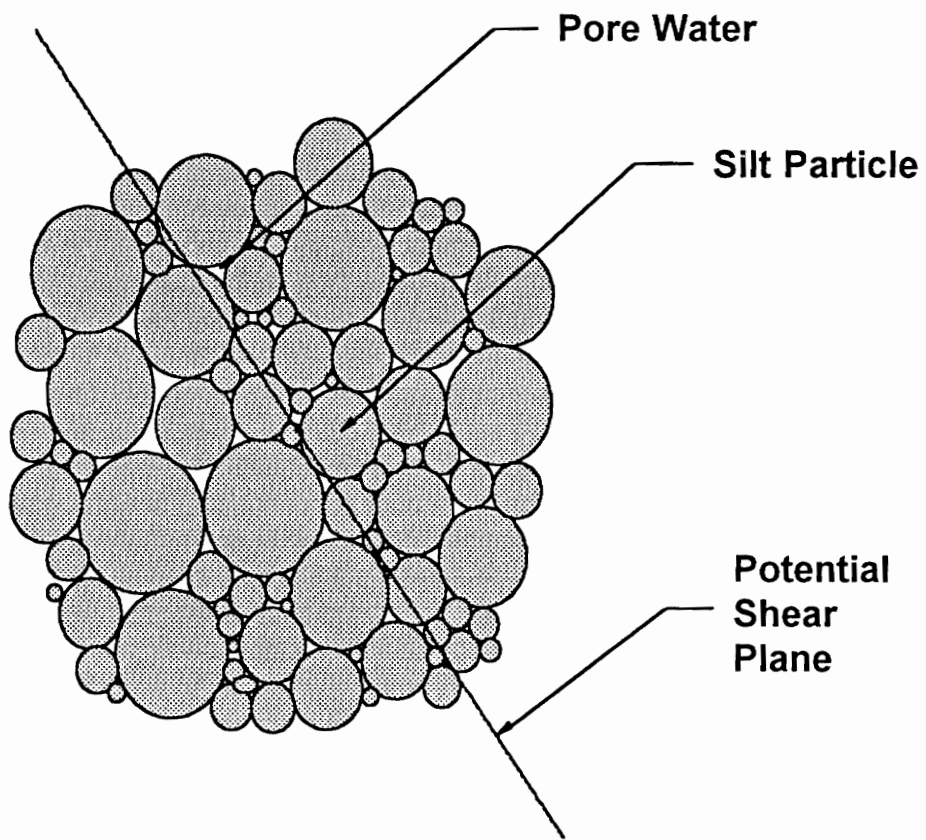


**Figure 6.27. Schematic diagram showing a cross-section through a saturated silt along with a potential shear plane**

Because the contact area between the silt particles is very small, the pore water pressures which develop during undrained shear will essentially act equally all around the silt particles (Bishop and Eldin, 1950). Due to the dilatant tendencies of the soil, the pore water pressure will decrease in a saturated silt Q test specimen. If the decrease in pore water pressure results in the pore water pressure going below atmospheric pressure, the pore pressure will have a negative gage pressure and the pore water will be in tension.

Although the magnitude of the pore water pressure may vary within a Q test specimen depending on the rate of shear, at the scale of individual soil particles, the negative pore water pressure will tend to pull the silt particle equally in all directions, as shown in Figure 6.28. This will apply tension to the soil particles but will not alter the intergranular forces between the particles. The pore water will also be placed in tension. The tensile strength of the silt grains is higher than that of the pore water. Therefore, if the pore water pressure continues to decrease, the water will fail in tension before the soil particles will. When the liquid fails in tension, a vapor- or gas-filled bubble will form within the liquid. This is illustrated in Figure 6.29.

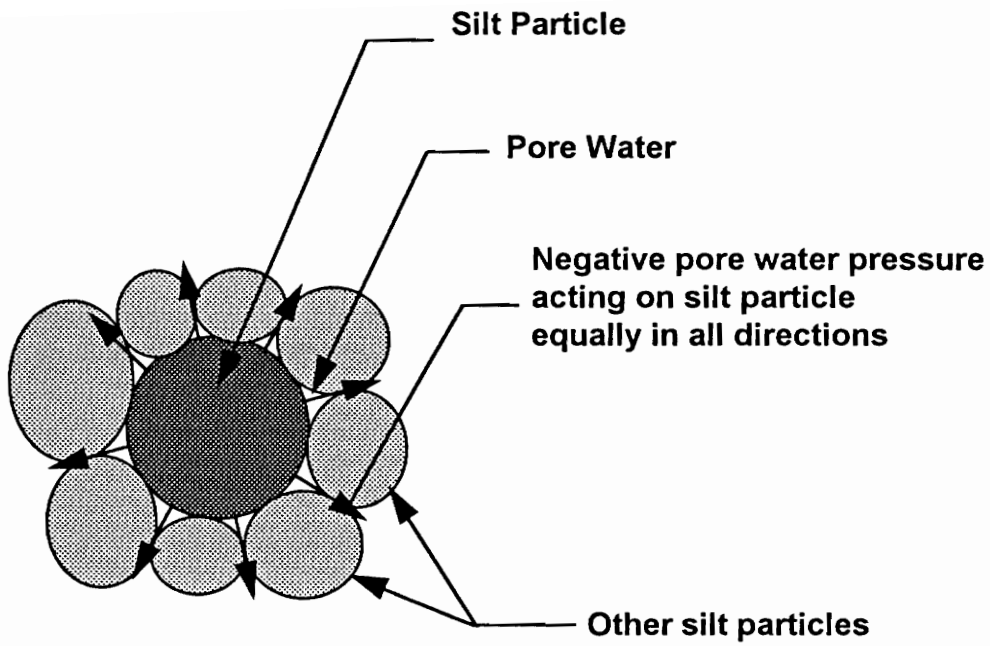


**Figure 6.28.** Schematic diagram showing how negative pore water pressure acts essentially equally all around the silt particle, resulting in no change in the intergranular forces between the silt particles

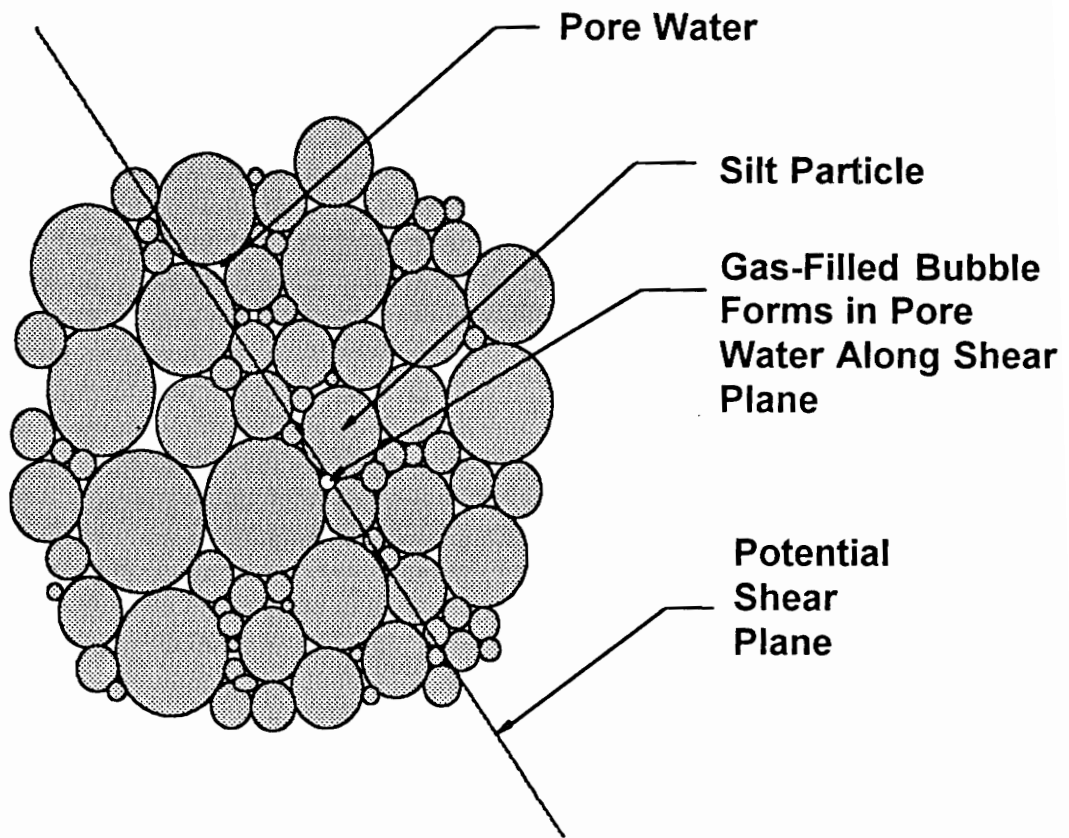


**Figure 6.29.** Schematic diagram showing a cross-section through a saturated silt in which, as a result of the pore water pressure reduction which occurred during undrained shear, a gas-filled bubble has formed within the pore water along the potential shear plane

In a Q test on a saturated silt, if gas- or vapor-filled bubbles form within the specimen at reduced pore water pressures, they would be expected to form and grow where the greatest decrease in pore pressure occurred. For a typical Q test performed at a strain rate of about one percent per minute, the maximum decrease in pore water pressure would occur in the region of maximum displacement. The decrease in pore water pressure may lead to bubble formation within the pore water in this region, as shown in Figure 6.29. The phenomenon of tribonucleation identified by Hayward (1967) may also have some influence on bubble formation. The rubbing of the silt particles against each other along the shear plane, combined with the negative pressure in the pore water, could possibly help facilitate the formation of bubbles in the pore water along the shear plane.

Figure 6.30 shows that once a bubble forms within the pore water adjacent to a silt particle, the negative pore water pressure which was essentially acting equally all around the silt particle, is no longer acting as strongly in the direction where the bubble has formed. The air or gas pressure in the bubble will probably exert some negative pressure on the silt particle. The magnitude of the gas pressure, however, will be greater than the water pressure due to surface tension effects. Equation 4-29 related the

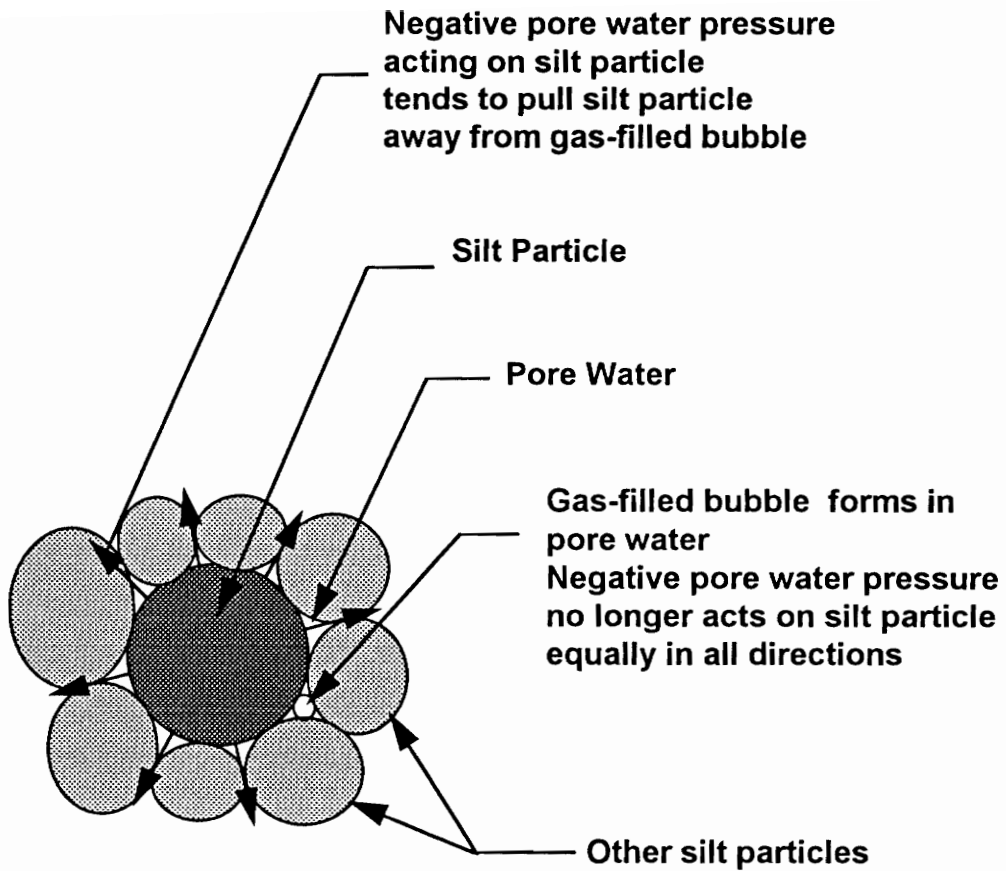


**Figure 6.30.** Schematic diagram showing that once a gas-filled bubble has formed in the pore water adjacent to the silt particle, the negative pore water pressure tends to pull the silt particle away from the bubble, thereby reducing the intergranular forces between the silt particles near where the bubble has formed

difference between the air and water pressures to the surface tension of the water and the radius of a bubble as:

$$P_a - P_w = \frac{2 T_s}{r} \cos \theta \quad (4-29)$$

For a spherical bubble,  $\theta = 0$  and the pressure of the air inside the bubble is equal to:

$$P_a = P_w + \frac{2 T_s}{r} \quad (6-16)$$

The surface tension of water,  $T_s$ , is equal to 0.0004154 lbf/in at 20°C. If an air bubble the size of a medium sized silt particle, or about 0.0004 in., forms within the pores of the soil, the pore air pressure would be approximately 2.1 psi greater than the pore water pressure.

Thus, the pressure of the air in the bubble would not be as negative as the pressure in the pore water. As a result, the pore water would tend to pull the silt particle away from the location of the gas bubble. This would be true for all of the silt particles which surround the pore where the bubble has formed. These silt particles all would tend to be pulled away from the bubble, and from each other. The ultimate effect of this is that the intergranular forces between the silt particles adjacent to the bubble, would be reduced. Any change in the intergranular forces would affect the shear strength of the soil.

If this bubble forms within the pores of the soil adjacent to the shear plane, the force acting on the silt particle due to the negative pore water pressure within the specimen will tend to act in a direction away from the bubble and the shear plane as well. This may cause a decrease in the interparticle forces between the silt grains along the shear plane where the bubble has formed. If a sufficient number of silt particles are similarly affected by the formation and growth of bubbles in the pore water along the shear plane, the decrease in interparticle forces could possibly result in abrupt yielding along the shear plane. Under this condition, the specimen could be expected to experience an increase in axial strain with little to no increase in deviator stress. A decrease in deviator stress or strain-softening would seem reasonable as well.

Even if bubble formation and growth along or near the shear plane do not occur to the extent that abrupt yielding and strain-softening resulted, bubble formation and reductions in intergranular forces could cause changes in the slopes of the stress-strain curves. Bubble formation and growth to different extents in a series of Q tests may result in the stress-strain curves varying for the different specimens. More bubble growth would be expected to reduce a larger number of the intergranular forces leading to lower strengths being measured. If little to no bubble growth

occurred, few intergranular forces would be reduced and stronger specimens with steeper stress-strain curves would result. Variables such as the dissolved gas content of the pore water, temperature variations, the presence and size of pre-existing bubbles, strain rate variations, disturbance factors, and the cell pressure used in the test may influence the formation and growth of bubbles during undrained shear, and therefore, the observed stress-strain behavior.

For a typical Q test performed on a saturated silt at a strain rate of approximately one percent per minute, equalization of pore water pressure throughout the entire specimen will very likely not take place over the time that undrained shear occurs. Pore water further away from the shear plane will tend to flow toward the shear plane since this is where the pore pressure will have decreased the most. Pore pressure equalization over time would increase the pore water pressure along the shear plane and may possibly collapse some of the bubbles which had previously formed.

Wheeler (1988b) noted that if the pore water pressure increases, the pressure in the bubbles would increase as well, resulting in stiffer bubbles with lower compressibility. The lower compressibility of the stiffer

bubbles could perhaps result in the measurement of an increase in deviator stress or strain-hardening as the bubbles are compressed and air is forced back into solution. Wheeler (1988b) noted, however, that if the solubility of the gas in the liquid was considered as well, the bubble stiffness would decrease somewhat, and the strain-hardening effect would be reduced.

Further evidence that the formation and growth of air bubbles within soil pore water may lead to strain-softening behavior is provided by the Q tests performed in this research in which the midheight pore pressure monitoring system failed during shear. In these tests, the failure of the system is believed to have occurred at the rubber cement seal at the needle-membrane interface. This would have resulted in air being drawn or forced into the triaxial specimen from the triaxial cell at about the midheight of the specimen, near the shear plane. This entry of air into the specimen would have occurred due to the negative pore water pressure developed within the specimen as well as by the positive cell pressure applied outside the specimen.

The result of this failure is that the pore pressure measurements became erratic or showed that the pore pressure within the specimen was equal to the cell pressure applied outside the membrane. This likely entry of air into the

previously saturated triaxial specimen near where the shear plane formed tended to coincide with strain-softening behavior. This was observed in a number of the Q tests at axial strains slightly greater than those at which the erratic pore pressure measurements began. The deviator stress-strain curves and pore pressure responses measured in two of these tests are given in Figure 6.31.

Although a number of the Q tests showed strain-softening behavior at some point during the test, other tests did not show any strain-softening behavior. For the Q tests in which continuous strain-hardening was observed and no strain-softening took place, one possible explanation is that no bubbles of air or water vapor formed within the pores of the soil during these tests. This could have resulted from two different circumstances:

- (1) The specimen could have contained pore water which had a very low dissolved air content relative to the reductions in pore pressure developed within the specimen, or in other words, the decrease in pore water pressure could have been too small to cause air to exit solution; or
- (2) Insufficient time may have been available for air to come out of solution and form bubbles within the soil.

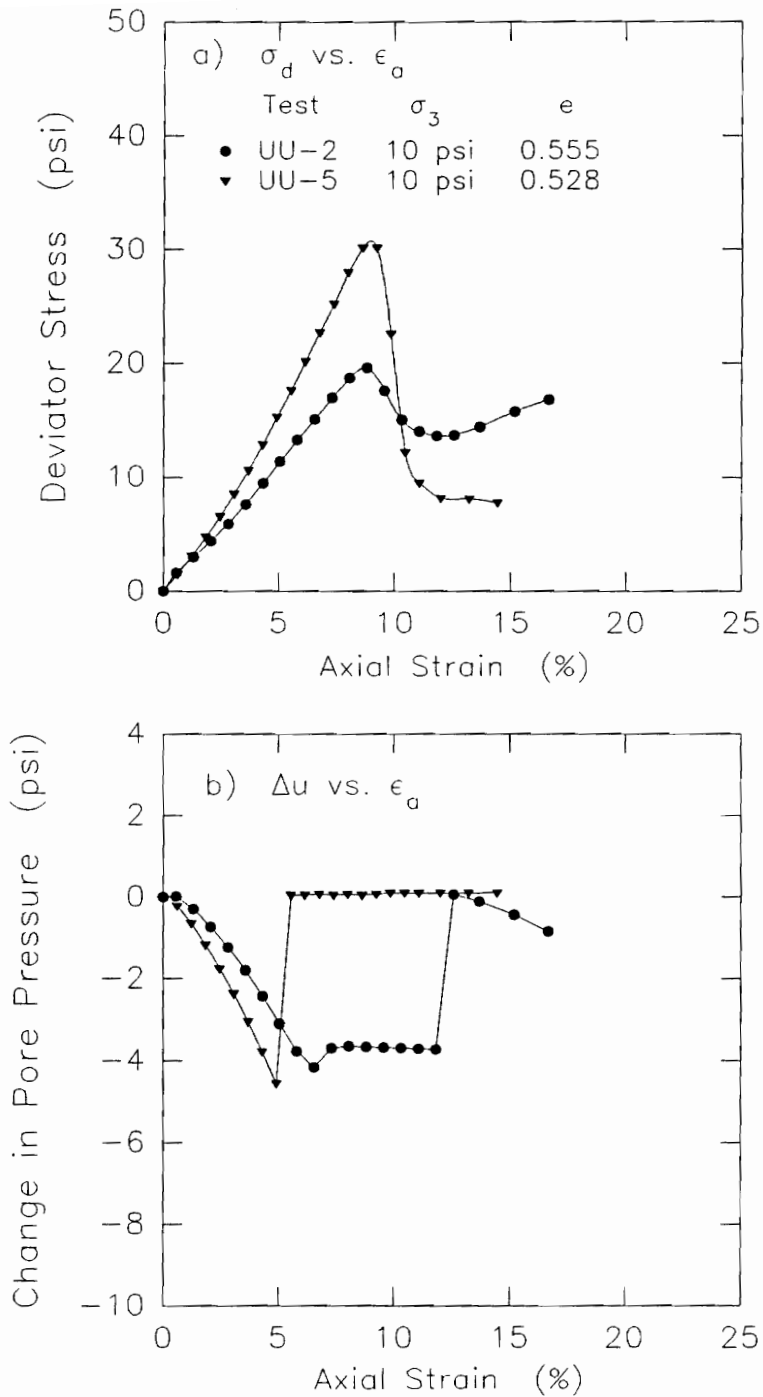


**Figure 6.31. Deviator stress-strain and change in pore pressure-strain relationships measured in two Q tests on remolded old LMVD silt, in which failure of the pore pressure monitoring system occurred**

Since the preparation procedures for the remolded specimens were essentially the same in all cases, it is believed that the dissolved air content of the pore water of the different specimens would have been quite similar. In addition, these Q tests were all performed at approximately the same strain rate. The time available for dissolved air to come out of solution should have been essentially the same for all of the specimens. Thus, it would be expected that the behavior of the different specimens would have been similar as well.

The decrease in pore water pressure which occurs in the specimen during undrained shear is dependent on the dilatant tendency of the soil which, in turn, is related to the density of the specimen. Therefore, if a set of specimens all had the same void ratio and were fully saturated, the reduction in pore water pressure should have been the same for all samples, regardless of the cell pressure used in the test. The cell pressure used in each test, however, can play a very important role in the undrained behavior and therefore, must be considered. This is because it is the absolute pore water pressure which controls gas coming out of solution, and not just the change in pore water pressure which occurs during the test.

For Q tests performed on identical specimens, the test in which a higher cell pressure was used would be expected to have less air come out of solution than a test at a lower cell pressure. This would be expected for two identical specimens in which the initial dissolved air content of the pore water and the pore pressure reduction were the same in both tests. The higher the cell pressure used in a given test, the higher the pore water pressure in the specimen prior to shear. Therefore, the decrease in pore water pressure which occurred during the test at the highest cell pressure would be less likely to cause air to exit solution.

If the pore water of the soil was saturated with dissolved air at atmospheric pressure, when the cell pressure was applied to the specimen, the pore water pressure would increase. The pore water would then be undersaturated with dissolved air at the higher pore pressure. During shear, dissolved air would not be expected to come out of solution until the reduction in pore water pressure equaled the pore pressure increase resulting from the applied cell pressure. Thus, the higher the cell pressure, the greater the reduction in pore pressure necessary to cause air to come out of solution.

It can be inferred from this that for a group of specimens with the same void ratio, air would tend to come

out of solution at smaller axial strains for tests conducted at lower cell pressures than for tests at higher cell pressures. This is because at lower cell pressures, the smaller decrease in pore pressure necessary for air to come out of solution can be reached at smaller axial strains. In the tests at higher cell pressures, the larger pore pressure reductions necessary would not take place until more attempted dilation had occurred and therefore, not until higher axial strains had been reached.

Assuming that the occurrence of a peak deviator stress followed by abrupt strain-softening is a sign that dissolved air has come out of solution, the behavior discussed above is illustrated in Figures 6.32 and 6.33. In Figure 6.32, the Q tests were performed on samples with similar initial void ratios. These tests were performed at cell pressures of 0, 5, and 10 psi. The stress-strain curves show similar behavior initially. Strain-softening then occurred in these Q tests at about 10 percent axial strain. By close observation, it can be seen that the axial strain at which the strain-softening took place showed a slight increase with increasing cell pressure.

Figure 6.33 shows the stress-strain curves for three Q tests performed on saturated silt samples with similar void ratios. These tests were performed at cell pressures of

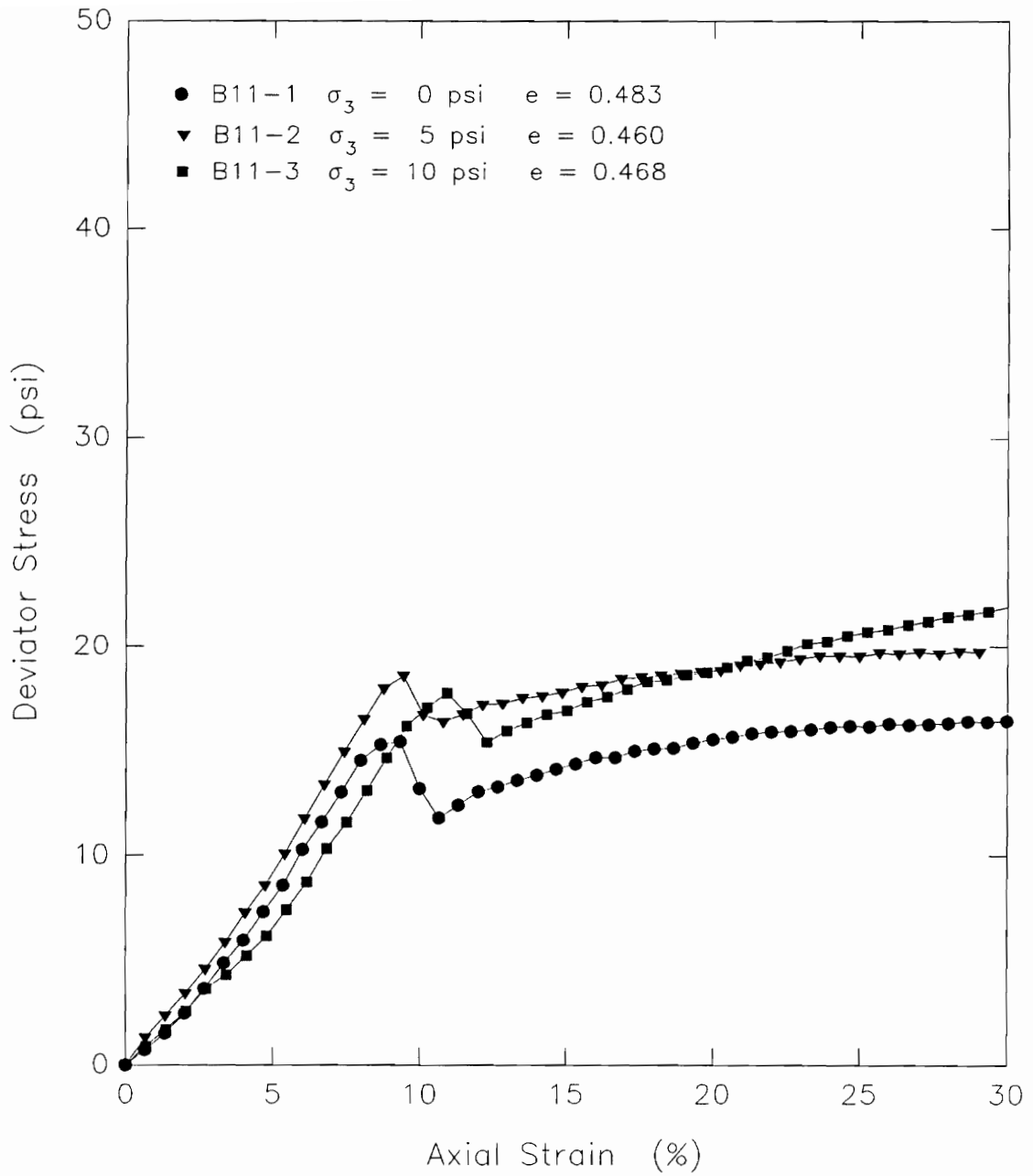


**Figure 6.32. Stress-strain curves for Q tests performed on Batch 11 of remolded old LMVD silt**

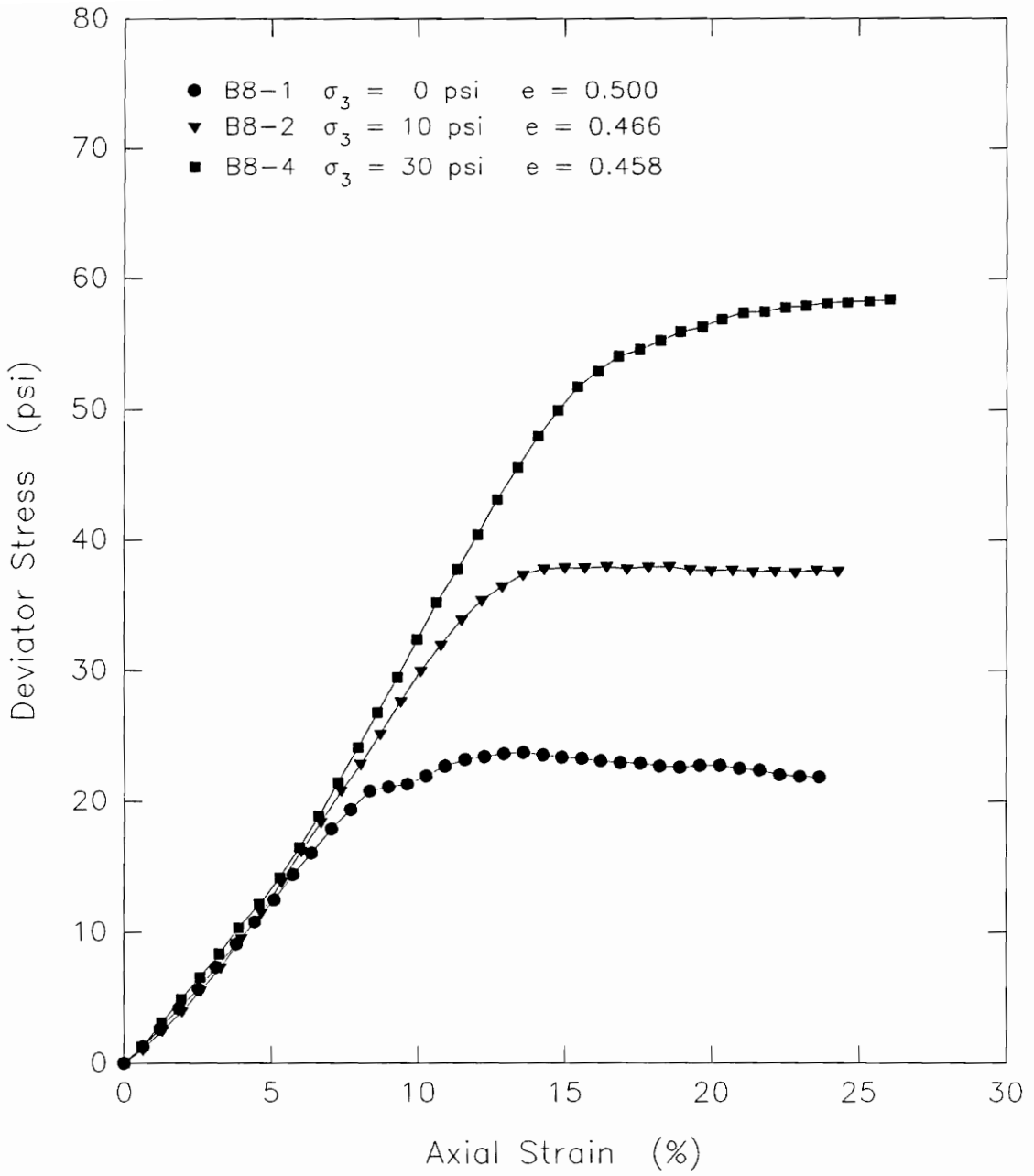


**Figure 6.33. Stress-strain curves for Q tests performed on Batch 8 of remolded old LMVD silt**

0, 10, and 30 psi. The stress-strain behavior of these specimens exhibit peak values of deviator stress but no abrupt strain-softening. It can be seen from the results of these three tests that the maximum deviator stress increased with increasing cell pressure. For the test performed at 0 psi cell pressure, the peak in the deviator stress-strain curves was followed by slight strain-softening behavior. All three tests reached a relatively constant value of deviator stress at high axial strains. The axial strain at which the deviator stress reached its maximum and became relatively constant in each test, increased with increasing cell pressure.

The stress-strain curves shown in Figure 6.1 for other Q tests performed on saturated remolded LMVD silt in this research are also worth discussion. These tests were performed with midheight pore pressure monitoring and had pore pressure measurements which were not felt to be erratic. Review of these stress-strain curves indicates that the tests in which strain-softening occurred tended to be those performed at cell pressures of 0 and 10 psi. For the tests performed at a cell pressure of 20 psi, strain-softening was either not observed or did not occur until very high strains. The strain-softening which occurred in the Q tests performed at 0 and 10 psi generally occurred between 7 and 12 percent strain and was more erratic in

nature. The strain-softening observed in the tests at 20 psi cell pressure did not occur until 18 to 20 percent strain. The stress-strain curves shown in Figure 6.1 emphasize the wide variations in undrained strength often measured in Q tests on saturated silts. It can be easily imagined the difficulty involved in interpreting this strength data for use in engineering analysis and design.

Another possible reason why some Q tests showed strain-softening behavior while others did not is that the samples may have contained different amounts of pre-existing air bubbles to serve as nuclei for additional air to come out of solution. If different amounts or sizes of pre-existing bubbles were present in the specimens initially, dissolved air may have been able to come out of solution to different extents as the pore water pressure decreased during undrained shear. The different amounts of pre-existing air bubbles in different specimens may have resulted from different environmental conditions, such as temperature and humidity in the laboratory during sample trimming and testing, or the possibility that the specimens experienced different levels of disturbance during sample preparation.

At first observation, the preparation procedures for the remolded specimens appear to have been essentially the same in all cases. Further consideration, however,

indicates that environmental conditions in the laboratory may have varied. No measurement or control of laboratory temperature or humidity was used in this research. Although care was taken during trimming, handling, and preparing the specimens for testing, some disturbance was unavoidable and slight variations in the level of disturbance each specimen experienced very likely occurred. The relative levels of disturbance each specimen experienced and how these variations may have influenced the volume of free air in pre-existing air bubbles within the different samples are not known and it is uncertain if they could be quantified in a reliable way.

Another important consideration was the nature of the erratic stress-strain behavior observed in Q tests on saturated silts performed by others. Of special interest was whether or not the stress-strain behavior of other Q tests, showed any abrupt strain-softening. Early research papers on the undrained behavior of saturated silts (Golder and Skempton, 1948; Penman, 1953) did not present stress-strain curves or presented only a typical stress-curve for the Q tests. This makes it difficult to assess the strength interpretations of these researchers. In addition, in some of these tests deaired water was used or the specimens were back pressure saturated and slightly consolidated, which would have affected the observed stress-strain behavior.

Recent studies on the undrained behavior of saturated silts, have presented stress-strain curves for Q tests. These stress-strain curves have been reviewed to observe whether or not abrupt strain-softening was a characteristic of any of these Q tests.

Fleming and Duncan (1990) tested normally consolidated specimens of reconstituted Alaskan silt. The deviator stress-strain curves given in Figure 6.34 were presented by dela Pena (1991) from the work of Fleming and Duncan (1990). The Q tests performed can be seen to have given very similar stress-strain behavior at the different cell pressures used in the tests. The resulting undrained strength envelope of the soil was characterized by a  $\phi_u = 0$  condition. The smooth stress-strain curves obtained by Fleming and Duncan (1990) for reconstituted Alaskan silt did not exhibit erratic behavior similar to that obtained for remolded LMVD silt in this research.

Brandon, Duncan, and Huffman (1990) tested undisturbed and remolded specimens of Yazoo silt. The stress-strain curves for Q tests on undisturbed specimens are shown in Figure 6.35. The stress-strain curves vary for the different specimens tested. The measured strength increased with increasing cell pressure. The stress-strain curves for the tests at lower cell pressures tended to be less smooth,

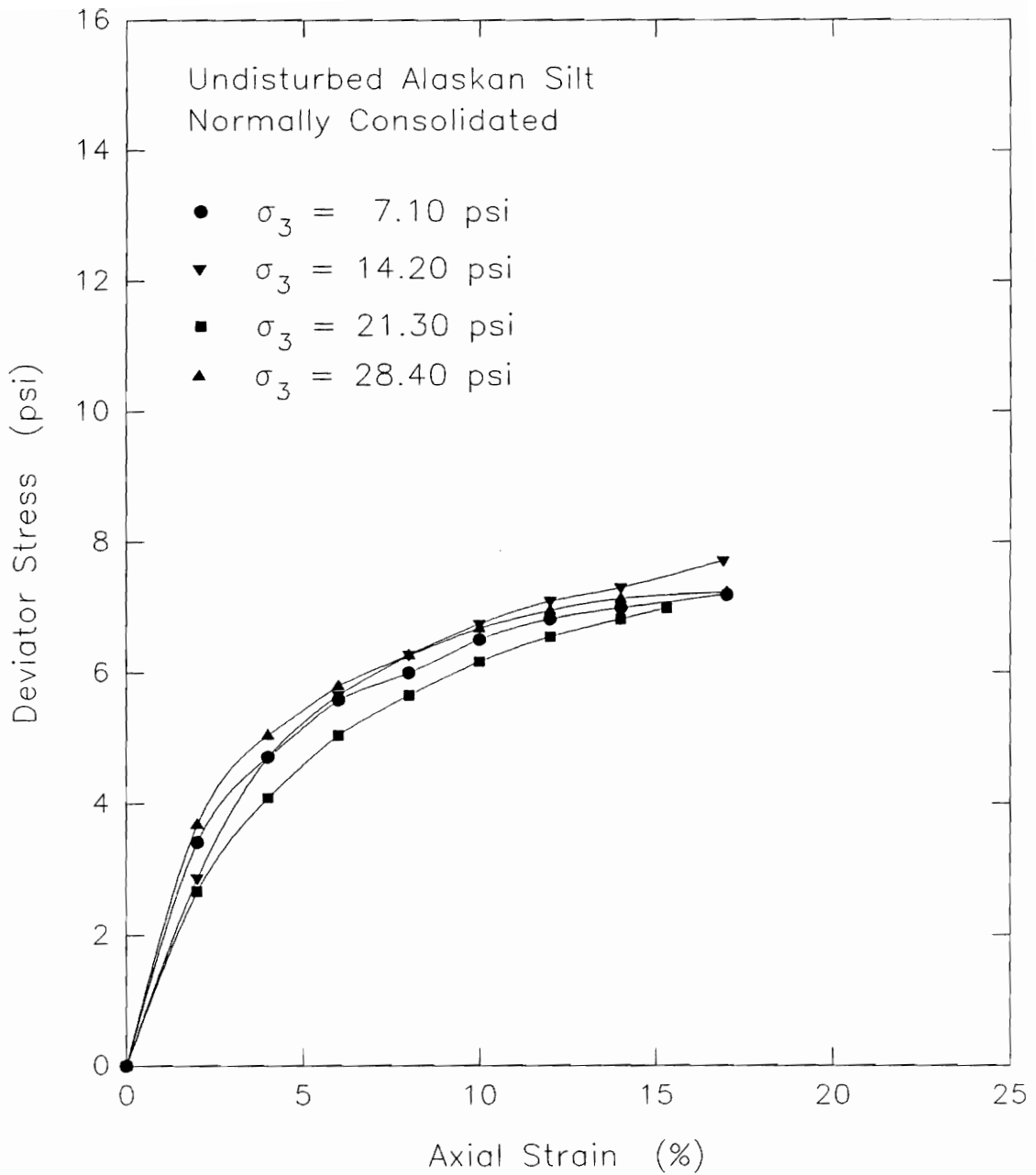


**Figure 6.34. Deviator stress-strain curves for Q tests on reconstituted specimens of Alaskan Silt tested by Fleming and Duncan (1990) (after dela Pena, 1991)**

### Yazoo Silt Undisturbed Samples

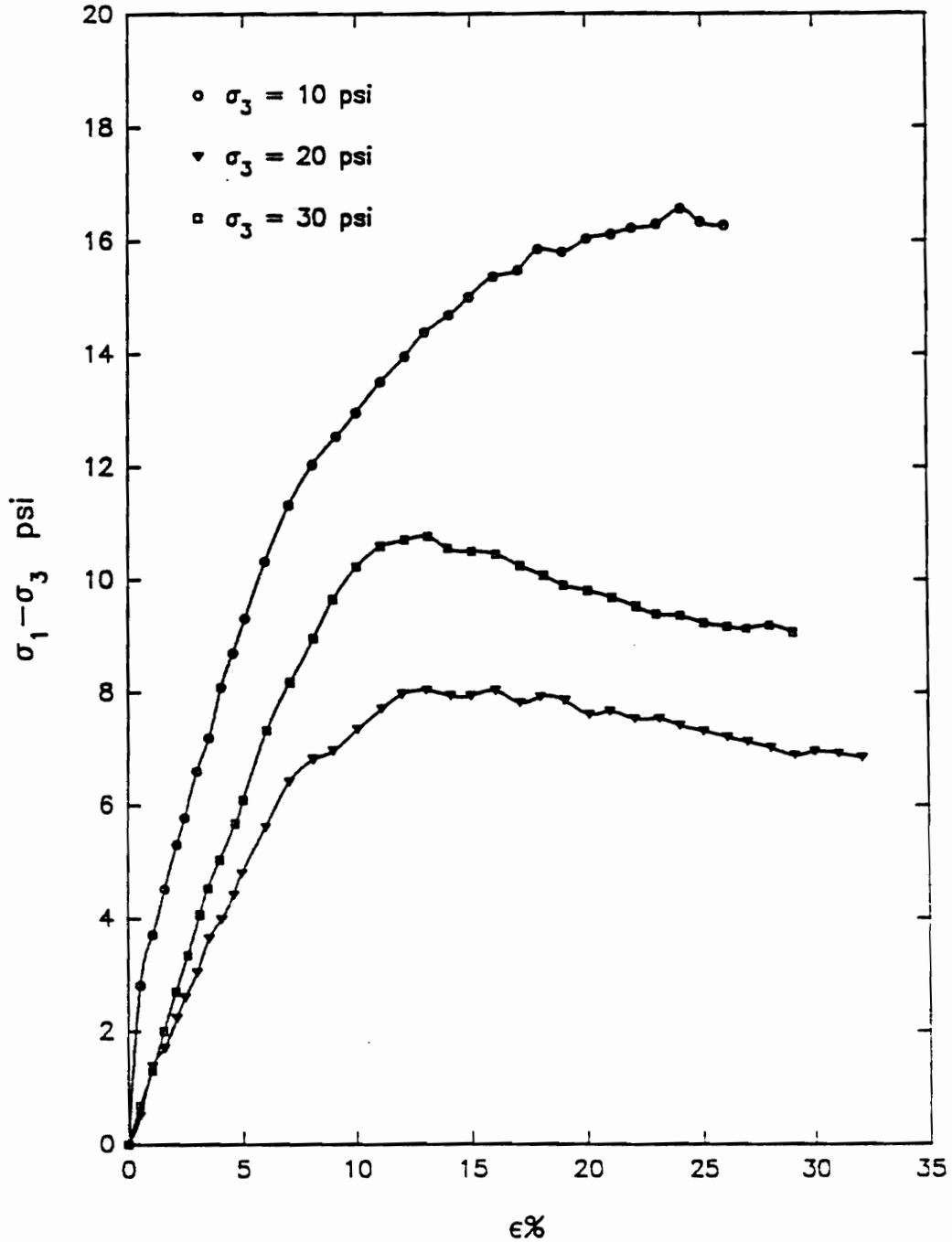


**Figure 6.35.** Deviator stress-strain curves for Q tests on undisturbed specimens of Yazoo silt (from Brandon, Duncan, and Huffman, 1990)

but not necessarily erratic. Abrupt strain-softening similar to that observed for remolded LMVD silt in this research, did not occur in the Q tests on undisturbed Yazoo silt.

Figure 6.36 shows the stress-strain curves for Q tests performed by Brandon, Duncan, and Huffman (1990) on remolded specimens of Yazoo silt. The stress-strain behavior is similar at low axial strains. With increasing axial strain, the undrained strength of the specimens shows more variation. The peak strength tended to increase with increasing cell pressure. The strain-softening that occurred after the peak values were reached tended to be more gradual than abrupt.

Brandon, Duncan, and Huffman (1990) also tested remolded specimens of LMVD silt. The stress-strain curves for Q tests on this soil are shown in Figure 6.37. The stress-strain curves varied for these tests. Higher undrained strengths were measured at higher cell pressures. The test performed at the lowest cell pressure, 10 psi, showed erratic stress-strain behavior similar to that observed in Q tests on LMVD silt in this research. After reaching a peak value of deviator stress, the strength of this specimen decreased slightly and then increased with further increase in strain. No tests were performed as

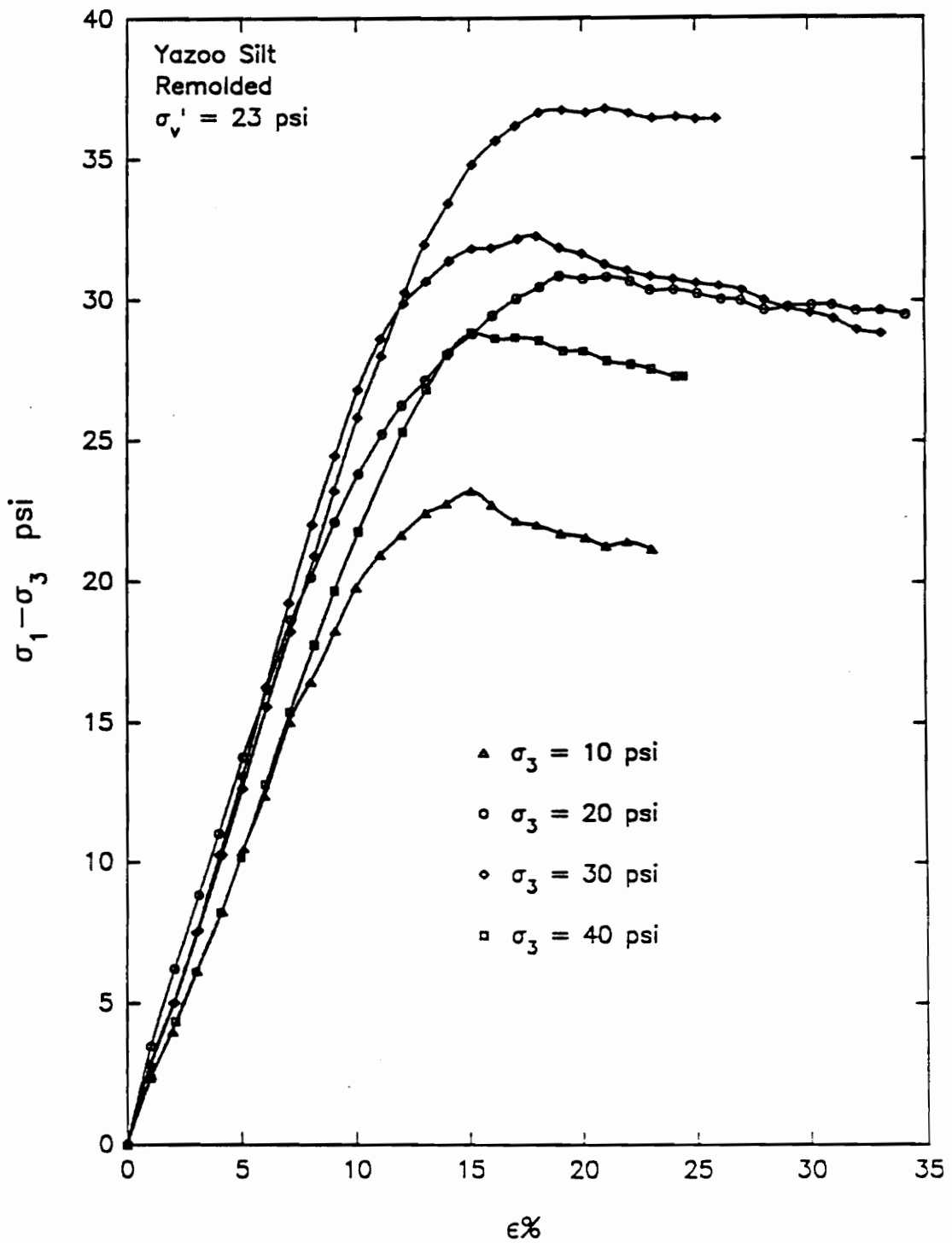


Figure 6.36. Deviator stress-strain curves for Q tests on remolded specimens of Yazoo silt (from Brandon, Duncan, and Huffman, 1990)

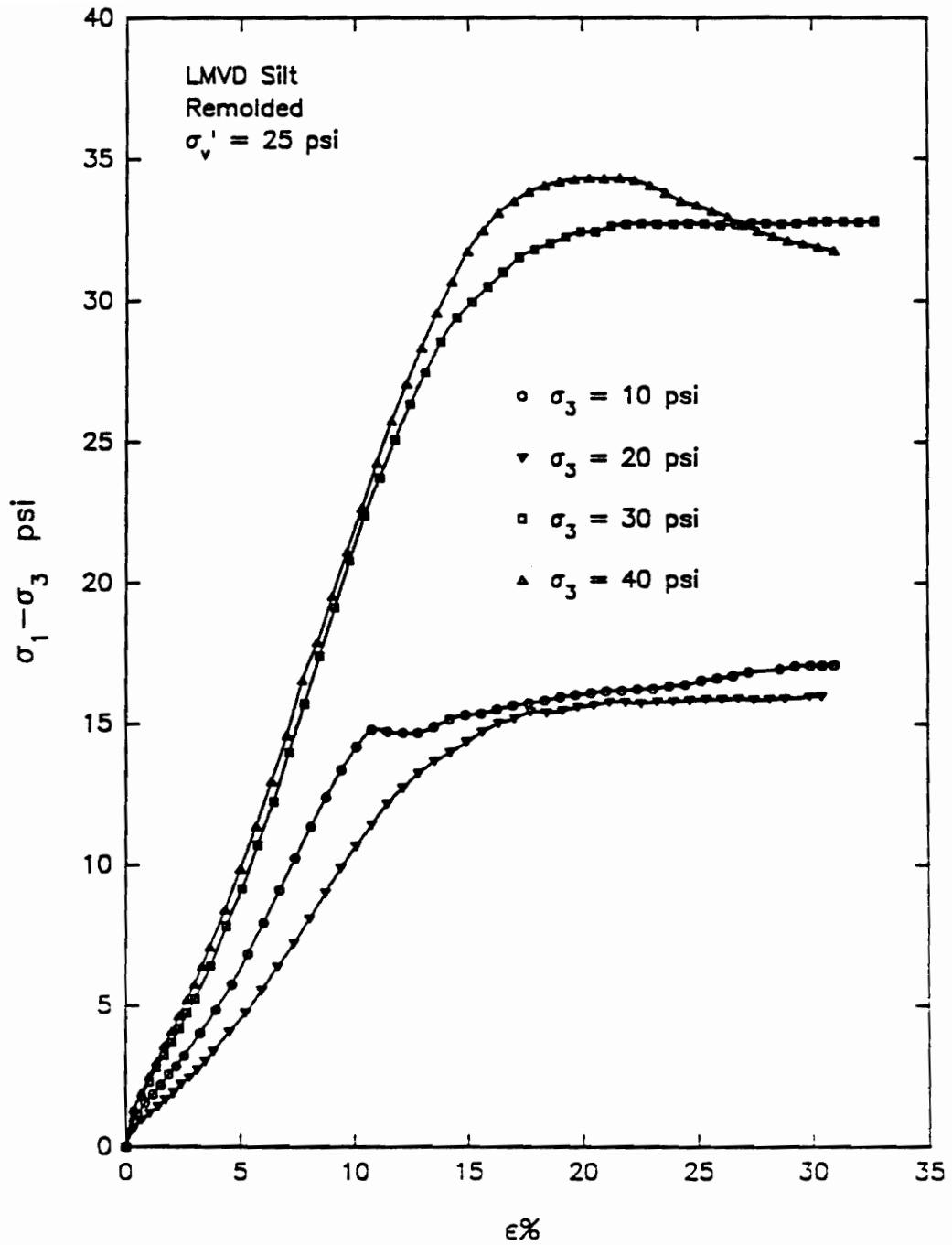
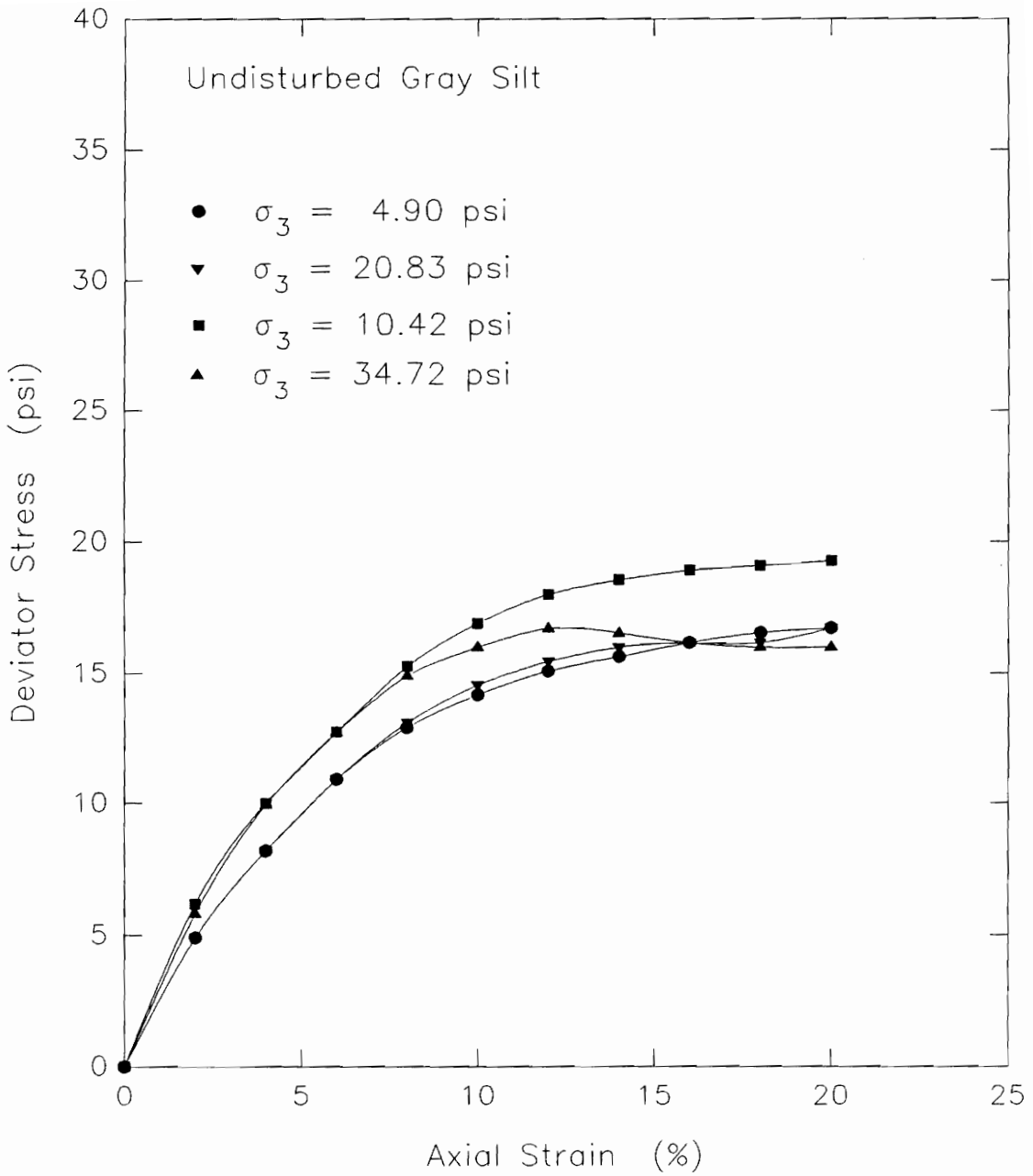


Figure 6.37. Deviator stress-strain curves for Q tests on remolded specimens of LMVD silt (from Brandon, Duncan, and Huffman, 1990)

unconfined compression tests. If they had been, they might have shown more erratic behavior.

Dela Pena (1991) reviewed the strength data of a number of silts. Two of these were gray and brown silt from the West Williamson L.P.P. Pump Station, tested by Duncan and Sehn (1987). The stress-strain curves for Q tests on undisturbed specimens of the gray silt are presented in Figure 6.38. These Q tests gave very similar stress-strain behavior and did not exhibit abrupt or unusual strain-softening.

The stress-strain curves for two sets of Q tests on undisturbed specimens of brown silt, are shown in Figures 6.39 and 6.40. The stress-strain behavior of these Q test specimens tended to be erratic. The curves shown in Figure 6.39 show similar strengths at small axial strains. At higher values of axial strain the stress-strain behavior of the specimens began to vary. The undrained strength of the specimens increased with increasing cell pressure. The stress-strain curves also showed definite changes in slope which are of an unusual nature. Slight peaks and leveling off of the deviator stress, followed by increasing deviator stress with further strain, are noticeable in the stress-strain curves for these specimens of brown silt.



**Figure 6.38.** Deviator stress-strain curves for Q tests on undisturbed samples of Gray silt, West Williamson L.P.P. Pump Station (Sample UD-101-S2-A), tested by Duncan and Sehn (1987) (after dela Pena, 1991)

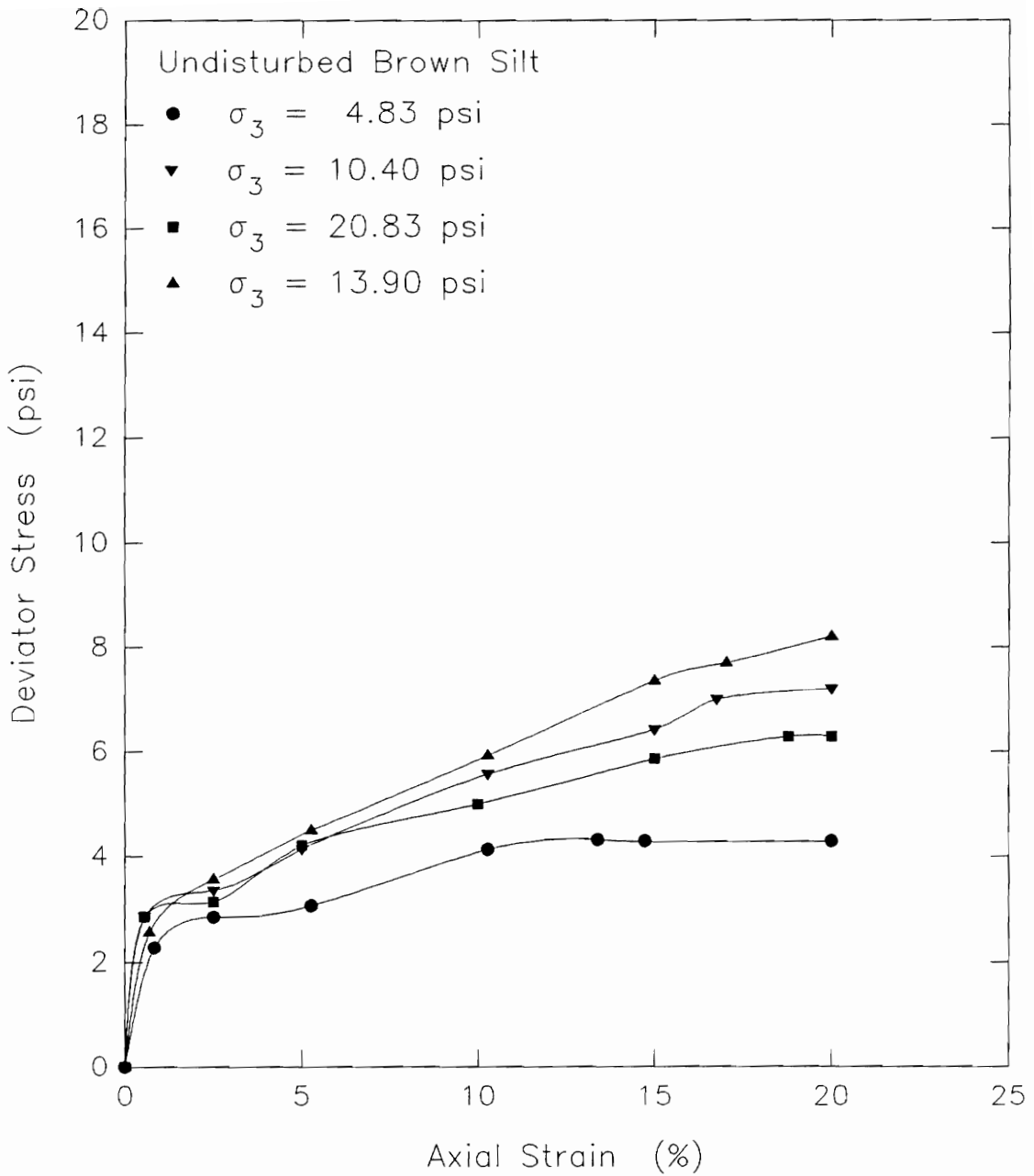


**Figure 6.39.** Deviator stress-strain curves for Q tests on undisturbed samples of Brown silt, West Williamson L.P.P. Pump Station (Sample UD-85-4-9), tested by Duncan and Sehn (1987) (after dela Pena, 1991)

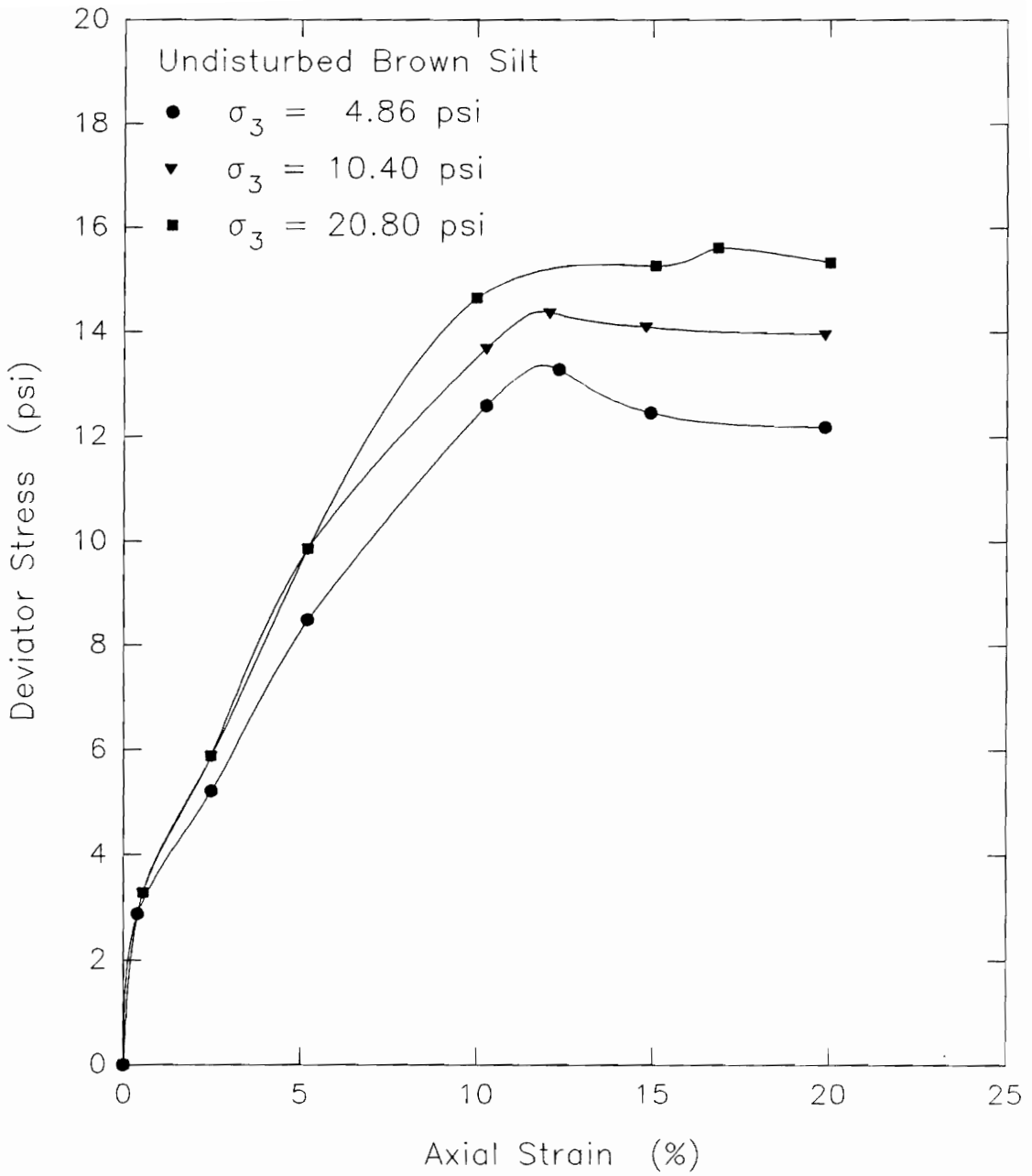


**Figure 6.40.** Deviator stress-strain curves for Q tests on undisturbed samples of Brown silt, West Williamson L.P.P. Pump Station (Sample UD-85-4-11B), tested by Duncan and Sehn (1987) (after dela Pena, 1991)

The stress-strain curves for the brown silt shown in Figure 6.40 also show noticeable changes in slope. The stress-strain curves tended to be similar at small axial strains with more variation occurring as axial strain increased. The test specimens all reached peak values of deviator stress. The strength of these specimens increased with increasing cell pressure. Gradual strain softening occurred in several of these tests.

Some of the stress-strain behavior observed in Q tests performed by Brandon, Duncan, and Huffman (1990) and Duncan and Sehn (1987) was slightly erratic. The erratic behavior was not as pronounced as it was for the Q tests performed on LMVD silt in this research. Abrupt strain-softening also was not observed in these limited number of tests performed by others.

Most of the Q tests discussed by other researchers were performed at cell pressures of 5 psi and above. The erratic stress-strain behavior observed for the LMVD silt in this research tended to occur most in tests performed at 0, 5, and 10 psi. At higher cell pressures, the tests often did not exhibit erratic stress-strain behavior and abrupt strain-softening was much less frequent. Variations in the slopes of the stress-strain curves and different values of

peak undrained shear strength were still observed in Q tests at higher cell pressures in this research.

A possible useful future study would be to review the available stress-strain data for numerous Q tests on different saturated silts. From the available information, possible correlations may be found between the occurrence of erratic stress-strain behavior, the plasticity index of the soil and the liquidity index of the specimen. A survey of the laboratory testing records of the Corps of Engineers, state and local government agencies, and engineering firms in regions of the country where saturated silts are commonly encountered, may provide a significant source of useful information in this respect.

An interesting experimental study would be to obtain several low plasticity silts with different plasticity indices and to run Q tests on remolded specimens. The different silts could be tested in Q tests at the same cell pressures and at similar values of liquidity index. This could be repeated over a range of liquidity index values. Comparison of the results may provide some type of useful guidelines in assessing when erratic stress-strain behavior would be expected in Q tests on saturated, dilatant silts.

### 6.13 Summary and Conclusions

Results obtained in the laboratory testing program have been used with information presented in Chapter 4 to assess the undrained behavior of saturated, dilatant silts. In addition, the stress-strain behavior observed in the Q tests performed in this research has been considered and a possible explanation of the erratic behavior has been proposed.

The changes in pore water pressure measured in Q tests were used to estimate the approximate amount of desaturation which could have taken place in the specimens. These calculations showed that if air came out of solution due the reduction in pore pressure measured in the tests, the degree of saturation of the specimens could have decreased from 100% initially to about 97.8%. It is stressed that the final degrees of saturation calculated in this procedure were only approximate because they were based on several assumptions. These assumptions included that the specimens were initially fully saturated, the pore water in the sample was saturated with dissolved air initially, the entire volume of soil pore water was subjected to the pore pressure reduction measured at the midheight of the specimen, the time necessary for air to come out of solution was sufficient, and the difference between the pore air and pore water pressures were the same throughout the test.

The presence of negative pore water pressures in the specimens initially suggests that surface tension forces were acting across air-water interfaces within the specimens. As a result of surface tension, the air-water interfaces were estimated to have radii ranging from 0.000386 in. to 0.000938 in. Negative pore water pressures and air-water interfaces in the specimens suggests that the Q test specimens were slightly less than fully saturated. This small amount of air was undetectable when measuring the degree of saturation of the specimen, as had been noted by Bishop and Eldin (1950).

According to Ladd and Lambe (1963), the negative pore water pressure measured in these specimens is equal to the residual effective stress in the soil. The measured values of residual effective stress were only 4 to 12 percent of the perfect sampling effective stress, or the effective stress in the soil if no disturbance had occurred during sampling. The low values of residual effective stress in the Q test specimens suggests that the Q test specimens may have had considerable disturbance (Ladd and Lambe, 1963). This disturbance may have affected the undrained behavior of the soil. Because of disturbance, the undrained strength of the soil measured in the Q tests may have been considerably less than the perfect sampling and in-situ strengths of the soil.

Another analysis of the amount of desaturation that could have occurred during undrained shear was performed considering an estimated amount of air that may have been initially present in the specimen. This analysis yielded a final degree of saturation which was similar to the value determined when the specimen was assumed to be initially 100 percent saturated. Considering the degree of saturation of the specimen to be slightly less than 100 percent did not have a significant effect on the calculated amount of desaturation which could possibly have occurred in the sample during the Q test.

An analysis was performed using the equations of Adeney and Becker (1918, 1919) and Dorsey (1940) to consider the rate at which air comes out of solution from soil pore water. During the time in which the pore pressure reduction occurs in a Q test, if the assumptions of the streaming process are true, all of the dissolved air that could possibly come out of solution may actually be able to do so, in accordance with Henry's law.

This analysis emphasized the significance of the area across which the dissolved air can diffuse to come out of solution. The magnitude of this area is unknown and has only been estimated in this study. It appears to be a major uncertainty in the consideration of the rate at which air

exits solution within the pores of a silt specimen. A further uncertainty is the applicability of the streaming process of Adeney and Becker (1918, 1919) to water contained in the pores of a soil. As a result, the slower diffusion process by which dissolved air moves through water, may be dominant.

Another analysis of the rate at which dissolved air comes out of solution from soil pore water was performed based on the diffusion principle. Using the equations of Epstein and Plesset (1950), the growth of an existing bubble was considered, due to dissolved air coming out of solution as the pore pressure decreased. For the measured reduction in pore water pressure, this analysis indicated that an existing air bubble with radius  $r = 0.000513$  in., could grow up to 25 times larger during the 21 minutes over which the Q test was performed. The growth of a pre-existing bubble to such a size during a Q test may very well be significant enough to affect the undrained behavior of the soil. The growth and interaction of multiple bubbles within the soil pores would be expected to have an even more significant effect.

Research on soils has suggested that air goes into solution in soil pore water at a slower rate than it diffuses into open water (Barden and Sides, 1967; Lee and

Black, 1972). It is expected that a similar condition would hold for air coming out of solution as well. Air was observed to come out of solution from soil pore water at a slower rate than it went into solution (Chace 1975, 1985). This tends to indicate that during the approximate 20 minute duration of a Q test, dissolved air may not be able to fully come out of solution from the soil pore water, due to the ultimate reduction in pore water pressure which occurs in the test. With the magnitude of the pore pressure reduction and the amount of time involved, however, some dissolved air will very likely come out of solution from the soil pore water and increase the sample volume and decrease the degree of saturation of the specimen to some extent. Even the slightest amount of air coming out of solution during the test may have a significant effect on the behavior of the silt in a Q test.

The results of the undrained unloading tests were used to calculate the change in pore water pressure for a saturated silt sampled from various depths. The amounts of desaturation which could occur due to the pore pressure decreases were also estimated. For the values of  $\bar{A}_u$  measured in the unloading tests, a saturated silt sampled from depths of up to 50 feet below the ground water level could experience a decrease in the degree of saturation of the soil from 100 percent down to 96.3 percent, due to air

coming out of solution as a result of the pore pressure reduction. This analysis, however, is felt to be unrealistic since it assumes that the soil pore water was saturated with dissolved air at a pressure corresponding to the hydrostatic pressure of the soil pore water. This would be unlikely, however, because the dissolved gas content of a body of water should depend only on the pressure of the gas above the water. For normal ground water conditions, the soil gas pressure may be very similar to atmospheric pressure conditions. During sampling, dissolved gas would very likely come out of solution due to the temperature increase that the soil pore water will likely experience. The pressure decrease during sampling could then expand the volume of this newly released gas, in accordance with Boyle's law.

The changes in pore water pressure resulting from sampling indicate that after sampling, the pore water pressure in the soil is negative. The development of negative pore water pressures during sampling suggests that surface tension forces are acting within the sample across air-water interfaces. Air-water interfaces would develop if some amount of air came out of solution during sampling.

Lambe and Whitman (1969) and Sowers (1979) stated that negative pore water pressures are present in soils after

sampling due to the presence of curved air-water interfaces which form as evaporation of water occurs along the surface of the soil sample exposed to the atmosphere. Although the magnitude of the negative pore water pressure developed during sampling can be estimated, the amount of air which comes out of solution can not be directly determined.

Numerous sets of Q tests performed on saturated silts in this research tended to show similar stress-strain behavior at low values of axial strain. This resulted in Mohr-Coulomb strength envelopes characterized by  $\phi_u = 0$ ,  $S_u = c$  undrained strength parameters, as expected (Bishop and Eldin, 1950). At higher axial strains, the stress-strain behavior in these Q tests showed more variation, often giving  $\phi_u > 0$  undrained strength envelopes for the soil. The higher values of peak strength in the specimens tested at higher cell pressures resulted from the higher values of pore water pressure in the specimens initially. The higher values of pore water pressure initially in the specimens allowed for larger decreases in pore water pressure and more dilatant hardening of the specimens.

The axial strain at which the Q tests went from a  $\phi_u = 0$  condition to a  $\phi_u > 0$  condition, varied for the different sets of Q tests. In some cases, variation from a  $\phi_u = 0$  condition began at axial strains of 4 or 5%. In

other cases,  $\phi_u = 0$  behavior continued through 9 or 10% axial strain. Certain groups of tests indicated that as the void ratio of the specimens decreased, the axial strain at which deviations from  $\phi_u = 0$  behavior began, tended to decrease, as well.

For the cases where  $\phi_u > 0$  undrained strength envelopes were obtained, the values of undrained friction angle,  $\phi_u$ , were less than the effective stress friction angle of the soil. This suggests that if dissolved air came out of solution and expanded the volume of the specimens, the soil did not experience fully drained conditions, but rather, something between undrained and drained conditions.

In addition, when considering Q tests performed over a wide range of cell pressures, at values of axial strain at failure of 10% or for peak deviator stress conditions, bilinear strength envelopes were observed. In these cases, at low cell pressures, the undrained strength of the soil was defined by a  $\phi_u > 0$  envelope. Above a certain value of cell pressure, the undrained strength of the soil was defined by a  $\phi_u = 0$ ,  $S_u = c$  condition. This was similar to the observations of Penman (1953).

Some groups of Q tests and comparisons between Q test results from different groups of tests did not show any similarity in their stress-strain behavior. These types of

Q test results emphasize the erratic nature of undrained strength measurements on saturated silts and the difficulty in interpreting the undrained strengths of these soils. This type of erratic stress-strain behavior may be more the result of specimen disturbance rather than the result of cavitation of the soil pore water. Silts are noted to be easily disturbed (Fleming and Duncan, 1990). The magnitude and influence of this disturbance is extremely difficult, if not impossible, to quantify.

Desaturation of CU test specimens as pore water pressures decreased and eliminated the back pressures initially in the specimens, corresponded with peak values in the deviator stress-axial strain curves for the tests. The occurrence of peak values of deviator stress in conventional Q tests and back pressure saturated Q tests performed in this research is believed to correspond with desaturation of these specimens, as well. Dissolved gases released from solution in the pore water due to the decreases in pore water pressure during undrained shear would desaturate the Q test specimens.

The formation and growth of gas bubbles within the pores of a soil due to pore pressure reductions would have an effect on the intergranular forces between the soil particles. When a gas bubble forms, the pressure of the gas

in the bubble would be greater than the pressure in the surrounding pore water. The lower pore water pressure would tend to pull soil particles away from the gas bubble, thereby reducing the intergranular forces between the soil particles adjacent to the bubble.

Gas bubble formation and the reduction of intergranular forces would influence the stress-strain behavior of the soil. Variations in the amount of bubble growth from specimen to specimen could result in the erratic stress-strain behavior often observed in Q tests on saturated, dilatant silts. Significant bubble growth could eventually lead to an abrupt shear failure and strain-softening, as was observed in many of the Q tests performed in this research.

The formation and growth of gas bubbles within the pores of saturated, dilatant silt Q test specimens during undrained shear, appears to be a plausible explanation for the erratic behavior often observed in these tests.

## Chapter 7

### SUMMARY, CONCLUSIONS AND RECOMMENDATIONS

Undrained strength tests on saturated, dilatant silts tend to exhibit erratic behavior. This makes the determination and use of undrained strengths for these soils difficult for geotechnical engineers. The erratic behavior is believed to result from the dilatant tendencies of the soil, the corresponding decreases in pore water pressure, and the physical behavior of water when subjected to a decrease in pressure. Cavitation or gases coming out of solution from soil pore water during undrained shear, has been proposed as a possible cause of the observed behavior (Bishop and Eldin, 1950; Brandon, Duncan, and Huffman, 1990). The findings of this research support this.

The purpose of this research was to investigate more fully the phenomenon of cavitation, the possibility of its occurrence in the pore water of saturated silts, and the influence that its occurrence would have on the undrained behavior of the soil.

This chapter presents a summary of the work accomplished in this research, conclusions resulting from the work, and recommendations for further study.

## 7.1 Summary of the Work Accomplished

The following work was accomplished in this research:

- 1.) Literature was reviewed in the following areas which had significance in this research:
  - The undrained behavior of saturated, dilatant soils,
  - Cavitation of water and related phenomena,
  - The solubility of air in water,
  - The rate at which air goes into and comes out of solution in water,
  - The dissolved gas content of ground water, and
  - Void growth within soils and other materials and its influence on their engineering behavior.
- 2.) Laboratory experiments were performed to:
  - Measure the dissolved oxygen content of soil pore water,
  - Measure the decrease in pore water pressure which occurs in Q tests on saturated, dilatant silts,
  - Investigate the behavior of saturated, dilatant silts during sampling and undrained shear,
  - Investigate the behavior of saturated, dilatant silts sheared in Q tests at different strain rates,
  - Provide data to evaluate the undrained shear strength and stress-strain behavior of saturated, dilatant silts, and
  - Investigate possible testing procedures for improving the determination and interpretation of the undrained strength of saturated, dilatant silts.
- 3.) Information obtained from the literature review was used along with data obtained from laboratory experiments to:
  - Estimate the amount of air which could possibly come out of solution from soil pore water during sampling and Q tests,

- Assess whether the time over which a Q test is performed is sufficient for dissolved air to come out of solution,
- Evaluate whether the erratic behavior observed in Q tests on saturated, dilatant silts can be explained by the occurrence of dissolved gases exiting solution from the pore water during undrained shear, and
- Suggest possible improvements to the procedures used to determine the undrained strengths of saturated, dilatant silts, as well as to propose areas in which further research is felt to be warranted.

## 7.2 Conclusions

The conclusions of this research study are related to three areas which this research investigated: cavitation phenomena and the physical properties of water; characteristics of the undrained behavior of saturated, dilatant silts; and the influence of the properties and behavior of water on the undrained behavior of saturated, dilatant silts.

The conclusions regarding cavitation phenomena and the physical properties of water are as follows:

- 1.) Dissolved gas coming out of solution from water is considered *gaseous cavitation* and can occur at pressures above -14.7 psig. Gas bubble formation and growth in water occurs in accordance with Henry's and Boyle's laws and is dependent on temperature and pressure. The pressure at which dissolved gases will begin to come out of solution will depend on the dissolved gas content of the water. The magnitude and duration of a change in pressure, will influence the amount of gas which will go into or come out of solution in water.

- 2.) Cavitation bubbles are believed to initiate from nuclei in the form of pockets of air trapped in cracks and crevices present on solid surfaces in contact with the liquid. Soil grains could potentially contain a number of such nuclei on their surfaces. In addition, *tribonucleation* or the formation of cavitation bubbles as a result of soil grains rubbing against each other within a liquid under negative pressure, may be a potential cause of cavitation in saturated, dilatant soils.
- 3.) The dissolved gas content of ground water can be expected to vary, depending on the chemical, biological and physical conditions in the ground. In addition, the gases commonly dissolved in ground water may be different from the gases present in atmospheric air (Freeze and Cherry, 1979). Ground water may be saturated with certain dissolved gases while being supersaturated or undersaturated with other dissolved gases, relative to atmospheric conditions of gas composition, temperature and pressure. When a saturated soil is sampled and brought to the ground surface, gases which the pore water is supersaturated with will tend to come out of solution, while gases which the water is undersaturated with will tend to go into solution.
- 4.) Cavitation of soil pore water, in the form of gases dissolved in the pore water coming out of solution during sampling and undrained shear tests, appears to be a distinct possibility for saturated dilatant soils such as silts. This concept of cavitation in saturated silts is different than the conventional idea of cavitation in soil mechanics presented by Seed and Lee (1967). Instead of the pore water pressure having to decrease to -14.7 psig for cavitation to occur, saturated, dilatant silts may experience cavitation in the form of dissolved gases exiting solution from the pore water at pressures greater than -14.7 psig. This is a result of soil pore water containing dissolved gases in-situ and the pore size of saturated, dilatant silts being suitable for gas bubble growth as pore water pressures decrease during undrained shear.

The conclusions concerning the characteristics of the undrained behavior of saturated, dilatant silts are as follows:

- 1.) Saturated silts can experience a decrease in pore water pressure due to the attempted dilation during undrained shear as well as the stress release associated with sampling the soil from some depth in the ground.
- 2.) The magnitude of the decrease in pore water pressure measured at the midheight of the Q test specimens, tended to increase with increasing cell pressure in the tests. The higher the value of pore water pressure at the start of undrained shear, the larger the decrease in pore water pressure measured within the specimens. In all of the Q tests with midheight pore pressure monitoring, the value of the pore water pressure never decreased to -13.7 psig, or zero pressure absolute, where vaporous cavitation would have been expected to occur. This suggests that some other limitation existed on the decrease in pore water pressure possible in the specimens.
- 3.) Unloading tests conducted on anisotropically consolidated undrained samples of remolded and undisturbed LMVD silt indicate that the measured values of the pore pressure parameter for unloading,  $A$ , are similar to the values reported for clayey-silt by Ladd and Lambe (1963). These results were used to calculate the change in pore water pressure that a saturated silt could experience when sampled from various depths.
- 4.) The calculated changes in pore water pressure resulting from sampling indicate that the soil has a negative pore water pressure after sampling. In addition, negative pore water pressures were measured in the Q test specimens initially. This suggests that somewhere within the soil, air-water interfaces existed. The soil after sampling, as well as the Q test specimens prior to shear, therefore, were not actually 100 percent saturated, but had a degree of saturation slightly less than 100%. Others have also noted that during sampling and trimming of saturated soil specimens, negative pore water pressures and air pockets will develop as evaporation occurs from the exposed specimen surface (Lambe and Whitman, 1969; Sowers, 1979). In addition, it is difficult if not impossible, to place a rubber membrane around the specimen in the triaxial cell without trapping some small amount of air between the specimen and membrane (Bishop and Henkel, 1962; Head, 1986). It may very well be that these tiny pockets of trapped air serve as initiation points for dissolved gases to come out of solution from the soil pore water, as the soil attempts to dilate during undrained shear. These small amounts

of free air trapped between the specimen and membrane, however, are very often not detected by ordinary measurements used to determine the degree of saturation of the specimen (Bishop and Eldin, 1950).

- 5.) The Q tests performed on saturated, dilatant silts in this research tended to exhibit erratic behavior. At low values of axial strain the Q tests often showed similar stress-strain behavior. At higher axial strains, the stress-strain behavior observed in the Q tests began to show increasing variation. This resulted in Mohr-Coulomb strength envelopes characterized by  $\phi_u = 0$ ,  $S_u = c$  undrained strength parameters at low axial strains. At higher values of axial strain,  $\phi_u > 0$  undrained strength envelopes resulted. The higher values of peak strength in the specimens tested at higher cell pressures, resulted from the higher values of pore water pressure in the specimens initially. This allowed for larger decreases in pore water pressure and more dilatant hardening in the specimens tested at higher cell pressures.
- 6.) Some groups of Q tests and comparisons between Q test results from different groups of tests did not show any similarity in their stress-strain behavior. These types of Q test results for saturated silts emphasize the erratic nature of undrained strength measurements and the difficulty in interpreting the undrained strengths of these soils. This type of erratic stress-strain behavior may be the result of specimen disturbance, which can be considerable for silts (Fleming and Duncan, 1990), but which is extremely difficult, if not impossible, to quantify.
- 7.) The axial strain at which the Q tests went from a  $\phi_u = 0$  condition to a  $\phi_u > 0$  condition, varied for the different sets of Q tests. In some cases, variation from a  $\phi_u = 0$  condition began at axial strains of 4 or 5%. In other cases,  $\phi_u = 0$  behavior continued through 9 or 10% axial strain. This makes it difficult to use a single value of axial strain as a failure criterion to determine the undrained strengths of saturated, dilatant silts on a given engineering project. Certain groups of tests indicated that as the void ratio of the specimens decreased, the axial strains at which deviations from  $\phi_u = 0$  behavior began, tended to decrease, as well. For the cases where  $\phi_u > 0$  undrained strength envelopes were obtained, the values of undrained friction angle,  $\phi_u$ , were less than the effective stress friction angle of the soil. This suggests that if dissolved air came out of solution and

expanded the volume of the specimens, the soil did not experience fully drained conditions, but rather, something between undrained and drained conditions.

The conclusions regarding the influence of the properties and behavior of water on the undrained behavior of saturated, dilatant silts are as follows:

- 1.) Pockets or bubbles of undissolved gas are very likely present in Q test specimens thought to be fully saturated. These undissolved gas bubbles may serve as a significant source of cavitation nuclei within the pore water, as pore water pressures decrease. These bubbles will grow larger more readily in the larger pores of a silt than in the smaller pores of a clay (Terzaghi, 1943).
- 2.) The decrease in pore water pressure which occurs in Q tests on saturated, dilatant silts can be expected to allow dissolved gases to exit solution from the pore water to some extent, during the duration of the test. This will increase the volume and void ratio of the Q test specimen while decreasing its degree of saturation.
- 3.) The formation and growth of gas bubbles within the soil pore water will influence the intergranular forces within Q test specimens. This, in turn, will affect the stress-strain behavior observed for the soil. Variations in the level of bubble formation and growth from specimen to specimen would likely result in variations in the observed stress-strain behavior of the soil. Bubble formation and growth may lead to the formation of distinct shear planes in saturated silt Q test specimens. This is believed to correspond with the abrupt strain-softening observed in this research for Q test specimens tested under certain conditions. It may also correspond with the erratic stress-strain behavior observed in Q tests on saturated, dilatant silts performed by others (Duncan and Sehn, 1987; Brandon, Duncan, and Huffman, 1990).
- 4.) The conditions under which abrupt strain-softening was observed most frequently in Q tests in this research were as follows:
  - Q test specimens tested at low cell pressures,

- Q test specimens tested at rapid strain rates, and
- Q test specimens tested without a back pressure applied to the specimen.

These are also the conditions under which cavitation or dissolved gases coming out of solution from soil pore water, are felt to be most likely to occur.

- 5.) Disturbance effects may also be considerable for saturated, dilatant silts. These effects are difficult to quantify, and therefore, they add to the difficulty in measuring and interpreting undrained strengths of these soils. Extreme care should be taken so that disturbance of saturated, dilatant silt Q test specimens will be minimized as much as possible.
- 6.) The undrained shear strength of saturated, dilatant silts can be obtained from Q tests based on a limiting value of axial strain. The appropriate value of limiting axial strain to use as a failure criterion will depend on the engineering project. In order to obtain a  $\phi_u = 0$  undrained strength envelope for the soil, the value of axial strain chosen as a failure criterion may vary from one silt to another, as well as for the same silt tested at different void ratios. A limiting value of 10% axial strain at failure was found to be the upper limit for which a  $\phi_u = 0$  undrained strength envelope was obtained in the Q tests performed on LMVD silt in this research. Unconfined compression tests tended to give the most erratic results in this research and should be avoided in determining the undrained strength of such soils for use in engineering analysis and design. Saturated, dilatant silts containing pore water with a high dissolved gas content, such as in a marine environment, may have an undrained strength which can only be defined by a  $\phi_u > 0$  envelope at all values of axial strain.
- 7.) Cavitation of soil pore water in-situ may be a possibility in saturated, dilatant silts under certain conditions of loading, initial hydrostatic pressure and the dilatant characteristics of the silt. Soil pore water containing sufficient amounts of dissolved gas may cavitate during undrained loading conditions if the decrease in pore water pressure is large enough to allow gases to exit solution. This could result in  $\phi_u > 0$  undrained strength behavior and may possibly lead to abrupt yielding of the soil along a shear plane in the field. The likely presence of free gas bubbles in laboratory test specimens may make cavitation of soil

pore water a more likely occurrence during laboratory tests than for in-situ conditions. The lack of free gas bubbles or air-water interfaces in the soil pore water may lead to soil pore water being less likely to cavitate in the field.

### 7.3 Recommendations for Further Study

Based on the findings of this research study, several recommendations can be made for further study:

- 1.) A review of available Q test stress-strain curves for saturated silts, the plasticity index of the soils tested, and the liquidity indices of the specimens may provide some type of correlation between these indices and when erratic stress-strain behavior is most likely to occur. Experimental research could also be used to further develop these types of correlations.
- 2.) Actual measurement of the volume of dissolved gases coming out of solution from Q test specimens of saturated, dilatant silts during undrained shear could be attempted using special equipment, similar to that discussed by Chan and Duncan (1967), Withiam and Kulhawy (1976), and Wheeler (1988b). In these devices the volume change of the triaxial specimen could be determined by measuring changes in the volume of the fluid in the triaxial cell during undrained shear. There are calibration factors involved with measurements of this type and the sensitivity of the device used would have to be accurate enough to measure the extremely small changes in specimen volume which might occur as dissolved gases come out of solution from the soil pore water. Tests of this type performed at different values of cell pressure may show that dissolved gases exit solution to different extents from the specimens and are the cause of the erratic behavior observed. Although this would not improve the methods used to perform and interpret the undrained strengths of saturated, dilatant silts, it would help to determine whether dissolved gases coming out of solution from soil pore water is the cause of the erratic behavior observed. It would also be interesting to note whether the specimens experienced noticeably abrupt volume increases when a distinct shear plane failure occurred in the specimens.

- 3.) Further consideration should be given to the possibility that cavitation of the pore water of saturated, dilatant silts occurs in the field. This could include the review of case histories of saturated silt failures. Back calculation of the silt strengths at failure could then be compared to strengths measured in laboratory tests. Measurement of the dissolved gas content of soil pore water may also be useful in comparing the failure conditions of the silts at different sites.
- 4.) Further consideration should be given to the influence that specimen disturbance may have on the undrained behavior of saturated, dilatant silts.

## REFERENCES

- Adeney, W. E. (1905). "Unrecognized Factors in the Transmission of Gases Through Water." *The London, Edinburgh, and Dublin Phil. Mag. and J. of Sci.*, Ser. 6, Vol. 9, 360-369.
- Adeney, W. E. and Becker, H. G. (1918). "The Determination of the Rate of Solution of Atmospheric Nitrogen and Oxygen by Water: Part I." *Sci. Proc. of the Royal Dublin Soc.*, 15(N.S. 31), 385-404.
- Adeney, W. E. and Becker, H. G. (1919). "The Determination of the Rate of Solution of Atmospheric Nitrogen and Oxygen by Water: Part II." *Sci. Proc. of the Royal Dublin Soc.*, 15(N.S. 44), 609-628.
- Adeney, W. E. and Becker, H. G. (1920). "The Determination of the Rate of Solution of Atmospheric Nitrogen and Oxygen by Water." *Sci. Proc. of the Royal Dublin Soc.*, 16(N.S. 13), 143-152.
- Adeney, W. E., Leonard, A. G. G., and Richardson, A. (1922). "On the Aeration of Quiescent Columns of Distilled Water and of Solutions of Sodium Chloride." *Sci. Proc. of the Royal Dublin Soc.*, 17(N.S. 3), 19-28.
- Adeney, W. E. (1926). "On the Rate and Mechanism of the Aeration of Water Under Open-Air Conditions." *The London, Edinburgh, and Dublin Phil. Mag. and J. of Sci.*, Ser. 7, Vol. 2(11), 1140-1148.
- Apfel, R. E. (1970). "The Role of Impurities in Cavitation Threshold Determination." *J. of the Acoust. Soc. of America*, 48, 1179-1186.
- Axelsson, K., Runesson, K., Sture, S., Yu, Y., and Alawaji, H. (1989). "Characteristics and Intergration of Undrained Response of Silty Soils." *3rd Int. Symp. on Num. Models in Geomechanics*, Niagara Falls, Canada, 195-203.
- Bair, F. E., Ed. (1992). *The Weather Almanac*, 6th ed., Gale Research, Inc., Detroit, p. 275.

- Baldi, G., Hight, D. W., and Thomas, G. E. (1988). "A Reevaluation of Conventional Triaxial Test Methods." *Advanced Triaxial Testing of Soil and Rock*, ASTM STP 977, Robert T. Donaghe, Ronald C. Chaney, and Marshall L. Silver, Eds., ASTM, Philadelphia, 219-263.
- Barden, L. and Sides, G. R. (1967). "The Diffusion of Air Through the Pore Water of Soils." *Proc., 3rd Asian Conf. Soil Mech. and Found. Engrg.*, Haifa, Israel, 135-138.
- Barker, J. F. and Patrick, G. C. (1985). "Natural Attenuation of Aromatic Hydrocarbons in a Shallow Sand Aquifer." *Proc., API/NWWA Conf. on Petroleum Hydrocarbons and Organic Compounds in Ground Water*, Houston, 160-177.
- Barrow, G. M. (1979). *Physical Chemistry*, 4th ed., McGraw Hill, NY, 832 p.
- Becker, H. G. and Pearson, E. F. (1923). "Irregularities in the Rate of Solution of Oxygen by Water." *Sci. Proc. of the Royal Dublin Soc.*, 17(N.S. No. 22), 197-200.
- Berg, C. A. (1970). "Plastic dilation and Void Interaction." *Inelastic Behavior of Solids*, M. F. Kanninen, W. F. Adler, A. R. Rosenfield, and R. I. Jaffee, Eds., Battelle Institute Materials Science Colloquia, McGraw-Hill Book Company, NY, 171-210.
- Bishop, A. W. (1960). "The Measurement of Pore Pressure in the Triaxial Test." *Proc., Conf. on Pore Pressure and Suction in Soils*, Butterworth & Co., London, 38-46.
- Bishop, A. W., Blight, G. E., and Donald, I. B. (1960). Closure of "Factors Controlling the Strength of Partly Saturated Cohesive Soils." *ASCE Res. Conf. on Shear Strength of Cohesive Soils*, Boulder, Colorado, 1027-1042.
- Bishop, A. W. and Eldin, G. (1950). "Undrained Triaxial Tests on Saturated Sands and Their Significance in the General Theory of Shear Strength." *Geotechnique*, 2, 13-32.
- Bishop, A. W. and Eldin, A. K. G. (1953). "The Effect of Stress History on the Relation between  $\phi$  and Porosity in Sand." *Proc., 3rd Int. Conf. on Soil Mech. and Found. Engrg.*, 1, Switzerland, 100-105.

- Bishop, A. W. and Henkel, D. J. (1962). *The Measurement of Soil Properties in the Triaxial Test*, Edward Arnold, London, 228 p.
- Black, D. K. and Lee, K. L. (1973). "Saturating Laboratory Samples by Back Pressure." *J. Soil Mech. and Found. Div.*, ASCE, 99(1), 75-93.
- Blake, F. G. (1949). "The Properties of Gaseous Solutions as Revealed by Acoustic Cavitation Measurements." *J. of the Acoust. Soc. of America*, 21, p. 464.
- Blight, G.E. (1965). "Shear Stress and Pore Pressure in Triaxial Testing." *J. Soil Mech. and Found. Div.*, ASCE, 91(6), 25-39.
- Bloomsburg, G. L. and Corey, A. T. (1964). "Diffusion of Entrapped Air from Porous Media." *Hydrology Papers*, No. 5, Colorado State University, Fort Collins, CO, 27 p.
- Börgesson, L. (1981). "Shear Strength of Inorganic Silty Soils." *Proc., 10th Int. Conf. on Soil Mech. and Found. Engrg.*, 1, Stockholm, 567-572.
- Brace, W. F. and Martin, R. J. (1968). "A test of the Law of Effective Stress for Crystalline Rocks of Low Porosity." *Int. J. of Rock Mech. and Mining Sci.*, 5, 415-426.
- Brandon, T. L., Duncan, J. M., and Huffman, J. T. (1990). "Classification and Engineering Behavior of Silt." Final report submitted to the U. S. Army Corps of Engineers Lower Mississippi Valley Division, Contract DACW39-89-M-2985, 145 p.
- Briggs, L. J. (1950). "Limiting Negative Pressure of Water." *J. of Applied Physics*, 21, 721-722.
- Brubaker, G. R. (1993). "In situ Bioremediation of Groundwater." *Geotechnical Practice for Waste Disposal*, David E. Daniel, Ed., Chapman and Hall, New York, 551-584.
- Bruggeman, J. R., Zangar, C. N., and Brahtz, J. H. A. (1939). "Notes on Analytical Soil Mechanics." US Dept. of the Interior, Bur. of Rec., Technical Memorandum No. 592, Denver, 153 p.

- Chace, A. B. (1975). "Pressure and Density in Marine Sediment." PhD dissertation, Univ. of Rhode Island, Kingston, RI, 121 p.
- Chace, A. B. (1985). "Pressure Release Disturbance in Simulated Marine Cores as Indicated by a Laboratory Gamma-Ray Densitometer." *Strength Testing of Marine Sediments: Laboratory and In-Situ Measurements*, ASTM STP 883, R.C. Chaney and K.R. Demars, Eds., ASTM, Philadelphia, 154-165.
- Chahal, R. S. (1964). "Effect of Temperature and Trapped Air on the Energy Status of Water in Porous Media." *Soil Science*, 98, 107-112.
- Chahal, R. S. and Yong, R. N. (1965). "Validity of the Soil Water Characteristics Determined with the Pressurized Apparatus." *Soil Science*, 99, 98-103.
- Chan, C. K. and Duncan, J. M. (1967). "A New Device for Measuring Volume Changes and Pressures in Triaxial Tests on Soils." *Materials Research & Standards*, 7(7), 312-314.
- Connolly, W. and Fox, F. E. (1954). "Ultrasonic Cavitation Thresholds in Water." *J. of the Acoust. Soc. of America*, 26, 843-848.
- Crawford, C.B. (1963). "Pore pressures within Soil Specimens in Triaxial Compression." *Laboratory Shear Testing of Soils*, ASTM STP No. 361, ASTM, Philadelphia, 192-199.
- CRC Handbook of Chemistry and Physics*, 69th ed., (1988). Robert C. Weast, editor-in-chief, CRC Press, Boca Raton, FL, p. B-457.
- CRC Handbook of Chemistry and Physics*, 74th ed., (1993). Robert C. Weast, editor-in-chief, CRC Press, Inc., Boca Raton, FL.
- Crum, L. A. (1979). "Tensile Strength of Water." *Nature*, 278, 148-149.
- Davis, S. N. and DeWiest, R. J. M. (1966). *Hydrogeology*, John Wiley & Sons, NY, 643 p.
- dela Pena, B. I. (1991). "Effective and Total Stress Strength Interpretation for Silts." MS Thesis, Civil Engineering Department, Virginia Polytechnic Institute & State University, Blacksburg, VA, 282 p.

- Dorsey, N. E. (1940). *Properties of Ordinary Water-Substance*, American Chem. Soc. Monograph Series, Reinhold Publishing Co., NY.
- Dowling, N. E. (1993). *Mechanical Behavior of Materials*, Prentice Hall, Englewood Cliffs, NJ, 773 p.
- Duncan, J. M. and Campanella, R. G. (1965). *The Effect of Temperature Changes During Undrained Tests*, Report No. TE-65-10, College of Engineering, University of California, Berkeley, 23 p.
- Duncan, J. M. and Sehn, A. (1987). "Investigation of the Cause of Failure of the Corrugated Metal Culvert at the West Williamson L.P.P. Pump Station, West Williamson, West Virginia." A Report Prepared for the U.S. Army Corps of Engineers, Huntington District, 117 p.
- Dupas, J.-M., Parker, A., Bozetto, P., and Fry, J.-J. (1988). "A 300-mm Diameter Triaxial Cell with a Double Measuring Device." *Advanced Triaxial Testing of Soil and Rock*, ASTM STP 977, Robert T. Donaghe, Ronald C. Chaney, and Marshall L. Silver, Eds., ASTM, Philadelphia, 132-142.
- Eisenberg, P. (1961). "Mechanics of Cavitation." *Handbook of Fluid Dynamics*, V. L. Streeter, Ed., McGraw-Hill, NY, 12-2 - 12-24.
- Elrick, D. E. (1963). "Unsaturated Flow Properties of Soils." *Australian J. of Soils Research*, 1, 1-8.
- Epstein, P. S. and Plesset, M. S. (1950). "On the Stability of Gas Bubbles in Liquid-Gas Solutions." *J. of Chemical Physics*, 18, 1505-1509.
- Esrig, M. I. and Kirby, R. C. (1977). "Implications of Gas Content for Predicting the Stability of Submarine Slopes." *Marine Geotechnology*, 2, 81-100.
- Evans, A. G. and Rana, A. (1980). "High Temperature Failure Mechanisms in Ceramics." *Acta Metallurgica*, 28, 129-141.
- Fleming, L. N. and Duncan, J. M. (1990). "Stress-Deformation Characteristics of an Alaskan Silt." *J. of Geotech. Engrg.*, ASCE, 116(3), 377-393.
- Fogg, P. G. T. and Gerrard, W. (1991). *Solubility of Gases in Liquids*, John Wiley & Sons, NY, 332 p.

- Fourie, A. B. and Xiaobi, D. (1991). "Advantages of Midheight Pore Pressure Measurements in Undrained Triaxial Testing." *Geotech. Test. J.*, 14(2), 138-145.
- Fox, F. E. and Herzfeld, K. F. (1954). "Gas Bubbles with Organic Skins as Cavitation Nuclei." *J. of the Acoust. Soc. of America*, 26, 984-989.
- Frederick, D. and Chang, T. S. (1972). *Continuum Mechanics*, Scientific Publishers, Boston, 218 p.
- Fredlund, D. G. (1976). "Density and Compressibility Characteristics of Air-Water Mixtures." *Canadian Geotech. J.*, 13, 386-396.
- Fredlund, D. G. and Rahardjo, H. (1993). *Soil Mechanics for Unsaturated Soils*, John Wiley & Sons, NY, 517 p.
- Freeze, R. A. and Cherry, J. A. (1979). *Groundwater*, Prentice-Hall, Englewood Cliffs, NJ, 604 p.
- Galloway, W. J. (1954). "An Experimental Study of Acoustically Induced Cavitation in Liquids." *J. of the Acoust. Soc. of America*, 26, 849-857.
- Gibbs, H. J., Hilf, J. W., Holtz, W. G., and Walker, F. C. (1960). "Shear Strength of Cohesive Soils." *ASCE Res. Conf. on Shear Strength of Cohesive Soils*, Boulder, Colorado, 33-162.
- Golder, H. Q. and Skempton, A. W. (1948). "The Angle of Shearing Resistance in Cohesive Soils for Tests at Constant Water Content." *Proc., 2nd Int. Conf. on Soil Mech. and Found. Engrg.*, 1, Rotterdam, The Netherlands, 185-192.
- Green, R. J. (1972). "A Plasticity Theory for Porous Solids." *Int. J. of Mechanical Sciences*, 14, 215-224.
- Gurson, A. L. (1977). "Continuum Theory of Ductile Rupture by Void Nucleation and Growth: Part I - Yield Criteria and Flow rules for Porous Ductile Media." *Trans., ASME, Series H, J. of Engrg. Materials and Technology*, 99, 2-15.
- Hamilton, L. W. (1939). "The Effects of Internal Hydrostatic Pressure on the Shearing Strength of Soils." *Proc., ASTM*, 39, 1100-1121.

- Harvey, E. N., Barnes, D. K., McElroy, W. D., Whiteley, A. H., Pease, D. C., and Cooper, K. W. (1944a). "Bubble Formation in Animals: I. Physical Factors." *J. of Cellular and Comparative Physiology*, 24, 1-22.
- Harvey, E. N., Whiteley, A. H., McElroy, W. D., Pease, D. C., and Barnes, D. K. (1944b). "Bubble Formation in Animals: II. Gas Nuclei and Their Distribution in Blood and Tissues." *J. of Cellular and Comparative Physiology*, 24, 23-34.
- Harvey, E. N., Barnes, D. K., McElroy, W. D., Whiteley, A. H., and Pease, D. C. (1945). "Removal of Gas Nuclei from Liquids and Surfaces." *J. of the Am. Chem. Soc.*, 67, 156-157.
- Harvey, E. N., McElroy, W. D., and Whiteley, A. H. (1947). "On Cavity Formation in Water." *J. of Applied Physics*, 18, 162-172.
- Hawley's Condensed Chemical Dictionary*, 11th ed., (1987). N.I. Sax and R.J. Lewis, Eds., VanNostrand Reinhold, NY, p. 592.
- Hayward, A. T. J. (1967). "Tribonucleation of Bubbles." *Brit. J. of Applied Physics*, 18, 641-644.
- Hayward, A. T. J. (1970). "The Role of Stabilized Gas Nuclei in Hydrodynamic Cavitation Inception." *J. of Physics D: Applied Physics*, 3, 574-579.
- Head, K. H. (1986). *Manual of Soil Laboratory Testing; Volume 3: Effective Stress Tests*, John Wiley & Sons, NY, 495 p.
- Heaton, T. H. E. and Vogel, J. C. (1980). "Rate of Oxygen Removal in Some South African Groundwaters." *Hydrological Sciences Bulletin*, 25, 373-377.
- Henry, W. (1803). "Experiments on the Quantity of Gases Absorbed by Water, at Different Temperatures, and Under Different Pressures." *Philosophical Trans. of the Royal Soc. of London*, Part 1, 29-43, 274-276.
- Heuer, A. H., Tighe, N. J., and Cannon, R. M. (1980). "Plastic Deformation of Fine-Grained Alumina ( $Al_2O_3$ ): II, Basal Slip and Nonaccommodated Grain-Boundary Sliding." *American Ceramic Soc. J.*, 63, 53-58.

- Hight, D. W. (1982). "A simple piezometer probe for the routine measurement of pore pressure in triaxial tests on saturated soils." *Geotechnique*, 32(4), 396-401.
- Hilf, J. W. (1956). *An Investigation of Pore water Pressure in Compacted Cohesive Soils*, US Dept. of the Interior, Bur. of Rec., Technical Memorandum 654, Denver, 109 p.
- Hillel, D. (1980). *Fundamentals of Soil Physics*, Academic Press, NY, 413 p.
- Iyengar, K. S. and Richardson, E. G. (1958). "Measurements on the Air-Nuclei in Natural Water which Give Rise to Cavitation." *Brit. J. of Applied Physics*, 9, 154-158.
- Johnson, V. E. (1963). "Mechanics of Cavitation." *J. of the Hydraulics Div., ASCE*, 89(3), 251-275.
- Knapp, R. T. (1958). "Cavitation and Nuclei." *Trans., American Soc. of Mech. Engrs.*, 80, 1315-1324.
- Knapp, R. T., Daily, J. W., and Hammitt, F. G. (1970). *Cavitation*, McGraw-Hill, NY, 578 p.
- Kuper, C. G. and Trevena, D. H. (1952). "The Effect of Dissolved Gases on the Tensile Strength of Liquids." *Proc., Physical Society, Section A*, 65, 46-54.
- Ladd, C. C. and Lambe, T. W. (1963). "The Strength of "Undisturbed" Clay Determined from Undrained Tests." *Laboratory Shear Testing of Soils*, ASTM STP No. 361, ASTM, Philadelphia, 342-371.
- Ladd, C. C., Weaver, J. S., Germaine, J. T., and Sauls, D. P. (1985). "Strength-Deformation Properties of Arctic Silt." *ASCE Specialty Conference Arctic '85*, San Francisco, 820-829.
- Lambe, T. W. and Whitman, R. V. (1969). *Soil Mechanics*, John Wiley & Sons, NY, 553 p.
- Lee, H. J. (1985). "State of the Art: Laboratory Determination of the Strength of Marine Soils." *Strength Testing of Marine Sediments: Laboratory and In-Situ Measurements*, ASTM STP 883, R.C. Chaney and K.R. Demars, Eds., ASTM, Philadelphia, 181-250.
- Lee, K. L. and Black, D. K. (1972). "Time to Dissolve Air Bubble in Drain Line." *J. of the Soil Mech. and Found. Div., ASCE*, 98(2), 181-194.

- Lloyd, J. W. and Heathcote, J. A. (1985). *Natural Inorganic Hydrochemistry in Relation to Groundwater: An Introduction*, Clarendon Press, London, 296 p.
- Lowe, J. and Johnson, T. C. (1960). "Use of Back Pressure to Increase Degree of Saturation of Triaxial Test Specimens." *ASCE Res. Conf. on Shear Strength of Cohesive Soils*, Boulder, Colorado, 819-836.
- Marsal, R. J. and Resines, J. S. (1960). "Pore Pressure and Volumetric Measurements in Triaxial Compression Tests." *ASCE Res. Conf. on Shear Strength of Cohesive Soils*, Boulder, Colorado, 965-983.
- Masterton, W. L., Slowinski, E. J., and Stanitski, C. L. (1981). *Chemical Principles*, 5th ed., Saunders College Publishing, Philadelphia.
- Matthess, G. and Harvey, J. C. (1982). *The Properties of Groundwater*, John Wiley & Sons, NY, 406 p.
- Mead, W. J. (1925). "The Geologic Role of Dilatancy." *J. of Geol.*, 33, 685-698.
- Mitchell, J. K. (1993). *Fundamentals of Soil Behavior*, 2nd. ed., John Wiley & Sons, NY, 437 p.
- Moore, E. M. (1953). "Sea Foam." *Nature*, 171, p. 913.
- Nash, K. L. (1953). "The Shearing Resistance of a Fine Closely Graded Sand." *Proc., 3rd Int. Conf. on Soil Mech. and Found. Engrg.*, 1, Zurich, Switzerland, 160-164.
- National Research Council (1933). *International Critical Tables of Numerical Data*, Vol. IV, McGraw-Hill, NY, p. 447.
- Odenstad, S. (1948). "Stresses and Strains in the Undrained Compression Test." *Geotechnique*, 1, 242-249.
- Olson, R.E. (1963). Discussion, *Laboratory Shear Testing of Soils*, ASTM STP No. 361, ASTM, Philadelphia, 204-207.
- Pease, D. C. and Blinks, L. R. (1947). "Cavitation from Solid Surfaces in the Absence of Gas Nuclei." *J. of Physical and Colloid Chem.*, 51, 556-567.

- Penman, A. D. M. (1953). "Shear Characteristics of a Saturated Silt Measured in Triaxial Compression." *Geotechnique*, 3, 312-328.
- Pionke, H. B. and Urban, J. B. (1987). "Sampling the Chemistry of Shallow Aquifer Systems - A Case Study." *Ground Water Monitoring Review*, 7, 79-88.
- Plesset, M. S. (1949). "The Dynamics of Cavitation Bubbles." *J. of Applied Mech.*, 16, 277-282.
- Rau, G. and Chaney, R. C. (1988). "Triaxial Testing of Marine Sediments with High Gas Contents." *Advanced Triaxial Testing of Soil and Rock*, ASTM STP 977, R.T. Donaghe, R.C. Chaney, and M.L. Silver, Eds., ASTM, Philadelphia, 338-352.
- Reynolds, O. (1885). "On the Dilatancy of Media Composed of Rigid Particles in Contact." *The London, Edinburgh, and Dublin Phil. Mag. and J. of Sci.*, Ser. 5, Vol. 20, 469-481.
- Reynolds, O. (1886). "Experiments Showing Dilatancy, a Property of Granular Material, Possibly Connected with Gravitation." *Proc., Royal Institution of Great Britain*, 11, 354-363.
- Rice, J. R. (1975). "On the Stability of Dilatant Hardening for Saturated Rock Masses." *J. of Geophysical Research*, 80, 1531-1536.
- Richards, L. A. (1928). "The Usefulness of Capillary Potential to Soil-Moisture and Plant Investigators." *J. of Agricultural Research*, 37(12), 719-742.
- Rodehush, W. H. and Buswell, A. M. (1958). "Properties of Water Substance." *Water and its Conduction in Soils*, Highway Research Board, Special Report 40, H.F. Winterkorn, Ed., 5-13.
- Ronen, D., Magaritz, M., Almon, E., and Amiel, A. J. (1987). "Anthropogenic Anoxification ('Eutrophication') of the Water Table Region of a Deep Phreatic Aquifer." *Water Resources Research*, 23, 1554-1560.
- Roscoe, K. H., Schofield, A. N., and Wroth, C. P. (1958). "On the Yielding of Soils." *Geotechnique*, 8, 22-53.
- Rose, S. and Long, A. (1988). "Dissolved Oxygen Systematics in the Tuscon Basin Aquifer." *Water Resources Research*, 24, 127-136.

- Schuurman, I. E. (1966). "The Compressibility of an Air/Water Mixture and a Theoretical Relation Between the Air and Water Pressures." *Geotechnique*, 16(4), 269-281.
- Schweitzer, P. H. and Szebehely, V. G. (1950). "Gas Evolution in Liquids and Cavitation." *J. of Applied Physics*, 21, 1218-1224.
- Schultze, E. and Horn, A. (1965). "The Shear Strength of Silt." *Proc., 6th Int. Conf. on Soil Mech. and Found. Engrg.*, 1, Montreal, 350-353.
- Sedgewick, S. A. and Trevena, D. H. (1976). "Limiting Negative Pressure of Water Under Dynamic Stressing." *J. of Physics D: Applied Physics*, 9, 1983-1990.
- Seed, H. B. and Lee, K. L. (1967). "Undrained Strength Characteristics of Cohesionless Soils." *J. of the Soil Mech. and Found. Div., ASCE*, 93(6), 333-360.
- Sheikh, GH. R. and Pharr, G. M. (1985). "Further Observation on Creep Enhanced by a Liquid Phase in Porous Potassium Chloride." *Acta Metallurgica*, 33, 231-238.
- Smith, R. M. and Browning, D. R. (1942). "Persistent Water-Unsaturation of Natural Soil in Relation to Various Soil and Plant Factors." *Proc., Soil Sci. Soc. of America*, 7, 114-119.
- Skempton, A. W. (1954). "The Pore Pressure Coefficients A and B." *Geotechnique*, 4, 143-147.
- Sowers, G. F. (1979). *Introductory Soil Mechanics and Foundations: Geotechnical Engineering*, 4th ed., Macmillan Publishing, NY, 621 p.
- Standard Methods for the Examination of Water and Wastewater*, 18<sup>th</sup> ed. (1992). American Public Health Association, AWWA, Water Pollution Control Federation, p. 4-101.
- Strasberg, M. (1959). "Onset of Ultrasonic Cavitation in Tap Water." *J. of the Acoust. Soc. of America*, 31, 163-176.
- Taylor, D. W. (1948). *Fundamentals of Soil Mechanics*, John Wiley & Sons, NY, 700 p.

- Temperley, H. N. V. and Trevena, D. H. (1978). *Liquids and Their Properties: A Molecular and Macroscopic Treatise with Applications*, Halsted Press, NY, 274 p.
- Terzaghi, K. (1943). *Theoretical Soil Mechanics*, John Wiley & Sons, NY, 510 p.
- Terzaghi, K. and Peck, R. B. (1967). *Soil Mechanics in Engineering Practice*, John Wiley & Sons, NY, 729 p.
- Tomlinson, C. (1869). "On the Action of Solid Nuclei in Liberating Vapor from Boiling Liquids." *Proceedings of the Royal Society of London*, 17, 240-252.
- Torrey, V. H. (1982). "Laboratory Shear Strength of Dilative Silts." Report prepared for the Lower Mississippi Valley Division, U. S. Army Engineers Waterways Experiment Station, Vicksburg, MS, September, 1982, 26 p.
- Trainer, F. W. and Heath, R. C. (1976). "Bicarbonate Content of Groundwater in Carbonate Rock in Eastern North America." *Journal of Hydrology*, 31, 37-55.
- Trevena, D. H. (1967). "The Behavior of Liquids Under Tension." *Contemporary Physics*, 8, 185-195.
- Trevena, D. H. (1975). *The Liquid Phase*, Wykeham Publications (London) Ltd., 109 p.
- Trevena, D. H. (1984). "Cavitation and the Generation of Tension in Liquids." *J. of Physics D: Applied Physics*, 17, 2139-2164.
- Trevena, D. H. (1987). *Cavitation and Tension in Liquids*, Adam Hilger, Philadelphia, 125 p.
- U.S. Army Corps of Engineers (1980). *Laboratory Soils Testing*, Engineer Manual EM 1110-2-1906.
- United States Dictionary of Places*, 1st edition, (1988). Somerset Publishers, NY, p. 512.
- United States Environmental Protection Agency (1990). *Handbook, Ground Water, Volume I Ground Water and Contamination*, EPA/625/6-90/016a, U.S. Environmental Protection Agency, Office of Research and Development, Washington, DC.
- U.S. Navy Diving Manual (1970). NAVSHIPS 0994-001-9010, Navy Department, Washington, D.C., 687 p.

- Vaandrager, B. L. and Pharr, G. M. (1989). "Compressive Creep of Copper Containing a Liquid Bismuth Intergranular Phase." *Acta Metallurgica*, 37, 1057-1066.
- Vesilind, P. A. and Peirce, J. J. (1982). *Environmental Engineering*, Butterworth Publishers, Boston, 602 p.
- Wheeler, S. J. (1988a). "A Conceptual Model for Soils Containing Large Gas Bubbles." *Geotechnique*, 38, 389-397.
- Wheeler, S. J. (1988b). "The Undrained Shear Strength of Soils Containing Large Gas Bubbles." *Geotechnique*, 38, 399-413.
- Willard, G. W. (1953). "Ultrasonically Induced Cavitation in Water: A Step-by-Step Process." *J. of the Acoust. Soc. of America*, 25, 669-686.
- Williams, P. J. (1967). "Replacement of Water by Air in Soil Pores." *Norwegian Geotechnical Institute, Publication No. 72*, 75-90.
- Winograd, I. J. and Robertson, F. N. (1982). "Deep Oxygenated Ground Water: Anomaly or Common Occurrence?" *Science*, 216, 1227-1230.
- Winterton, R. H. S. (1977). "Nucleation of Boiling and Cavitation," *J. of Physics D: Applied Physics*, 10, 2041-2156.
- Withiam, J. L. and Kulhawy, F. H. (1976). "Undrained Volume Changes in Compacted Cohesive Soil." *J. of the Geotech. Engrg. Div., ASCE*, 102(10), 1029-1039.
- Wyman, J., Scholander, P. F., Edwards, G. A., and Irving, L. (1952). "On the Stability of Gas Bubbles in Sea Water." *J. of Marine Research*, 11, 47-62.
- Yong, R. N. and Warkentin, B. P. (1966). *Introduction to Soil Behavior*, Macmillan, NY, 300-301.
- Young, F. R. (1989). *Cavitation*, McGraw-Hill, NY, 418 p.
- Yount, D. E. (1979). "Skins of Varying Permeability: A Stabilization Mechanism for Gas Cavitation Nuclei." *J. of the Acoust. Soc. of America*, 65, 1429-1439.

Yount, D. E. (1982). "On the Evolution, Generation, and Regeneration of Gas Cavitation Nuclei." *J. of the Acoust. Soc. of America*, 71, 1473-1481.

## **APPENDICIES**

## Appendix A

### NOTATION

a	=	the initial rate of solution of the gas in the water
abs	=	absolute (pressure)
A	=	the surface area across which the gas diffuses into or out of solution
$\bar{A}_u$	=	the pore pressure parameter for unloading
b	=	a constant which is dependent on the gas and temperature
bar	=	unit of pressure (1 bar = 14.504 psi)
bw	=	the rate of escape of gas from water
B	=	pore pressure parameter, B = 1.0 for a degree of saturation of 100%
c	=	undrained cohesion
c	=	concentration of the gas in water at time t
c	=	concentration of dissolved air in the liquid
c'	=	effective stress cohesion
$c_i$	=	uniform concentration of dissolved air at the bubble boundary
$c_0$	=	concentration of the gas in water at time t = 0
$c_s$	=	the saturation dissolved air concentration in the liquid at a given temperature and pressure
$c_\infty$	=	concentration of the gas in water at time t = $\infty$
$C_s$	=	the volumetric compressibility of the soil structure

CU test	= consolidated undrained triaxial test ( $\bar{R}$ test)
d	= the thickness of the shell surrounding the bubble into which the gas diffuses
$\frac{dc}{dx}$	= the rate of change of the concentration of the solute in the liquid at point x occurring over time dt
dq	= the amount of the solute which passes in the positive x direction through the area dy dz at a point x during time dt
dt	= the time increment over which diffusion occurs
$\frac{dw}{dt}$	= the rate of solution of the gas in the water
dy dz	= the cross sectional area of the interface across which the solute diffuses into the liquid
dia.	= diameter
D	= the coefficient of diffusion or the diffusivity of the solute (air) in the liquid (water)
D <sub>10</sub>	= effective size of soil grains, soil grain diameter corresponding to 10% finer by weight on the grain size curve for the soil
e	= void ratio of soil
e	= exponential function
f	= the coefficient of escape of the gas from the liquid per unit area and volume, cm/min
f	= the degree of undersaturation of the water with dissolved air, or the ratio between the initial dissolved air content of the water and the saturation dissolved air content
H	= Henry's coefficient of solubility of air in water at a given temperature
I.D.	= inside diameter
K	= a constant

$K_o$	=	minor principal stress ratio for at-rest condition = $\sigma'_{3con}/\sigma'_{1con}$
$K_c$	=	in situ principal stress ratio corresponding to anisotropic conditions = $\sigma'_{1con}/\sigma'_{3con}$
$K_f$ line	=	failure envelope line from stress path plot
L	=	Ostwald coefficient of solubility
LMVD	=	Lower Mississippi Valley Division, U.S. Army Corps of Engineers
m	=	the mass of air going into or out of solution
M	=	the molecular weight of the gas
n	=	the initial porosity of the specimen
n	=	the number of moles of gas present
n	=	the number of moles of gas which entered the bubble in time t
O.D.	=	outside diameter
p	=	horizontal stress path coordinate in terms of total stresses = $\frac{1}{2}(\sigma_1 + \sigma_3)$
p'	=	horizontal stress path coordinate in terms of effective stresses = $\frac{1}{2}(\sigma'_1 + \sigma'_3)$
$p_a$	=	atmospheric pressure
P	=	gas pressure
$P_a$	=	pore air pressure
$P_{af}$	=	the final pressure of the dissolved air
$P_{ai}$	=	the initial pressure of the dissolved air
$P_{air}$	=	pore air pressure
$P_{atm}$	=	atmospheric pressure
$P_b$	=	applied back pressure

$P_f$	=	final pore air pressure (absolute)
$P_g$	=	gas pressure
$P_{gf}$	=	final pore-gas pressure
$P_{gi}$	=	initial pore-gas pressure
$P_{go}$	=	the initial absolute gas pressure
$P_{g1}$	=	the final absolute gas pressure in the bubble
$P_i$	=	the initial absolute air pressure corresponding to the initial degree of saturation, $S_i$
$P_o$	=	the initial pressure of the air in the voids when the sample is unconfined (absolute)
$P_w$	=	pore water pressure
$P_{water}$	=	pore water pressure
$P_{wf}$	=	final pore water pressure
$P_{wi}$	=	initial pore water pressure
$P_{100}$	=	the minimum increase in back pressure required to achieve 100% saturation, $P_{100} = 49P_i(1 - S_i)$
PPT	=	prepressurization threshold
psi	=	pounds per square inch (pressure or stress)
psia	=	pounds per square inch (absolute pressure)
psig	=	pounds per square inch (gauge pressure)
$q$	=	vertical stress path coordinate in terms of total and effective stresses = $\frac{1}{2}(\sigma_1 - \sigma_3) = \frac{1}{2}(\sigma'_1 - \sigma'_3)$
Q test	=	unconsolidated undrained (quick) triaxial test
$r$	=	the radius of curvature of the air-water interface
$r$	=	bubble radius
$r$	=	final radius of the bubble

- $r$  = the radial distance from the center of the bubble
- $r_1$  = the bubble radius,  $r$ , for which the denominator in Eq. 4-33 will be equal to zero
- $r_0$  = the initial radius of the gas bubble
- $R$  = the gas constant
- $R$  = ratio between back pressure applied,  $P_b$ , and minimum back pressure required to reach 100% saturation,  $P_{100}$ ,  $= \frac{P_b}{P_{100}}$
- $R_a$  = the specific gas constant for air (converted from the universal gas constant in terms of moles of gas to specific gas constant for air in terms of average molecular weight of air)
- $R_0$  = the initial radius of the air bubble
- $\bar{R}$  test = consolidated undrained triaxial test (CU test) with pore pressure measurements
- $S$  = the degree of saturation of the soil
- $S_f$  = final degree of saturation of the soil
- $S_i$  = initial degree of saturation of the soil
- $S_r$  = degree of saturation
- $S_u$  = undrained shear strength of soil
- $t$  = time
- $t_A$  = the approximate time for an air bubble to dissolve, neglecting surface tension effects
- $t_d$  = the time in minutes required for the free air to dissolve due to an increase in back pressure so that the soil specimen goes from an initial degree of saturation  $S_i$  to a final degree of saturation  $S_f$
- $t_s$  = the approximate time for an air bubble to dissolve in water, including the effects of surface tension

$T$	=	the absolute temperature
$T_s$	=	surface tension
$u$	=	pore water pressure
$u$	=	the final absolute pore water pressure
$u_a$	=	pore air pressure
$u_f$	=	pore water pressure at failure
$u_{min}$	=	minimum pore water pressure measured in Q test
$u_o$	=	the initial absolute pressure of the water (the hydrostatic pressure of the water plus atmospheric pressure)
$u_w$	=	pore water pressure
$u_1$	=	the absolute pore water pressure for a bubble radius of $r_1$
$u_{w1}$	=	the hydrostatic (gage) pressure of the pore water
UU test	=	unconsolidated undrained triaxial test (Q test)
$V$	=	volume of gas
$V_{air}$	=	volume of free air
$V_{df}$	=	the final volume of dissolved air
$V_{dg}$	=	the volume of gas dissolved in the liquid at equilibrium conditions
$V_{di}$	=	the initial volume of dissolved air
$V_{free\ air}$	=	volume of free air in the specimen initially
$V_g$	=	volume of free air
$V_{gf}$	=	final volume of free gas in specimen
$V_{gi}$	=	initial volume of free gas in specimen
$V_T$	=	total volume of triaxial specimen
$V_v$	=	volume of voids

$V_{vf}$	=	final volume of voids
$V_{vi}$	=	initial volume of voids
$V_w$	=	volume of water
$V_{wf}$	=	final volume of water
$V_{wi}$	=	initial volume of water
$w$	=	water content of the soil
$w$	=	the weight per unit volume of gas which dissolved in the liquid during time $t$
$w_{df}$	=	the final mass of dissolved air
$w_{di}$	=	the initial mass of dissolved air
$w_0$	=	the weight per unit volume of dissolved gas present in the liquid at $t = \infty$
$w_1$	=	the weight per unit volume of gas dissolved in the liquid initially
$x$	=	a constant
$z$	=	depth
$\alpha$	=	angle $K_f$ line makes with the horizontal axis
$\alpha$	=	the solubility of the gas in the water
$\beta$	=	angle $K_0$ line makes with the horizontal axis
$\beta$	=	the exit coefficient from water of a given gas at a given temperature, $\beta = 0.0099(T - 239)$ where $T = ^\circ\text{C} + 273$ , and $\beta$ is in units of cm/minute
$\chi$	=	the fraction of voids filled with free air at the initial pressure of an unconfined specimen, $\chi = \frac{V_{\text{free air}}}{V_v}$ , ( $\chi = 1 - S_i$ , where $S_i$ = the initial degree of saturation of the specimen)
$\delta$	=	$\frac{\Delta\alpha}{d}$

$\Delta$	=	the diffusion coefficient of the gas in the water
$\Delta\sigma_1$	=	the change in major principal total stress
$\Delta\sigma_3$	=	the change in minor principal total stress
$\Delta u_{\max}$	=	maximum change in pore water pressure measured in the Q test
$\Delta u_v$	=	the increase in back pressure required to go from an initial degree of saturation, $S_i$ , to a final degree of saturation, $S_f$ , for a constant volume, increasing water content condition
$\Delta u_w$	=	the change in pore water pressure
$\Delta V_g$	=	change in volume of free gas due to a change in gas pressure
$\epsilon_a$	=	axial strain
$\mu D$	=	linear attenuation coefficient
$\phi'$	=	effective stress friction angle of the soil
$\phi_u$	=	undrained friction angle of soil
$\gamma_d$	=	dry unit weight of soil
$\gamma_{\text{sat}}$	=	saturated unit weight of soil
$\rho_a$	=	the density of air at atmospheric pressure and the temperature of the system
$\sigma'$	=	effective stress
$\sigma_{\text{cell}}$	=	cell pressure at which Q test was performed
$\sigma_{d\max}$	=	maximum deviator stress measured in triaxial test
$\sigma_s$	=	the saturation pressure or the minimum cell pressure, above atmospheric, needed to completely dissolve all free air

$\sigma_1$	=	major principal total stress at failure
$\sigma_3$	=	minor principal total stress at failure
$\sigma_3$	=	cell pressure used in Q test
$\sigma'_{1con}$	=	major principal consolidation stress
$\sigma'_{3con}$	=	minor principal consolidation stress
$\theta$	=	the angle of intersection between the air-water surface and the soil grains
$^{\circ}C$	=	degree Centigrade

## Appendix B

### Conversion Factors

Non-SI units of measurement used in this report can be converted to SI (metric) units as follows:

Multiply	By	To Obtain
angstroms	$1 \times 10^{-8}$	cm
atmospheres	1.0332	kg/cm <sup>2</sup>
bars	1.0197	kg/cm <sup>2</sup>
inches (in)	2.54	cm
square inches (in <sup>2</sup> )	6.4516	cm <sup>2</sup>
cubic inches (in <sup>3</sup> )	16.387	cm <sup>3</sup>
pounds per square inch (psi)	0.070307	kg/cm <sup>2</sup>

## VITA

Andrew Thomas Rose was born on January 10, 1964 in Bridgeport, Connecticut. He received his Bachelor of Science degree in Engineering from the University of Connecticut in May, 1985. He received a Master of Science degree in Civil Engineering from the University of Connecticut in December, 1986. He obtained experience as a consulting engineer in Connecticut from January, 1987 to August, 1990 with Heynen Engineers, Seelye, Stevenson, Value & Knecht, and Roald Haestad, Inc. He has been a registered professional engineer in Connecticut since August, 1990.

Mr. Rose enrolled in the Graduate School at Virginia Polytechnic Institute & State University in August, 1990 to pursue a doctoral degree in civil engineering, with emphasis in geotechnical engineering. He was employed by the university as a teaching assistant for two years and as a research assistant for two years.

As of October, 1994, Mr. Rose will be employed by GAI Consultants of Monroeville, Pennsylvania.

A handwritten signature in cursive script that reads "Andrew T. Rose". The signature is written in dark ink and is positioned at the end of the text block.